CORROSION BEHAVIOUR OF ALUMINIUM BASED METAL MATRIX COMPOSITES REINFORCED WITH SiC AND ZIRCON SAND

A
Thesis
Submitted in partial fulfilment of the requirement for the award of degree of

MASTER OF ENGINEERING
IN
PRODUCTION & INDUSTRIAL

Submitted By

Avdesh
Roll No. 800982002

Under the Guidance of

Yogesh Kumar Singla
Lecturer,
Deptt. Of Mechanical Engg.
Thapar University,
Patiala-147004

Dr. Shweta Goyal
Assistant Professor,
Deptt. Of Civil Engg.
Thapar University,
Patiala-147004

DEPARTMENT OF MECHANICAL ENGINEERING
THAPAR UNIVERSITY
PATIALA-147004, INDIA
JUNE-2011

CERTIFICATE

This is to certify that the work done in this thesis report entitled **"CORROSION BEHAVIOUR OF ALUMINIUM BASED METAL MATRIX COMPOSITES REINFORCED WITH SiC AND ZIRCON SAND"** submitted in partial fulfilment of requirement for the award of **Master of Engineering degree in Production & Industrial Engineering** submitted in the mechanical engineering department of Thapar University, Patiala, is an authentic record of work carried out by me under the guidance of **Mr. Yogesh Kumar Singla**, Lecturer, Mechanical Engineering Department, TU, Patiala **and Dr. Shweta Goyal,** Assistant Professor, Civil Engineering Department, TU, Patiala.

The matter embodied in this report has not been submitted in part or full to any other university or institute for the award of any degree.

(Avdesh)

This is to certify that above declaration made by the student concerned is correct to the best of my knowledge & belief

Mr. Yogesh Kumar Singla
Lecturer,
Deptt. Of Mechanical Engineering
Thapar University,
Patiala-147004

Dr. Shweta Goyal
Assistant Professor
Deptt. Of Civil Engineering
Thapar University,
Patiala-147004

(Counter-signed by)

Dr. Ajay Batish
Professor & HOD,
Deptt. Of Mechanical Engineering
Thapar University,
Patiala-147004

Dr. S.K. Mohapatra
Dean of Academic Affairs
Thapar University,
Patiala- 147004

ACKNOWLEDGEMENT

I am highly grateful to the authorities of Thapar University, Patiala for providing this opportunity to carry out the thesis work.

I would like to express a deep sense of gratitude and thank profusely to my thesis guide Mr. Yogesh Kumar Singla & Dr. Shewta Goyal for their sincere & invaluable guidance, suggestions and attitude which inspired me to submit thesis report in the present form.

I am also thankful to other faculty members of Mechanical Engineering Department, Thapar University, Patiala for their intellectual support. My special thanks are due to my family members and friends who constantly encouraged me to complete this work.

Dated: Avdesh

ABSTRACT

Metal Matrix Composites (MMCs) have evoked a keen interest in recent times for potential applications in marines, aerospace and automotive industries owing to their superior strength to weight ratio and high temperature resistance. The excellent mechanical properties of these materials and relatively low production cost make them a very attractive candidate for a variety of applications both from scientific and technological viewpoints.

Present work is focused on the study of corrosion behaviour of Aluminium alloy (6063) /SiC /ZIRCON SAND composite produced by the stir casting technique by controlling various casting parameters. The electrochemical behaviour of Aluminium alloy 6063/SiC/ZIRCON SAND metal matrix composite was investigated in 3.5% NaCl aqueous solution by ACM field machine. Results of the corrosion tests were determined using the potentiodynamic method, half cell method, potential measurement and by recording corrosion current density (Icorr) and corrosion rate in the 3.5 % water solution of NaCl indicate that corrosion of the investigated composite materials depends on the volume fraction of the reinforcing particles.

Microhardness tester was used to evaluate the interfacial bonding between the particles and the matrix by indenting the microhardness indenter on the particle with the constant load (200 gm) and constant time (20 sec) at 100X optical zoom. X-ray Diffraction was performed to know the presence of the phases of reinforced material. Optical micrography and scanning electron microscopy was done to know the distribution of SiC/ZIRCON SAND particles in Aluminium alloy.

CONTENTS

LIST OF FIGURES

LIST OF TABLES

CHAPTER 1 INTRODUCTION

1.1 METAL MATRIX COMPOSITES (MMC)

In engineering designs, great interest is to search for new materials exhibiting good mechanical properties. For the development of such materials metal matrix composites (MMCs) have been proved to be one of the best selections for such materials. Metal matrix composites (MMCs), like all composites consist of at least two chemically and physically distinct phases, suitably distributed to provide properties not obtainable with either of the individual phases [1].

The constituents are combined at a microscopic level and are not soluble in each other. The reinforcing material may in the form of the fibres, particles or flakes. The matrix phase's materials are generally continuous. The matrix holds the reinforcement to form the desired shape while the reinforcement improves the overall mechanical properties of the matrix. When designed properly, the new combined material exhibits better strength than would each individual material [2].

Examples of composite system include concrete reinforcement with steel, epoxy reinforced with graphite fibers etc. By definition, MMC's are produced by means of processes other than conventional metal alloying. Like their polymer matrix counterparts, these composites are often produced by combining two pre-existing constituents [3].

Common types of MMC are

- Aluminium Matrix Composites (AMC)
- Magnesium Matrix Composite
- Titanium Matrix Composite
- Copper Matrix Composites

1.1.1 Matrix

The selection of suitable matrix alloys is mainly determined by the intended application of the composite materials. With the development of light metal composite materials that are mostly easy to process, conventional light metal alloys are applied as matrix materials.

The matrix is the monolithic material into which the reinforcement is embedded, and is completely continuous. In structural applications, the matrix is usually a lighter metal such as Aluminium, magnesium, or titanium, and provides a compliant support for the reinforcement. In high temperature applications, cobalt and cobalt-nickel alloy matrices are common [4].

1.1.2 Reinforcement

The second phase is imbedded in the matrix in a discontinuous form. This secondary phase is called dispersed phase. Dispersed phase is usually stronger than the matrix, therefore it is sometimes called reinforcing phase. Many of common materials (metal alloys, doped Ceramics and Polymers mixed with additives) also have a small amount of dispersed phases in their structures, however they are not considered as composite materials since their properties are similar to those of their base constituents [3].

The strength of the composite depends primarily on the amount, arrangement and type of fiber (or particle) reinforcement in the resin. Typically the higher the reinforcement content, the greater the strength. Reinforcing materials are strong with low densities while the matrix is usually a ductile, or tough, material. If the composite is designed and fabricated correctly, it combines the strength of the reinforcement with the toughness of the matrix to achieve a combination of desirable properties not available in any single conventional material [5]. Examples of some current application of composites include the tires, diesel piston, brake-shoes and pads.

1.1.3 Aluminium Matrix Composites

Aluminium matrix composites (AMCs) have been widely studied since the 1920s and are now used in sporting goods, electronic packaging, armours and automotive industries. Aluminium is the most popular matrix for the metal matrix composites (MMCs). The Al alloys are quite attractive due to their low density, their capability to be strengthened by precipitation, their good corrosion resistance, high thermal and electrical conductivity, and their high damping capacity [6].

They are usually reinforced by Al_2O_3, SiC, and carbon. As proposed by the American Aluminium Association the AMCs should be designated by their constituents: accepted designation of the matrix / abbreviation of the reinforcement's designation / arrangement and volume fraction in % with symbol of type (shape) of reinforcement. For example, an

Aluminium alloy AA6061 reinforced by particulates of alumina, 22 % volume fraction, is designated as "AA6061/Al_2 O_3/22p".

Aluminium Matrix Composites are manufactured by the following fabrication methods

- Powder metallurgy
- Stir casting
- Squeeze casting

1.2 PROCESSING OF MMCs

Accordingly to the temperature of the metallic matrix during processing the fabrication of MMCs can be classified into three categories:

(a) Liquid phase processes,

(b) Solid state processes, and

(c) Two phase (solid-liquid) processes.

1.2.1 Liquid Metal Techniques

Liquid state fabrication of Metal Matrix Composites involves incorporation of dispersed phase into a molten matrix metal, followed by its Solidification. In order to provide high level of mechanical properties of the composite, good interfacial bonding (wetting) between the dispersed phase and the liquid matrix should be obtained. Wetting improvement may be achieved by coating the dispersed phase particles (fibers). Proper coating not only reduces interfacial energy, but also prevents chemical interaction between the dispersed phase and the matrix. The simplest and the most cost effective method of liquid state fabrication is Stir Casting [7].

1.2.2 Stir Casting Method of Fabrication of MMCs

Stir Casting is a liquid state method of composite materials fabrication, in which a dispersed phase (ceramic particles, short fibers) is mixed with a molten matrix metal by means of mechanical stirring as shown in figure 1.1. The liquid composite material is then cast by conventional casting methods and may also be processed by conventional Metal forming technologies [7].

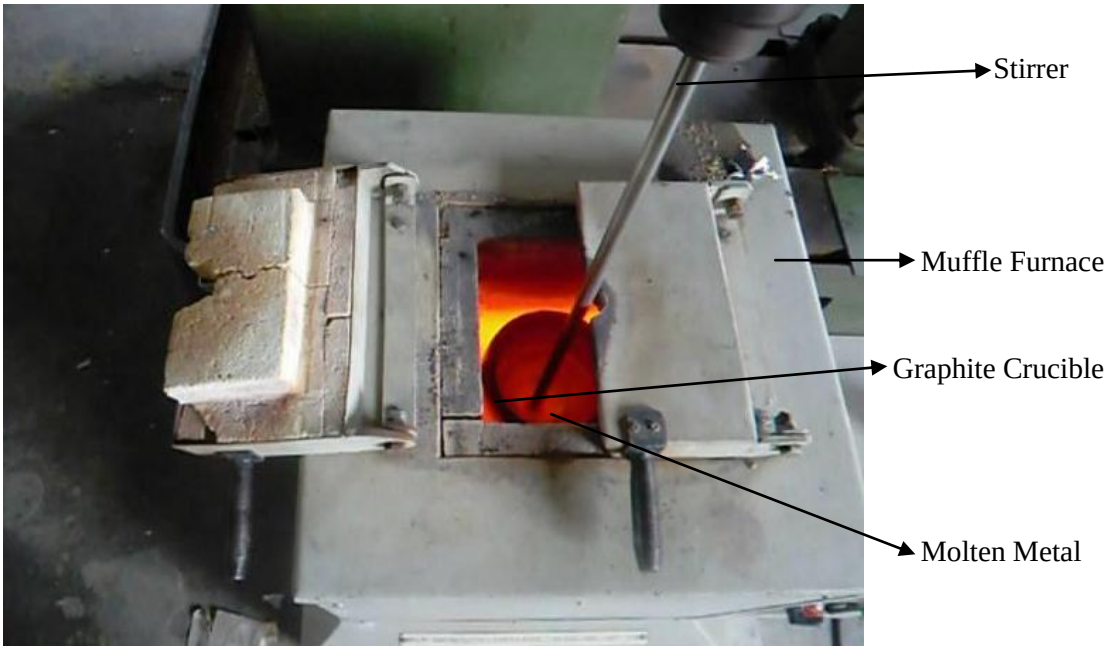

Figure 1.1 Stir casting set up

Stir Casting is characterized by the following features

- Content of dispersed phase is limited (usually not more than 30 vol. %).
- Distribution of dispersed phase throughout the matrix is not perfectly homogeneous:
    1. There are local clouds (clusters) of the dispersed particles (fibers).
    2. There may be gravity segregation of the dispersed phase due to a difference in the densities of the dispersed and matrix phase.
- The technology is relatively simple and low cost [7].

1.3 PROCESS VARIABLES AND THEIR EFFECTS ON PROPERTIES

1.3.1 Speed of rotation

The control of speed is very important for successful production of casting. Rotational speed also influences the structure, the most common effect of increase in speed being to promote refinement and instability of the liquid mass at very low speed. It is logical to use the highest speed consistent with the avoidance of tearing [8].

1.3.2 Pouring temperature

Pouring temperature exerts a major role on the mode of solidification and needs to determine partly in relation to type of structure required. Low temperature is associated with maximum grain refinement and equiaxed structures while higher temperature promotes columnar growth in many alloys. However practical consideration limits the

range .The pouring temperature must be sufficiently high to ensure satisfactory metal flow and freedom from cold laps whilst avoiding coarse structures [8].

1.3.3 Pouring speed

This is governed primarily by the need to finish casting before the metal become sluggish. Although too high a rate can cause excessive turbulence and rejection. In practice slow pouring offers number advantages. Directional solidification and feeding are promoted whilst the slow development of full centrifugal pressure on the other solidification skin reduces and risk of tearing. Excessive slow pouring rate and low pouring temperature would lead to form surface lap [9].

1.3.4 Mould temperature

The use of metal die produces marked refinement when compared with sand cast but mould temperature is only of secondary importance in relation to the structure formation. Its principal signification lies in the degree of expansion of the die with preheating. Expansion diminishes the risk of tearing in casting. In nonferrous castings, the mould temperature should neither be too low or too high. The mould should be at least 25 mm thick with the thickness increasing with size and weight of casting [9].

1.3.5 Mould coatings

Various types of coating materials are used. The coating material is sprayed on the inside of the metal mould. The purpose of the coating is to reduce the heat transfer to the mould. Defects like shrinkage and cracking that are likely to occur in metal moulds can be eliminated, thus increasing the die life. The role of coating and solidification can be adjusted to the optimum value for a particular alloy by varying the thickness of coating layer. For aluminium alloys, the coating is a mixture of Silicate and graphite in water.

1.3.6 Mould life

Metal mould in casting is subjected to thermal stresses due to continuous operation. This may lead to failure of the mould. The magnitude of the stresses depends on the mould thickness and thickness of the coating layer, both of which influence the production rate. Deterioration takes place faster in cast iron mould than in steel mould [9].

1.4 WETTABILITY BETWEEN REINFORCEMENT AND MATRIX ALLOY

Wettability can be defined as the ability of a liquid to spread on a solid surface. It also describes the extent of intimate contact between a liquid and a solid. Successful

incorporation of solid ceramic particles into casting requires that the melt should wet the solid ceramic phase. The basic means used to improve wetting are:

(a) Increasing the surface energies of the solid,

(b) Decreasing the surface tension of the liquid matrix alloy,

(c) Decreasing the solid-liquid interfacial energy at the particles-matrix

Several approaches have been taken to promote the wetting of the reinforcement particles with a molten matrix alloy, including the coating of the particles, the addition of alloying elements to the molten matrix alloy, the treatment of the particles, and ultrasonic irradiation of the melt. In general, the surface of non-metallic particles is not wetted by the metallic metal, regardless of the cleaning techniques carried out. Wetting has been achieved by coating with a wettable metal. Metal coating on ceramic particles increases the overall surface energy of the solid, and improves wetting by enhancing the contacting interface to metal-metal instead of metal-ceramic [4].

Nickel and copper are well wetted by many alloys and have been used for a number of low melting alloys. In general, these coatings are applied for three purposes, viz., to protect the reinforcement from damage in handling, to improve wetting, and to improve dispensability before addition to the matrix.

Heat treatment of the particles before dispersion into the melt aids their transfer by causing desorption of adsorbed gases from the particle surface. Heating Silicon Carbide particles to 900°C, for example, assists in removing surface impurities and in the desorption of gases, and alters the surface composition by forming an oxide layer on the surface. Hence a clean surface provides a better opportunity for melt-particles interaction, and thus, enhances wetting. Thus results in strong interfacial bonding [10].

1.5 SILICON CARBIDE AS REINFORCEMENT

Silicon Carbide is the only chemical compound of carbon and silicon. It was originally produced by a high temperature electro-chemical reaction of sand and carbon. Silicon Carbide is an excellent abrasive and has been produced and made into grinding wheels and other abrasive products for over one hundred years. Today the material has been developed into a high quality technical grade ceramic with very good mechanical properties.

It is used in abrasives, refractories, ceramics, and numerous high-performance applications. The material can also be made an electrical conductor and has applications in resistance heating, flame igniters and electronic components. Silicon Carbide is composed of tetrahedral of carbon and silicon atoms with strong bonds in the crystal lattice. This produces a very hard and strong material [8].

1.5.1 Properties of silicon carbide

- Low density
- High strength
- Low thermal expansion
- High thermal conductivity
- High hardness
- High elastic modulus
- Excellent thermal shock resistance
- Superior chemical inertness

Table 1.1 Properties of Silicon Carbide

Properties	Silicon carbide
M.P.	2200-2700
Limit of application (°C)	1400-1700
Hardness (Moh's Scale)	9
Density (g/cm^3)	3.2
Linear coeff. of expansion (10^{-6} K)	4.5
Fracture toughness (MPa-$m^{1/2}$)	4.6
Crystal structure	Hexagonal

1.6 ZIRCON SAND AS REINFORCEMENT

Zircon Sand consists of mostly ZIRCONIUM SILICATE ($ZrSiO_4$) and some hafnium in addition to some rare earth elements, titanium minerals, monazite, etc. Zircon Sand is used chiefly for facing on foundry moulds to increase the resistance against metal penetration. Milled Zircon Sand is used in refractory paint for coating the outside of moulds.

Zircon Sand deposits have been found in abundance near Indian coastal regions of Kerala, Tamil Nadu and Orissa. Zircon Sand was found to be a promising candidate as reinforcement material for aluminium, zinc and lead based composites. [10]

1.6.1 Advantages of using Zircon Sand as reinforcement

1. High hardness,
2. High modulus of elasticity,
3. High temperature resistance (melting point of 2500^{o}C),
4. Acid corrosion resistance and excellent thermal stability.

The last property is important since fabrication processes require drastic changes in temperature and large volumetric changes due to phase transformations can cause debonding at the interface. Furthermore, Zircon Sand possesses a very low thermal expansion coefficient compared to most other ceramic oxides. **[10]**

Therefore, a change in temperature would not give rise to very high thermal stresses within Zircon Sand particles. Zircon Sand particles can be incorporated to aluminium silicon alloy matrix by stir casting route and the dispersed amount can be further increased by the addition of magnesium in the melt.

Table 1.2: Properties of Zircon Sand

Properties	Zircon Sand
M.P. (°C)	2500
Limit of application (°C)	1870
Hardness (Moh's Scale)	7.5
Density (g/cm^3)	4.5-4.70
Linear coeff. of expansion (10^{-6} K)	4.5
Fracture toughness (MPa-m$^{1/2}$)	5
Crystal structure	Tetragonal

1.7 CORROSION

Corrosion is a slow, progressive or rapid deterioration of a metal's properties such as its appearance, its surface aspect, or its mechanical properties under the influence of the surrounding environment: atmosphere, water, seawater, various solutions, organic environments, etc. In the past, the term "oxidation" was frequently used to designate what is now a day's commonly called "corrosion". Nevertheless, the former was the right word because corrosion also is an electrochemical reaction during which the metal is oxidised, which usually implies its transformation into an oxide, i.e. into the state in which it existed in the mineral **[11]**.

1.8 TYPES OF CORROSION ON ALUMINIUM ALLOYS AND COMPOSITES

Different types of corrosion, more or less visible to the naked eye, can occur on aluminium, such as uniform (generalised) corrosion, pitting corrosion, stress corrosion, etc. The predominant type of corrosion will depend on a certain number of factors that are intrinsic to the metal, the medium and the conditions of use. There is no form of corrosion that is specific to aluminium and its alloys

1.8.1 Uniform Corrosion

This type of corrosion develops as pits of very small diameter, in the order of a micrometer, and results in a uniform and continuous decrease in thickness over the entire surface area of the metal as shown in figure 1.2. With aluminium, this type of corrosion is observed especially in highly acidic or alkaline media, in which the solubility of the natural oxide film is high. The dissolution rate of the film is greater than its rate of formation. However, the ratio of both rates can change over time [12].

As an example, in sodium hydroxide solutions the dissolution rate has been found to be lower for long-term exposure, in the order of 40 or 80 days, than for tests over 20 days. The dissolution rate can vary from a few micrometers per year up to a few micrometers per hour, depending on the nature of the acid or base. The rate of uniform corrosion can be easily determined by measuring the mass loss, or the quantity of released hydrogen.

Figure 1.2 Uniform Corrosion [12]

1.8.2 Pitting Corrosion

This localised form of corrosion is characterised by the formation of irregularly shaped cavities on the surface of the metal. Their diameter and depth depend on several parameters related to the metal, the medium and service conditions. Aluminium is prone to pitting corrosion in media with a pH close to neutral, which basically covers all natural environments such as surface water, seawater, and moist air.

Pitting is considered to be more dangerous than uniform corrosion damage because it is more difficult to detect, predict and design against. Corrosion products often cover the pits. As shown in figure 1.3 small, narrow pit with minimal overall metal loss can lead to

the failure of an entire engineering system. Pitting corrosion occurs when the metal is put into permanent or intermittent contact with aqueous media: water, seawater, rain water, and humidity. Experience shows that when pitting corrosion occurs, it will always develop during the first weeks of exposure [13].

Figure 1.3 Pitting Corrosion [13]

1.8.3 Galvanic Corrosion

When two dissimilar metals are in direct contact in a conducting liquid, experience shows that one of the two may corrode. This is called galvanic corrosion. This corrosion is different in its kind and intensity from the one that would occur if they were placed separately in the same liquid. Unlike other types of structural corrosion, galvanic corrosion does not depend on the metal's texture, temper, etc [12].

Galvanic corrosion may occur with any metal, as soon as two are in contact in a conductive liquid. It works like a battery; we will recall its principles below.

Galvanic corrosion works like a battery built from two electrodes:

- The cathode, where reduction takes place,
- The anode, where oxidation takes place.

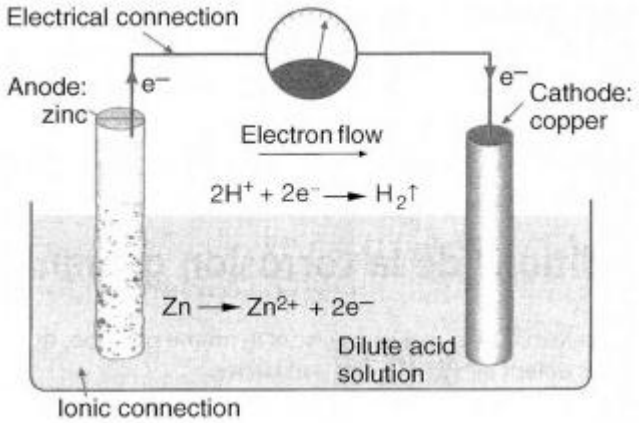

Figure 1.4 Principle of a galvanic cell [14]

As shown in the figure 1.4 these two electrodes are plunged into a conductive liquid called an electrolyte, which is normally a diluted acid solution, such as sulphuric acid, or a salt solution, such as copper sulphate. The two electrodes are externally linked by an

electrical circuit that ensures a circulation of electrons. Within the liquid, the transport of electrical current proceeds by the movement of ions, i.e. by ionic transport. The liquid thus provides an ionic junction [14].

Figure 1.4 shows a cell in which the electrolyte is a solution of sulphuric acid H_2SO_4 which totally dissociates in water (since it is a strong acid) by forming H^+ ions that are responsible for the acidity of the medium. The following electrochemical reactions occur:

- the zinc anode oxidises:

$$Zn \longrightarrow Zn^{2+} + 2e^- \quad \text{.....1.1}$$

- The copper cathode, protons H^+ are reduced (this is the only cation present which can be reduced):

$$2H^+ + 2e^- \longrightarrow H_2 \quad \text{.....1.2}$$

The net reaction is

$$Zn + 2H_20 \longrightarrow Zn(OH)^2 + H_2 \quad \text{.....1.3}$$

This cell produces electricity while consuming zinc that precipitates as zinc hydroxide $Zn(OH)_2$.

Three conditions must be met simultaneously for a cell to function:

- Two metals of a different nature which form the two electrodes, Presence of an electrolyte,
- Electrical continuity.

In galvanic corrosion, the cathodic reactions (on the metal which does not undergo corrosion) depend on the medium:

- If it is acid:

$$0_2 + 4H^+ + 4e^- \longrightarrow 2H_20 \quad \text{.....1.4}$$

Or

$$2H^+ + 2e^- \longrightarrow H_2 \quad \text{.....1.5}$$

If it is an alkali

$$0_2 + 2H_20 + 4e^- \longrightarrow 4OH^- \quad \text{.....1.6}$$

If one of these three conditions is not met, for example, if the electrical connection is interrupted, the cell will not produce a current, and the oxidation at the anode will not take place (nor the reduction at the cathode) [13].

1.8.4 Transgranular and Intergranular (intercrystalline) Corrosion

Within the metal, at the level of the grain, corrosion may propagate in two different ways:

- It spreads in all directions (Figure1.5): corrosion indifferently affects all the metallurgical constituents; there is no selective corrosion. This is called transgranular or transcrystalline corrosion because it propagates within the grains.
- It follows preferential paths (Figure1.6): corrosion propagates at grain boundaries. Unlike transgranular corrosion, this form of intercrystalline corrosion consumes only a very small amount of metal, which is why mass loss is not a significant parameter for assessment of this type of corrosion. It is not detectable with the naked eye but requires microscopic observation, typically at a magnification of 50X.

When penetrating into the bulk of the metal, intercystalline corrosion may lead to a reduction of mechanical properties, especially of elongation, and may even lead to the rupture of components. The propagation of intercrystalline corrosion starts at pits. There is no relationship between the penetration depth of intercrystalline corrosion and the diameter of corrosion pits. This means that intercyrstalline corrosion may also propagate from minute, superficial pits [15].

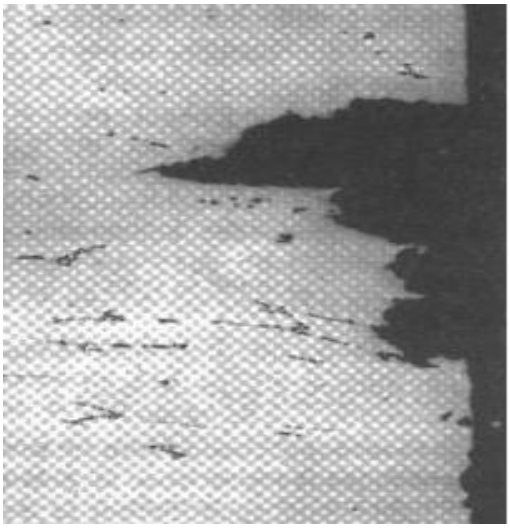

Figure 1.5 Transcrystalline corrosion [15]

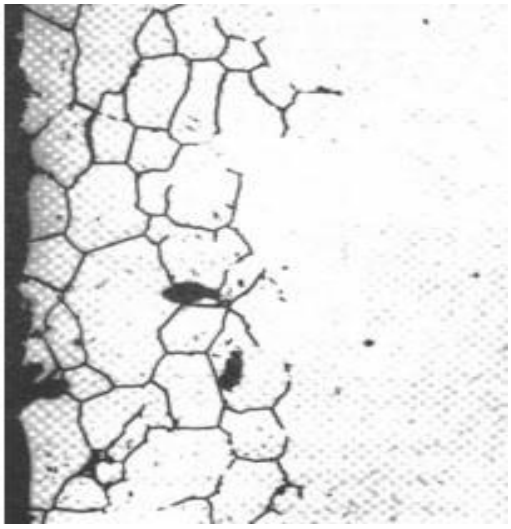

Figure 1.6 Intercrystalline corrosion [15]

1.8.5 Exfoliation Corrosion

Exfoliation corrosion is a type of selective corrosion that propagates along a large number of planes running parallel to the direction of rolling or extrusion [47]. Between these planes are very thin sheets of sound metal that are not attacked, but gradually pushed away by the swelling of corrosion products, peeling off like pages in a book; hence the term "exfoliation corrosion". The metal will swell, which results in the spectacular aspect of this form of corrosion (Figure 1.7).

This corrosion may be intercystalline in 2000 and 5000 alloys exhibiting a long-grained structure parallel to the direction of transformation. It can also be found in 7000 alloys with or without copper (which have a low susceptibility to intercrystalline corrosion). It results from the precipitation of parallel stripes of intermetallic phases such as $A1_6Mn$, Al_2CrMn, etc., which are cathodic with respect to the solid solution and between which there is an anodic zone depleted in Fe and Mn [16].

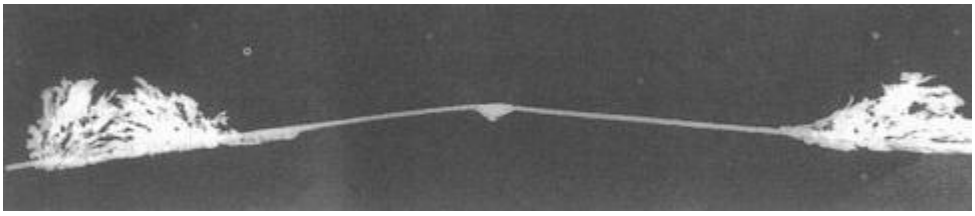

Figure 1.7 Exfoliation Corrosion [16]

1.8.6 Stress Corrosion

This type of corrosion results from the combined action of a mechanical stress (bending, tension) and a corrosive environment. Each of these parameters alone would not have such a significant effect on the resistance of the metal or would have no effect at all. Cold deformation and forming, welding, heat treatment, machining and grinding can introduce residual stresses.

The magnitude and importance of such stresses is often underestimated. The residual stresses set up as a result of welding operations tend to approach the yield strength. The build-up of corrosion products in confined spaces can also generate significant stresses. Usually, most of the surface remains unattacked, but with fine cracks penetrating into the material (figure 1.8). In the microstructure, these cracks can have intergranular or transgranular morphology [17].

Stress Corrosion is classified as a catastrophic form of corrosion, as the detection of such fine cracks can be very difficult and the damage not easily predicted. A disastrous failure may occur unexpectedly, with minimal overall material loss.

Figure 1.8 Stress corrosion cracking [17]

1.8.7 Filform Corrosion

Filiform corrosion is specific to lacquered metal. This is mainly an alteration of surface appearance. The underlying metal only suffers a very superficial attack, not exceeding a depth of a few tens of microns. It develops as narrow filaments, about 0.1-0.5 mm wide and a few millimetres long, which propagate at the metal-lacquer interface. Swelling of corrosion products deforms the lacquer film and appears as very narrow wires which progress like mole tunnels underneath the lacquer film (Figure 1.9).

Filiform corrosion always starts at coating defects, such as scratches, and weak points: beards, cut edges or holes. It can be seen after several years of service [12].

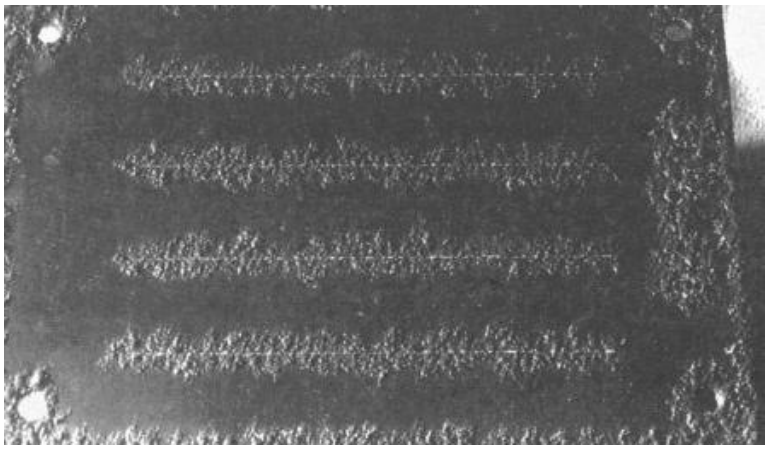

Figure 1.9 Filiform Corrosion [12]

1.8.8 Crevic Corossion

Crevice corrosion is a localised corrosion in recesses: overlapping zones for riveting, bolting or welding, zones under joints, and under various deposits (sand, slag, precipitates, etc.). These zones, also called crevices, are very tiny and difficult to access for the aqueous liquid that is covering the rest of the readily accessible surfaces (Figure1.10). This type of corrosion is also known as deposit attack.

As soon as an electrochemical reaction occurs in this confined volume, the composition of the contained liquid will change. As a consequence, the dissolution potential becomes more electronegative, and the surface in the recess becomes anodic with respect to the rest of the structure [39]. In the crevice, aluminium is oxidised according to the reaction [18].

$$A1 \longrightarrow A13^{+} + 3e^{-} \quad \text{.....1.7}$$

Whereas at the rim of the crevice, oxygen is reduced:

$$0_2 + 2H_20 + 4e^{-} \longrightarrow 4OH^{-} \quad \text{.....1.8}$$

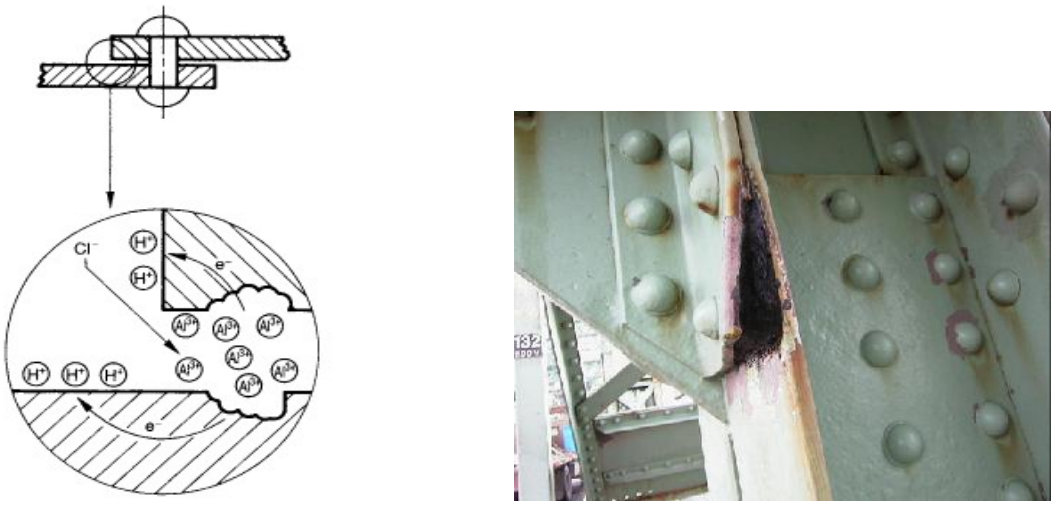

Figure 1.10 Crevice corrosion [18]

While the metal in the recess is being corroded, oxygen dissolved in the liquid will be consumed. Since the local geometry limits diffusion, the recess will be depleted in oxygen, with an excess of $A13^{+}$ ions. This leads to an inflow of $C1^{-}$ chloride ions. Aluminium chloride will hydrolyse:

$$A1C1_3 + 3H_20 \longrightarrow AI\,(OH)_3 + 3H^{+} + 3C1^{-} \quad \text{.....1.9}$$

1.8.9 Cavitation

Cavitation occurs when the hydrodynamic pressure exceeds the vapour pressure of a moving liquid. Gas bubbles form within the liquid, which thus becomes a two-phase system. These bubbles will be crushed against the metal surface at high speed, an attack that leads to cavities with rounded contours. This degradation is caused by the combination of a mechanical effect and corrosion of the metal (Figure1.11). The natural oxide film is destroyed and the aluminium is attacked. There is a competition between tearing off the film and reforming it. It is not possible to estimate the individual contributions of the mechanical effect and corrosion [15].

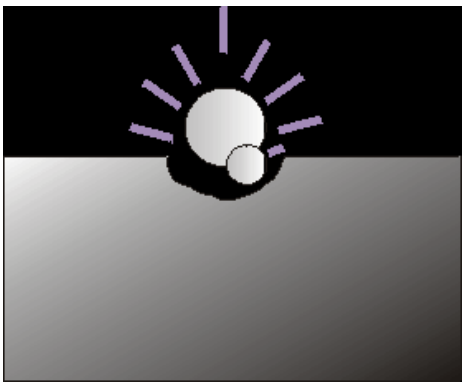

Figure 1.11 Cavitation [15]

Cavitation develops quickly: within a few days, and even within a few hours. Since this is partly a mechanical phenomenon, a high superficial hardness of the metal will favour resistance to cavitation. A direct relationship between hardness and resistance to cavitation has been found.

Aluminium is less resistant than other metals (cast iron, steel, etc.) and needs to be replaced by a harder metal such as cast iron if it is not possible to adapt the flow regime of the fluid. Cavitation is not a stable regime and can be avoided by increasing the diameter of the pipes that form the circuit, appropriate dimensioning of accessories such as pumps, and avoiding sudden changes in flow direction. Prevention of cavitation in aluminium equipment is based on the same problems and the same solution as for other metals.

1.8.10 Erosion

Corrosion by erosion occurs in moving media. This type of corrosion is related to the flow speed of the fluid. It leads to local thinning of the metal, which results in scratches, gullies, and undulations, which are always oriented in the same direction, namely the

flow direction as shown in figure 1.12. Experience with tubular heat exchangers in aluminium alloys of the series 3000, 5000 and 6000 used for desalination of seawater has shown that aluminium can withstand a flow speed in the order of 2.5-3 $m.s^{-1}$ at temperatures up to 130 °C with no erosion corrosion. This range corresponds to the usual flow speed in industrial installations [12]. Tests with distilled water at 100°C have shown that the erosion of aluminium starts at a flow speed in the order of 12-15 $m.s^{-1}$.

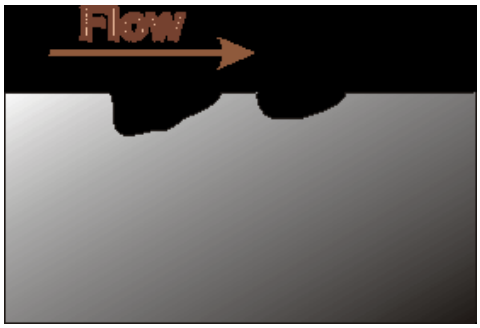

Figure 1.12 Erosion [12]

Avoiding erosion corrosion on aluminium does not require any specific precautions, only those commonly applied to other metals.

1.9 THE ELECTROCHEMICAL BASIS OF METAL CORROSION

Corrosion of metals is caused by the electrochemical reaction between a metal (or an alloy) and an aqueous phase. It proceeds according to a complex electrochemical process that is related to the atomic structure of matter. Matter is built up from elementary particles that carry electrical charges, namely ions and electrons, and from particles that are electrically neutral, namely atoms and molecules. In metals, the electrical environment of atoms is made up of free electrons capable of moving throughout the metal [19].

In the aqueous phase, which is a solution, the following species can be found:

- positive ions (cations) and negative ions (anions),
- Neutral molecules such as water and various undissociated compounds.

At the interface between metal and water, the transfer of electrical charges leads to electrochemical reactions (Figure 1.13):

- The metal atom is oxidised and forms M^{n+} ions that are released in the aqueous phase. This creates a flux of electrons within the metal in the direction from solution to metal. The resulting anodic oxidation current i_a flows from the metal to the solution.

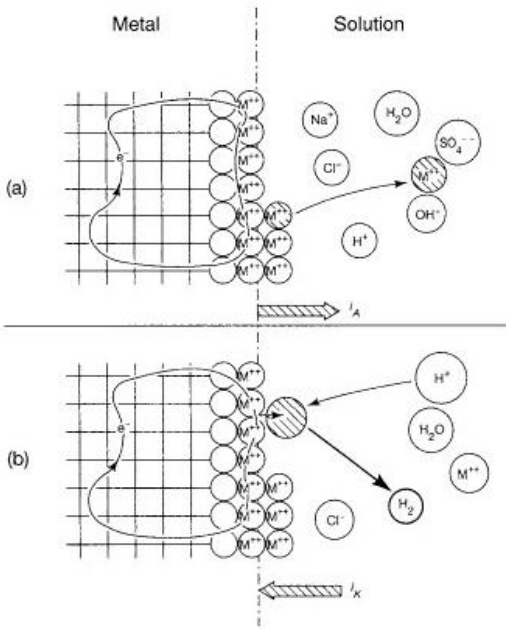

Figure 1.13 Electrochemical reactions at the metal-solution interface [19]

- The ions or molecules of the aqueous phase are reduced, which means that they take up electrons from the metal and get transformed into another chemical species. This creates a flux of electrons within the metal in the direction from metal to solution. The resulting cathodic current i_k flows from the solution to the metal.

1.10 ELEMENTORY ELECTROCHEMICAL REACTIONS OF CORROSION

The corrosion of a metal is the result of two simultaneous reactions that are in electrical equilibrium:

- the oxidation of the metal, resulting in a loss of electrons, according to the fundamental reaction

$$M \longrightarrow M^{n+} + n\,e^{-} \quad \text{.....1.10}$$

It results in an anodic current I_a that flows in the direction

$$\text{Metal} \longrightarrow \text{Solution} \quad \text{.....1.11}$$

- The reduction of an ion present in the aqueous solution according to the fundamental reaction

$$X^{n-} \longrightarrow X + ne^{--} \quad \text{.....1.12}$$

It results in a cathodic current i_k that flows in the direction

Solution ⟶ metal 1.13

- The reactions of oxidation and reduction proceed at distinct sites of the metal surface. The surface at which oxidation takes place is called the anode. It carries negative charges and is designated by the sign (-); the resulting current is called the anodic current. Reduction takes place on a surface called the cathode, designated by the sign (+); the reducing current is called the cathodic current.

  Except when connected to the electrodes of a generator, the metal is electrically neutral, which means that the electron and current fluxes are in equilibrium:

  $$\sum i_a = \sum i_k \quad \text{.....1.14}$$

  In a given system, all electrochemical reactions result in electrical currents that depend on the differences in potential between the two phases: metal and aqueous liquid. The kinetics of anodic and cathodic electrochemical reactions is represented by the relationship between the potential **e** and the reaction rate of the corresponding electrical intensity **I** (Figure 1.14).

  When an electrode is plunged into an aqueous solution, several anodic and cathodic reactions can take place simultaneously, and in principle they need not be related. However, because of the transfer of electrons, interactions between the anodic and cathodic reactions can occur [19].

Under the conditions of natural corrosion, i.e. without an external source of electrical current, the system formed by the metal and the aqueous solution constitutes an open electrical circuit. This means that the anodic current and the cathodic current, flowing in opposite directions, are necessarily equal (point C). This point, which forms the intersection between two polarisation curves, defines the corrosion potential e_{corr} and the intensity of corrosion I_{corr}.

By using Faraday's law

$$m = \frac{1}{96500}\frac{A}{n} It \quad \text{.....1.15}$$

Where

m is the mass,

A is the atomic mass of the metal (27 for Aluminium),

n is the valency (3 for Aluminium),

I is the intensity, in amperes, here I_{corr}

t is the time, in seconds,

The mass loss, i.e. the corrosion rate, can be calculated for a given intensity and a given time. However, this calculation makes sense only if the corrosion is uniform.

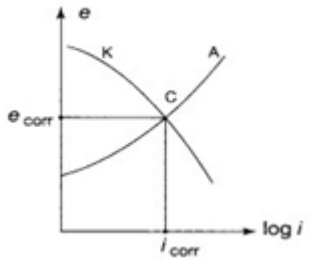

Figure 1.14 Relation between potential and current [19]

1.11 THE CORROSION BEHAVIOUR OF ALUMINIUM ALLOYS

Corrosion is a complex phenomenon that depends on many parameters that are related to the environment or to the metal. The occurrence of corrosion is sometimes difficult to explain because the cause of corrosion has not been identified, or because the theoretical foundations are sometimes insufficient to give a satisfactory answer.

No metal or alloy is capable of resisting all possible aqueous media, even at room temperature. The corrosion resistance of a metal or alloy depends on many factors that are inherent to the metal itself, the environment in which it is placed, and the conditions of use.

1.11.1 Factors related to the environment

The environment plays a very important role in the corrosion resistance of a metal or alloy, a fact that has been demonstrated time and again by experience. The following are the factors related to the environment:

(A) Nature of the environment

It is not easy to list a rigorous typology of environments with respect to corrosion phenomena observed on metals. Nonetheless, the following tendencies can be formulated:

- In aqueous, ionic media, the fundamental electrochemical reactions for corrosion of metals can take place;

- In nonaqueous, non-ionic, organic media, no oxidation and reduction phenomena can take place, and therefore a different behaviour can be expected. However, certain totally dehydrated organic products such as alcohols and phenols can react very violently with Aluminium at higher temperatures [19].

B) Concentration

Concentration is an important factor in the corrosion of metals. In general, the reaction rate increases with the concentration of the corrosive agents. However, there is not necessarily a proportional relationship between their concentration in air, water, etc and the corrosion rate.

C) Oxygen content

The rate and form of the corrosion of certain metals such as iron depend to a large extent on the oxygen content of the water. Oxygen is an oxidant and is corrosive in the sense that it depassivates the cathodes by starting up the cathodic reaction.

$$2H_20 + 0_2 + 4e^- \longrightarrow 4OH^- \quad \text{.....1.16}$$

This favours the oxidation reaction at the anode, i.e. corrosion

D) Temperature

It is well known that increasing temperature leads to an increase in the rate of chemical reactions. In the case of the corrosion of Aluminium, this applies to inorganic acids and bases and also to certain organic media such as alcohols, phenols and chlorinated derivatives, especially when the temperature approaches their boiling point. The corrosion resistance of Aluminium in water depends on the temperature.

1.11.2 Factors are related to the metal

Certain factors are related to the metal (or alloy) itself. Metallurgists try to adjust alloy compositions, transformation sequences and heat treatments in order to obtain the best possible corrosion resistance**.** Following are the factor related to the metal:

A) Alloy compositions

Since the beginning of the 20th century, many studies have tried to quantify the influence of most of the metallic and metalloid elements on the properties of Aluminium alloys,

and especially on their corrosion resistance. Contrary to a common misconception, the purity of the base metal does not improve the corrosion resistance of Aluminium.

B) Elaboration and transformation techniques

Several modes of elaboration are used for Aluminium alloys: casting, rolling, extrusion, etc. This is not an important factor. Experience shows that Aluminium casting alloys without copper generally have a better resistance to pitting corrosion than wrought alloys transformed by rolling or extrusion. This is probably due to the more resistant oxide layer of the as-cast surface compared to that of wrought semi-products

C) Heat treatments

Heat treatments of alloys lead to changes in the nature and the distribution of metallurgical constituents present in these alloys. They have an important influence on the susceptibility of these alloys to certain forms of corrosion, especially intercrystalline corrosion and stress corrosion. The temperature and duration of heat treatments also have a strong influence on the susceptibility to intercrystalline corrosion of these alloys.

D) Surface state

The surface state has an influence on the corrosion resistance of Aluminium. Experience has shown that scratched, scraped or ground surfaces are sites at which corrosion preferentially develops. This can be observed very frequently on ground and machined surfaces of welded structures of tanks, for example after hydraulic testing.

1.12 THE ELECTROCHEMICAL REACTIONS IN THE CORROSION OF ALUMINIUM

The fundamental reactions of the corrosion of Aluminium in aqueous medium have been the subject of many studies. In simplified terms, the oxidation of Aluminium in water proceeds according to the equation:

$$A1 \longrightarrow A1^{3+} + 3e- \quad .....1.17$$

Metallic Aluminium, in oxidation state 0, goes in solution as trivalent cation A^{3+} when losing three electrons. This reaction is balanced by a simultaneous reduction in ions present in the solution, which capture the released electrons.

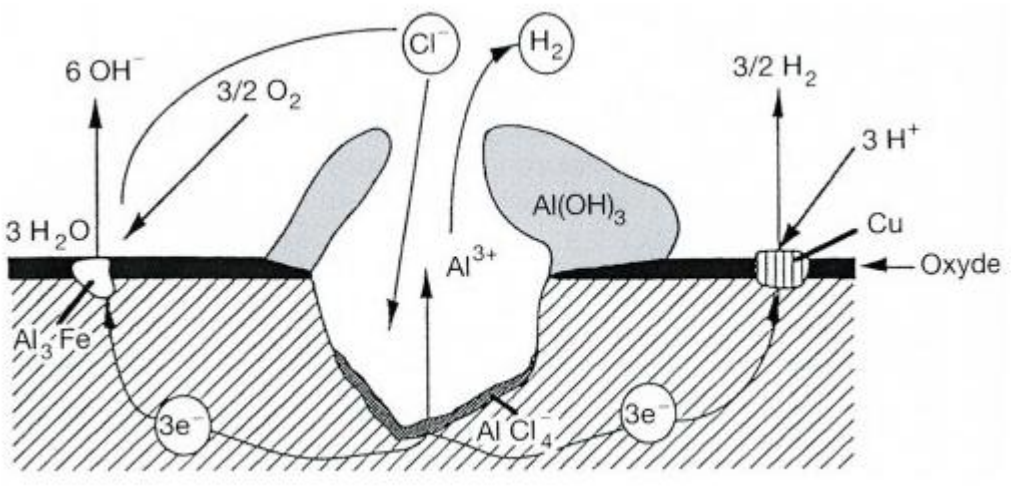

Figure 1.15 Mechanism of pitting corrosion of Aluminium [19]

In common aqueous media with a pH close to neutral such as fresh water, seawater, and moisture it can be shown by thermodynamic considerations that only two reduction reactions can occur:

- reduction of H^+ protons:

$$3H^+ + 3e^- \longrightarrow 3/2\ H_2 \quad \text{.....1.18}$$

H^+ protons result from the dissociation of water molecules:

$$H_2 0 \longrightarrow H^+ + OH^- \quad \text{.....1.19}$$

- reduction of oxygen dissolved in water:

- In alkaline or neutral media:

$$0_2 + 2H_2 0 + 4e^- \longrightarrow 4OH^- \quad \text{.....1.20}$$

- In acidic media:

$$0_2 + 2H^+ + 4e^- \longrightarrow 2H_20 \quad \text{.....1.21}$$

At 20°C and under atmospheric pressure, the solubility of oxygen in water is 43.4 $mg.kg^{-1}$. It decreases with increasing temperature and is no more than 30.8$mg.kg^{-1}$ at 40°C, and 13.8$mg.kg^{-1}$ at 80°C.

Globally, the corrosion of Aluminium in aqueous media is the sum of two electrochemical reactions, oxidation and reduction:

$$A1 \longrightarrow A1^{3+} + 3e-$$

$$3H^{+} + 3e^{-} \longrightarrow 3/2\ H_2$$

$$A1 + 3H^{+} \longrightarrow A1^{3+} + 3/2\ H_2 \quad \text{.....1.22}$$

Or

$$A1 + 3H_2\,0 \longrightarrow AI\,(OH)_3 + 3/2\ H_2 \quad \text{.....1.23}$$

This reaction is accompanied by a change in the oxidation state of Aluminium which, from the oxidation state 0 in the metal, is transformed into the oxidation state of alumina (+3), and by an exchange of electrons, since Aluminium loses three electrons that are picked up by $3H^{+}$.

Aluminium corrosion results in the formation of alumina $AI\,(OH)_3$, which is insoluble in water and precipitates as a white gel, which is found in corrosion pits as white gelatinous flakes [19].

1.13 CORROSION TESTING

Electrochemical techniques are the most widely used techniques for the study of corrosion in laboratories together with their application to real life structures. The reason for the frequent use of electrochemical techniques in practice is the increased number of Composites requiring an assessment of their residual health condition due to the premature deterioration caused by reinforcement corrosion. In addition it is necessary to evaluate the short-term performance of different components to know their early age behaviour by performing various corrosion tests at initial periods [20].

The commonly used techniques are

1. Electrochemical measurement,
2. Half cell Potential measurement,
3. Potentiodyanmic polarization measurement,

1.13.1 Electrochemcial Measurement

The corrosion medium is 3.5wt% NaCl neutral solution, prepared by analytical sodium chloride and distilled water. The test system is a 3-electrode system, the sample is the working electrode, and the reference electrode is a saturate calomel electrode and a platinum plate serves as the counter electrode. In this experiment the features of the

electrochemical noise and polarization curves are studied. The electrochemical measurements were performed using a potentiostat/frequency response analyzer (ACM instruments, UK) [20].

The sampling rate of the EN tests is 10 Hz and the potential noise is recorded. The potential noise recorded in this experiment is the fluctuation of the electrode potential between the working electrode and the reference electrode. Besides the EN measurements, the corrosion behaviour of the two materials are also studied by potentiodynamic polarization curves, the scan rate of the potentiodynamic tests is 1 mV/s. All the experiments are carried out at room temperature.

1.13.2 Half cell potential measurement

The detection of corrosion by using the method of potential measurement is one of the most common procedures for the routine inspection of reinforced composites. The half-cell potential is measure of electrode potential, represents the potential difference between the composite and the adjacent electrolyte. Thus in a given environment it may serve as an indicator of corrosion initiation since the threshold of depassivation depends mainly on the potential compared.

The half-cell potential value is measured with reference to a standard reference electrode. The various reference electrodes used for the potential measurement are standard hydrogen electrode (SHE), copper-copper sulphate electrode ($Cu/CuSO_4$), saturated calomel electrode (SCE), silver-silver chloride electrode (Ag/AgCl), and mercury-mercurous sulphate electrode (Hg/HgSO4). The technique is very well known and is described in ASTM C 876 [21].

The factors affecting potential measurements are reference electrode position, polarization phenomena induced by limited oxygen diffusion, presence of cracks, stray currents. Nonetheless, this technique is widely used as a first approach for corrosion detection. However quantification and reliable prediction of the corrosion rate requires the use of other electrochemical techniques.

Zuhair et al. [2002] [2]

In this paper the electrochemical behaviour of aluminium alloy 6061/Al_2O_3 metal matrix composite was investigated in 3.5% NaCl aqueous solution. Two composite compositions were examined containing 10% and 30% (by volume) of sub-micron alumina particulates as the reinforcement phase. The composites were fabricated via powder metallurgy processing. Cyclic polarization tests were carried out to determine pitting potentials and repassivation potentials in deaerated 3.5% NaCl solution. The pitting potential was 50 mV nobler for the higher-content reinforcement composite, while the repassivation potentials were essentially identical.

Excessive pitting of the matrix alloy was observed in both composites. Pits forming in the 6061/Al_2O_3 composite were more numerous and more uniformly dispersed compared to pits on the lower-content reinforcement composite which were deeper and more localized.

Vishal Sharma [2007] [4]

In the present investigation, Al-4.5wt%Cu/Zircon Sand/SiC hybrid composite has been synthesized by stir casting route by controlling various casting parameters. The as-cast samples were observed under optical and scanning electron microscope. Micro structural observations of the as-cast hybrid composite, shows uniform distribution of reinforcement particles and also good interfacial bonding between the particles and the matrix. Micro hardness tester is employed to evaluate the interfacial bonding between the particles and the matrix by indenting the micro hardness indenter on the particle with the varying load (100 gm, 200 gm, and 300 gm) and time (10 sec, 15 sec, 20 sec and 25 sec). It has been concluded that by the variation in hardness at constant load varying time or at constant time varying load, the bond strength can be compared.

Shailove Kumar [2010] [5]

Studied the age hardening behaviour of Aluminium alloy (6351) - 9%wt SiC composite produced by the stir casting technique. Water and Brine solution has been used as the quenching media. Thermal ageing has been done at different temperature, time and quenching media. Micro hardness and wear tests were performed on the samples

obtained from the stir casting process. The results of ageing demonstrate that the micro hardness of the composite depend on the quenching medium in which they are heat treated and peak hardness depends on quenching media and ageing time durations. X-ray Diffraction was performed to know the presence of the phases of reinforced material. Optical micrograph was taken to know the distribution of SiC particles in aluminium alloy.

Sanjeev Das et al. [2006] [7]

Zircon Sand particles of different size and amount have been incorporated in Al-4.5 wt% Cu alloy by stir casting route. Coarser particles of size between 90 and 135 μm can be dispersed in substantial amounts (up to 30 wt%), where as finer particles of size 15 and 65 μm have limited dispersion, 10 and 20 wt%, respectively. The matrix of the composites has cellular structure, where the size of the cell depends on Zircon Sand particle size and its amount in the composite. Segregation of copper rich phase ($CuAl_2$) has been found in the vicinity of the particle– matrix interface. The abrasive wear resistance of the composite improves with the increase in amount or decrease in size of Zircon Sand particles.

T.P.D. Rajan et al [2007] [9]

Investigated the effect of three different stir casting routes on the structure and properties of fine fly ash particles (13 μm average particle size) reinforced Al–7Si–0.35Mg alloy composite. Among liquid metal stir casting, compocasting (semi solid processing), modified compocasting and modified compocasting followed by squeeze casting routes evaluated, the latter has resulted in a well-dispersed and relatively agglomerate and porosity free fly ash particle dispersed composites. Interfacial reactions between the fly ash particle and the matrix leading to the formation of $MgAl_2O_4$ spinel and iron intermetallics are more in liquid metal stir cast composites than in compocast composites.

Nigamanada ray, Dilip kumar kerketta [2010] [10]

Investigated the method to produce a composite with cheap and simple production route i.e. stir casting method. They have chosen low grade iron ore as the reinforcement material and commercially pure aluminium as matrix phase. For the fabrication of in-situ composite wettability of the iron ore particles by liquid Al is essential. To improve wettability, Mg is added into Al melt. After fabrication; composites have been

characterized for their morphology, mechanical and wear properties to see their suitability as a wear resistance material. Wear test was performed as a function of sliding distance, applied load, sliding velocity with the help of Pin-On-Disc wear test machine. The worn surfaces were analyzed using scanning electron microscope. The mechanical properties such as hardness have been investigated.

Geetha Mable Pinto et al. [2009] [21]

Investigated the corrosion behaviour of SiC particulate reinforced in aluminium metal matrix composites. Silicon Carbide particulate - reinforced aluminium (SiCp-Al) composites possess a unique combination of high specific strength, high elastic modulus, good wear resistance and good thermal stability than the corresponding non-reinforced matrix alloy systems. These composites are potential structural material for aerospace and automotive applications. The corrosion characteristics of 6061 Al/SiCp composite and the base alloy were experimentally assessed.

A. Abdul Jameel et al. [2009] [22]

Studied the corrosion behaviour of Zircon Sand particulate reinforced aluminium 6061 metal matrix composites by weight loss corrosion studies and open circuit potential method. The composites were prepared by liquid melt metallurgy technique using vortex method. Specimens were designed according to ASTM standards. The corrodent used for the tests was natural seawater. Corrosion rates were calculated. In each case the corrosion rate and the potential decreases with increase in exposure time and become constant due to passivation induced by aluminium for matrix and metal matrix composites.

B. Bobic et al. [2010] [23]

Studied the corrosion behaviour of MMCs with aluminium alloy matrix. The corrosion characteristics of boron, graphite, silicon carbide, alumina and mica reinforced aluminium MMCs were reviewed. The reinforcing phase influence on MMCs corrosion rate as well as on various corrosion forms (galvanic, pitting, stress corrosion cracking, corrosion fatigue) was discussed. Some corrosion protection methods of aluminium based MMCs were described.

C. Monticelli et al. [1997] [24]

Investigated the corrosion behaviour and corrosion inhibition of AA 6061 and AA 2014 metal matrix composites (MMCs) reinforced with alumina particles, during exposures to

0.1_M NaCl solution is reported. Many tungsten and molybdenum-containing inorganic salts were tested as corrosion inhibitors. The techniques adopted included weight loss measurements, electron probe microanalysis (EPMA), scanning electron microscopy (SEM), linear polarization resistance measurements, polarization curve recordings and current noise analysis.

C. Chen and F. Mansfeld [1997] [25]

Investigated the corrosion resistance of an Al 6092/W, metal matrix composite (MMC) by recording of impedance spectra during immersion in 0.5 N NaCl for at least one week. Various methods of corrosion protection have been applied. These included surface modification in the Ce-MO process and anodizing in sulphuric acid. Anodized surfaces were sealed by immersion in hot water, cerium nitrate and two different dichromate solutions. Significant improvements of the corrosion resistance were only observed for the anodized surface with a dichromate seal.

Florian B. Manfeld et al. [1993] [26]

Studied the method for treating the surface of an aluminium-based material so as to make the surface resistant to corrosion includes the steps of contacting with an aqueous cerium non halide solution and then contacting the surface with an aqueous cerium halide solution. These steps may optionally be followed by a step of positively charging the metal surface while in contact with an aqueous molybdenum solution.

G. B. Veeresh Kumar et al. [2010] [27]

Presented the experimental results of the studies conducted regarding hardness, tensile strength and wear resistance properties of Al6061-SiC and Al7075-Al_2O_3 composites. The composites are prepared using the liquid metallurgy technique, in which 2-6 wt. Percentages of particulates were dispersed in the base matrix in steps of 2. The obtained cast composites of Al6061-SiC and Al7075-Al_2O_3 and the castings of the base alloys were carefully machined to prepare the test specimens for density, hardness, mechanical, and as well as for microstructural studies.

The SiC and Al_2O_3 resulted in improving the hardness and density of their respective composites. The microphotographs of the composites studied revealed the uniform distribution of the particles in the matrix system. The experimental density values were agreed with that of the theoretical density values of the composites obtained using the rule of mixture for composites.

Hosni Ezuber et al. [2008] [28]

Studied the aluimnium alloys AA5083 and AA1100 in seawater at 23 and 60 °C. Polarization plots showed that the alloys suffered from pitting attack. The breakdown potential of the two alloys decreased with an increase in test temperature with better corrosion resistance for alloy 1100. The weight loss tests revealed low corrosion rate values for both alloys, indicating a beneficial use for these alloys in marine environments. The pit morphology on the polarized aluminium alloys showed hemispherical isolated deeper pits on the 5083 alloy. Samples of the 1100 alloy revealed a higher number of shallow pits. The results showed that the type of intermetallic particles in the aluminium alloy played a major role in passivity breakdown and pit morphology in seawater.

H.J. Greene and F. Mansfeld [1997] [29]

Corrosion protection of aluminium metal-matrix composites (MMC) by anodizing treatments was investigated. Electrochemical behaviour of MMC without protection also was investigated. Electrochemical impedance spectroscopy (EIS) and potentiodynamic polarization measurements were used to characterize the properties of protective surface layers. Material studied was Al 6061/SiC. The MMC had similar corrosion (Ecorr) and pitting (Epit) potentials as the matrix alloy.

The cathodic current density for oxygen reduction in 0.5% N sodium chloride (NaCl) increased for Al 6061/SiC MMC with reinforcement concentration, which was attributed to electrochemically active interfaces between the matrix and the reinforcement particles. Anodizing and hot-water sealing were less effective for MMC than for the matrix aluminium alloys.

J. Bienia et al. [2003] [30]

Studied the microstructural characteristics of aluminium matrix AK12 composites containing of fly ash particles, obtained by gravity and squeeze casting techniques. Pitting corrosion behaviour and corrosion kinetics are presented and discussed. It was found that: (1) in comparison with gravity casting, squeeze casting technology is advantageous for obtaining higher structural homogeneity with minimum possible porosity levels, good interfacial bonding and quite a uniform distribution of reinforcement, (2) fly ash particles lead to an enhanced pitting corrosion of the AK12/9.0% fly ash (75-100μm fraction) composite in comparison with unreinforced

matrix (AK12 alloy), and (3) the presence of nobler second phase of fly ash particles, cast defects like pores, and higher silicon content formed as a result of reaction between aluminium and silica in AK12 alloy and aluminium fly ash composite determine the pitting corrosion behaviour and the properties of oxide film forming on the corroding surface.

J. Zhu, L.H. Hihara [2010] [31]

Studied the corrosion performance of a continuous alumina-fibre reinforced metal–matrix composite (MMC) and its monolithic matrix alloy (Al–2%Cu–T6) in 3.15 wt. % sodium chloride solution. Corrosion initiation sites, mapping of corrosion current density and pH at corrosion sites, mass loss resulting from immersion, and polarization behaviour were studied. Results show that the MMC exhibited inferior corrosion resistance as compared to its monolithic matrix alloy. Corrosion of the MMC initiated preferentially along the fibre/matrix interface or in regions of plastic deformation. The build-up of acidity at localized corrosion sites on the MMC was enhanced by the formation of micro-crevices caused by fibres left in relief as a result of corrosion.

L.A. Dobrza nski et al. [2005] [32]

Investigated the composite materials based on EN AW-2124 aluminium alloy reinforced with the Al_2O_3 particles with various weight ratios of 5, 10, and 15% are presented. The components were initially compacted at cold state in a die with the diameter of Ø26mm in the laboratory vertical unidirectional press with a capacity of 350 kN.

The obtained P/M compacts were heated to a temperature of 480–500 ◦C and finally extruded with the extrusion pressure of 500 kN. Bars with a diameter of 8mm were obtained as the end product. Based on the micro structural examinations of the obtained composite materials, the uniform distribution of the reinforcing particles in the aluminium matrix was revealed. Results of the corrosion tests, determined using the potentiodynamic method in the 3% water solution of NaCl indicate that corrosion of the investigated composite materials depends on the volume fraction of the reinforcing particles. It was found out, based on the determined anode polarisation curves that the investigated materials are susceptible to pitting corrosion.

Manoj Singla et al. [2009] [33]

Studied the modest attempt to develop aluminium based Silicon Carbide particulate MMCs with an objective to develop a conventional low cost method of producing

MMCs and to obtain homogenous dispersion of ceramic material. To achieve these objectives two step-mixing method of stir casting technique has been adopted and subsequent property analysis has been made. Aluminium (98.41% C.P) and SiC (320-grit) has been chosen as matrix and reinforcement material respectively. Experiments have been conducted by varying weight fraction of SiC (5%, 10%, 15%, 20%, 25%, and 30%), while keeping all other parameters constant. The results indicated that the 'developed method' is quite successful to obtain uniform dispersion of reinforcement in the matrix.

M. K. Surappa [2003] [34]

This paper presents an overview of AMC material systems on aspects relating to processing, microstructure, properties and applications. Aluminium matrix composites (AMCs) refer to the class of light weight high performance aluminium centric material systems. The reinforcement in AMCs could be in the form of continuous/discontinuous fibres, whisker or particulates, in volume fractions ranging from a few percent to 40%. Properties of AMCs can be tailored to the demands of different industrial applications by suitable combinations of matrix, reinforcement and processing route. Presently several grades of AMCs are manufactured by different routes.

Olivier et al. [2007] [35]

Studied the mechanical properties of high volume fraction SiC-particle reinforced Al-based metal matrix composites (MMCs) produced by means of pressurized liquid metal infiltration. It is distinguished between the effect of those alloying elements that only act on matrix strengthening, leaving the interface unaffected, and those alloying elements that interact with both (i.e. Mg).

Among the first category a further sub-division is made between pure solid solution and precipitation hardening elements (i.e. Zn and Cu, ZnMg, respectively). In particular, this study addresses the effect of alloying and age hardening for $AlCu_3$ and $AlZn_6Mg$ as well as the specific role of Mg additions to Al/SiC MMCs on interface microstructure formation, mechanical properties and fracture mode. For instance, it is shown that single additions of Mg catalyse the formation of Al_4C_3 whereas additions of Cu as well as (Zn + Mg) provide opportunities to enhance the composites' strength.

P.B. DA Silva-Mala et al. [1999] [36]

Investigated the corrosion resistance of 2014 aluminium matrix composites. The base alloy was manufactured through mechanical alloying, and reinforced with Ni_3Al (manufactured through atomisation). Composite materials were manufactured according to the following procedure: mixing, cold uniaxial compacting, and hot extrusion. All materials were tested as extruded and heat treated. The influence that the intermetallic and heat treatment have on the corrosion resistance of 2014 aluminium alloy has been studied. Results show that atomised Ni_3Al improves the intergranular corrosion resistance of base aluminium by a mechanism of cathodic protection. Heat treatment is also favourable.

S. Balasivanandha et al. [2006] [37]

Studied that the high silicon content aluminium alloy–Silicon Carbide metal matrix composite material, with 10% SiC were successfully synthesized, using different stirring speeds and stirring times. The microstructure of the produced composites was examined by optical microscope and scanning electron microscope. The Brinell hardness test was performed on the composite specimens from base of the cast to top. The results revealed that stirring speed and stirring time influenced the microstructure and the hardness of composite. Microstructure analysis revealed that at lower stirring speed with lower stirring time, the particle clustering was more.

Increase in stirring speed and stirring time resulted in better distribution of particles. The hardness test results also revealed that stirring speed and stirring time have their effect on the hardness of the composite. The uniform hardness values were achieved at 600 rpm with 10 min stirring. But beyond certain stir speed the properties degraded again. An attempt is made in this study to establish the trend between processing parameters such as stirring speed and stirring time with microstructure and hardness of composite

Sanjeev Kumar [2010] [38]

Investigated the Effects of Thermal Cycling on Cast Aluminium Composites Reinforced With Silicon Carbide And Fly Ash Particles. During this investigation, dry fly ash was used with Aluminium reinforced with SiC and a composite was prepared using Liquid metal stir casting route with the reducing quantity of SiC. During the research, Thermal cycling was carried out on the samples prepared and effects on samples before and after thermal cycling were observed.

S. L. Coleman et al. [1994] [39]

Investigated the corrosion characteristics, in 3.5 wt% NaCI solution, of aluminium alloy composites containing a range of reinforcements using potentiostatic measurements and simple immersion tests. Complementary microstructural studies carried out on corroded surfaces and sections through corroded material have identified a number of preferential corrosion sites; these include the fiber/matrix interface, especially where it contains chemical reaction products resulting from composite fabrication, as well as second phases and pores in the metal matrix. The effect on corrosion behaviour of the different reinforcements, with particular reference to their chemistry and geometry, is discussed, as is the influence of composite manufacturing route.

2.1 SUMMARY AND GAP IN LITERATURE REVIEW

A lot of work has been done in aluminium matrix composite at different types of reinforcements, different sizes and manufactured either by stir casting or by sintering technique then subjected to the corrosion test. Alloy composition and its condition influence the corrosion behaviour and corrosion rate. With increase in weight Percentage of SiC the potential and corrosion current density of composite decrease. The corrosion resistance of base matrix is more than that of composites. But wear resistance and hardness will increase with increase in weight Percentage of reinforcement.

In case of the hybrid composites the corrosion resistance do not depend on type of reinforcement, but corrosion potential and corrosion rate decreases with increasing the weight percentage of reinforcing materials. The corrosion rate of Al-based hybrid composites will be controlled by the protective coating provided on surface of composite. In case of SiC/Zircon Sand reinforced aluminium alloy cast samples the addition of increasing amounts of particulate SiC and Zircon Sand increases the hardness and wear resistance and decreases the ductility.

The ductility level of the cast composite is found to be lower than those of the based alloy. Lot of work need to be carried out on aluminium matrix composite with varying weight percentage reinforcement such as SiC, Zircon Sand and SiC & Zircon Sand as hybrid composite to find out the different mechanical property and corrosion behaviour. Corrosion behaviour, microstructure and hardness of SiC & Zircon Sand as hybrid composite need to be studied.

CHAPTER 3 PROBLEM FORMULATION

3.1 PROPOSED WORK

The problem is to study the corrosion behaviour Al-SiC/Zircon Sand metal matrix composite (MMC) of aluminium alloy of grade 6063 with addition of varying percentage composition of SiC particles and Zircon Sand made by stir casting technique. The corrosion behaviour, corrosion rate and the change in physical and mechanical properties will also be taken into consideration.

For the achievement of the above, an experimental set up is prepared where all the necessary inputs were made. The aim of the experiment is to study the effect of variation of the percentage composition to predict the rate of corrosion and corrosion behaviour and effect of corrosion on physical and mechanical properties of the metal matrix composites (MMC). The experiment was carried out by preparing the sample of different percentage composition by stir casting technique and then subjected to the corrosive medium and predicting the change in properties of metal matrix composites. Once again different tests are performed on specimens after subjecting to corrosive medium to find change in properties of material.

3.1.1 Objectives

1. To study the effect of percentage composition on corrosion behaviour, micro hardness and micro structure of metal matrix composites.

2. Analyze for microstructure to study the change in material properties as a result of the experimentation.

The tests performed on the samples are as below:

1. Micro Hardness Test, Optical micrograph
2. The Microstructure (SEM),
3. X-Ray Diffraction Test
4. Corrosion Test on ACM corrosion analyzer
5. Half cell potential measurement
6. Potentiodyanmic polarization measurement
7. Corrosion rate and corrosion current density measurement.

3.2 WORK PLAN

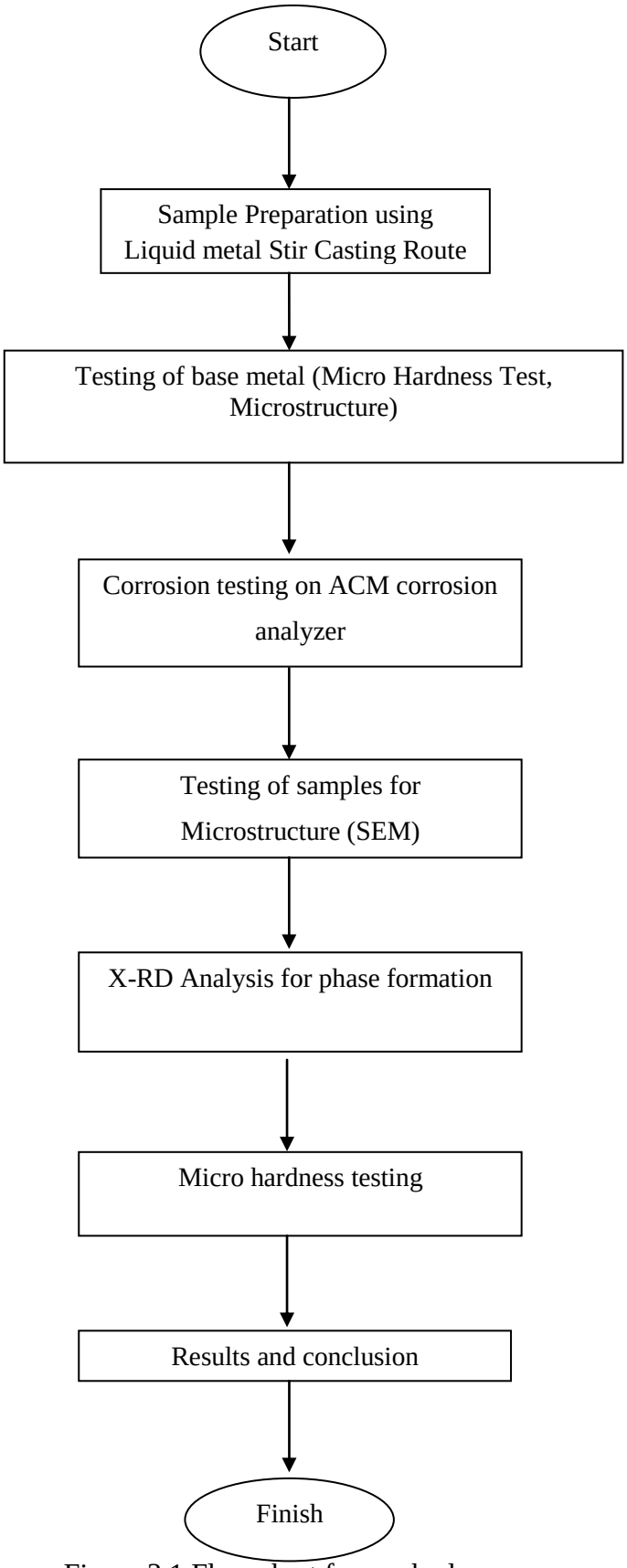

Figure 3.1 Flow chart for work plan

3.3 STEPS INVOLVED IN STIR CASTING

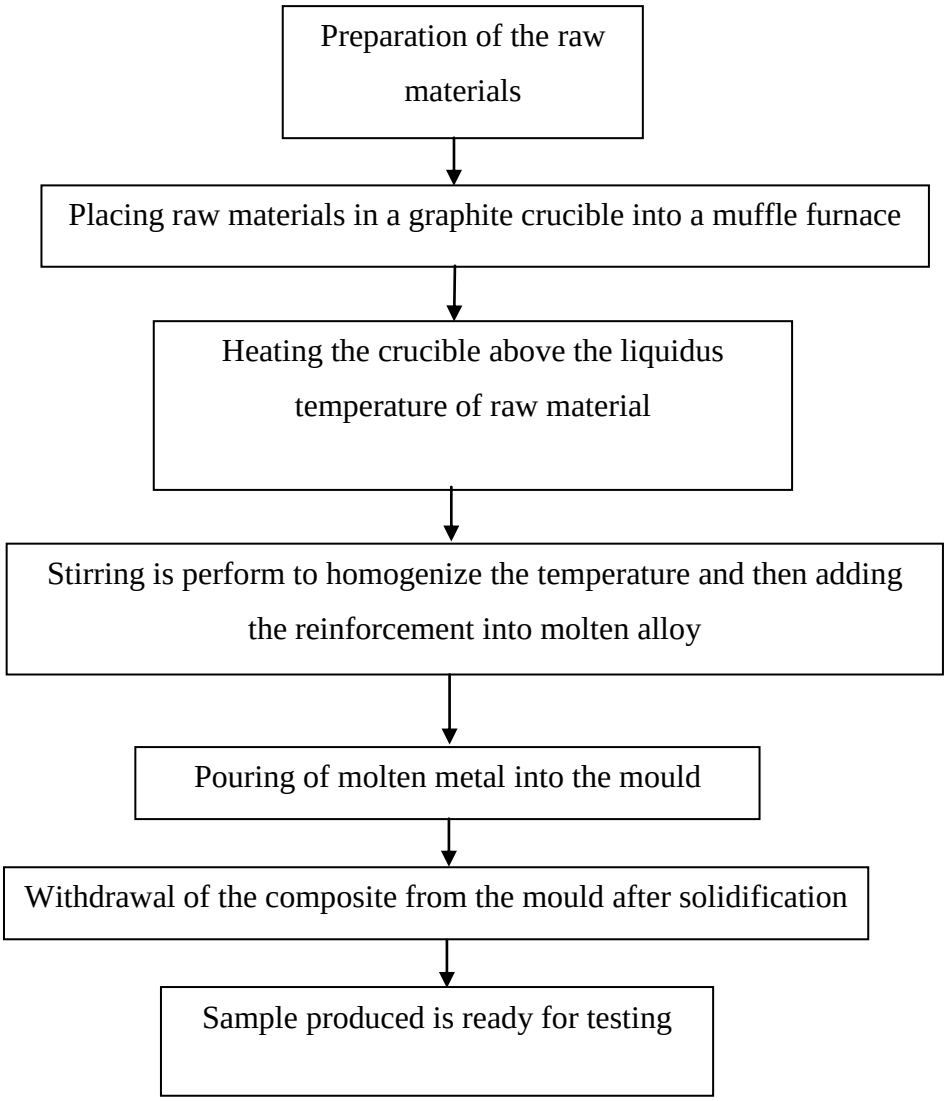

Figure 3.2 Flow Chart Showing Steps in Involved in Stir Casting

CHAPTER 4 EXPERIMENTAL WORK

4.1 EXPERIMENTAL SETUP FOR STIR CASTING

For performing the stir casting operation and testing of composites the following machines/equipments were used:

1. Sieve Analysis Tester
2. Reinforcement (SiC and Zircon Sand)
3. Matrix (Al alloy 6063)
4. Muffle Furnace
5. Radial Drilling Machine
6. Graphite Crucible/ mould
7. Graphite Stirrer
8. Stainless steel rod (SS3l6) of diameter 12mm, Length 600mm
9. ACM Corrosion analyzer
10. Micro hardness testing machine
11. Scanning electron microscope
12. Power Hacksaw

4.2 SYNTHESIS OF AL6063/SiC/ZIRCON SAND COMPOSITE

4.2.1 Details of raw materials

A brief description of the raw materials used in the synthesis of composite is presented as follows:

a) Matrix alloy

Aluminium alloy 6063 is used as matrix in the synthesis of composite. Aluminium alloy was cut from its ingot size into smaller pieces by an electric power saw in order to feed the crucible properly. Composition of matrix alloy was analyzed and the chemical composition of the matrix alloy is given in table 4.1.

Table 4.1 - Composition of 6063 aluminium alloy

Element	Si	Fe	Cu	Mn	Mg	Cr	Zn	Ti	Al
Wt%	0.42	0.35	0.1	0.1	0.74	0.1	0.10	0.1	rest

b) Reinforcement material

Zircon Sand and Silicon Carbide was used as reinforcement material. Particle size of Zircon Sand silicate was in the range between 100-200 µm and for Silicon Carbide it was 75–150 µm. The received reinforcement particles were sieved and required particle size were selected as given in the table 4.2

Table 4.2 - Particle size range of Zircon Sand and Silicon Carbide

Reinforcement	Particle size range (µm)
Silicon Carbide	100-120
Zircon Sand	125-150

c) Corrosive media

To predict the corrosion rate and corrosion behaviour of samples produced by stir casting, samples are immersed in corrosive media such as 3.5% NaCl aqueous solution.

4.3 COMPOSITES PREPARATION BY STIR CASTING

A stir casting setup (Figure. 4.1), which consisted of a resistance furnace and a stirrer assembly, was used to synthesize the composite. The stirrer assembly consisted of a graphite turbine stirrer, which was connected to a variable speed vertical drilling machine (speed 0 to 890 rpm) by means of a steel shaft. The stirrer was made by cutting and shaping a graphite block to desired shape and size manually. The stirrer consisted of three blades at angles of 120° apart. Figure 4.2 show the photograph of the stirrer from two different angles. Clay graphite crucible of 1.5 Kg capacity was placed inside the furnace.

The stirrer assembly consisted of a graphite turbine stirrer fixed to a steel rod. Approximately 1Kg of alloy was then melted at 820°C in the resistance furnace of stir casting setup. Preheating of Zircon Sand and Silicon Carbide mixture at 800°C was done for one hour to remove moisture and gases from the surface of the particulates. The stirrer was then lowered vertically up to 3 cm from the bottom of the crucible (total height of the melt was 9 cm). The speed of the stirrer was gradually raised to 800 rpm and the preheated Zircon Sand and Silicon Carbide particle was added with a spoon at the rate of 10- 20g/min into the melt.

The speed controller maintained a constant speed, as the stirrer speed got reduced by 50-60 rpm due to the increase in viscosity of the melt when particulates were added into the

melt. After the addition of Zircon Sand and Silicon Carbide particle, stirring was continued for 10 minutes for better distribution. The melt was kept in the crucible for one minute in static condition and it was then poured in the metal moulds.

4.3.1 Experimental Procedure

Following procedure was followed after the casting preparation

1. Specimens, prismatic in shape with dimensions 10 mm x 10 mm and 10 mm for SEM, XRD, Micro hardness and with dimensions 30 mm x 15mm x 5 mm (L x b x t) respectively were cut from the cast composite.
2. Micro hardness of specimen was measured on Vicker's Micro hardness testing machine.
3. The SEM and XRD analysis was done for the samples.
4. Each specimen of 1 cm^2 area was subjected to a corrosive medium (3.5% NaCl aqueous solution).
5. Potential measurement, Potentiodyanmic polarization measurement, electrochemical impedance measurement of specimens was carried out on ACM field machine as shown in Figure. 4.9
6. Analyzing the Microstructure of the specimens by optical microscope and by SEM before the corrosion and after the corrosion.
13. The data related to corrosion test was recorded for each specimen before and after corrosion testing.

Table 4.3 - Composition of Samples

Composition				
Samle No.	Aluminium(gm)	SiC(gm)	Zircon Sand(gm)	Remarks
1	1000	0	0	Weight of sample=1000 gm
2	975	25	0	SiC=2.5%
3	950	50	0	SiC=5%
4	925	75	0	SiC=7.5%
5	900	100	0	SiC=10%
6	975	0	25	Zircon Sand=2.5%
7	950	0	50	Zircon Sand=5%
8	925	0	75	Zircon Sand=7.5%
9	900	0	100	Zircon Sand=10%
10	950	25	25	SiC=2.5%+ Zircon Sand=2.5%
11	900	50	50	SiC=5%+ Zircon Sand=5%
12	850	75	75	SiC=7.5%+ Zircon Sand=7.5%
13	800	100	100	SiC=10%+Zircon Sand=10%

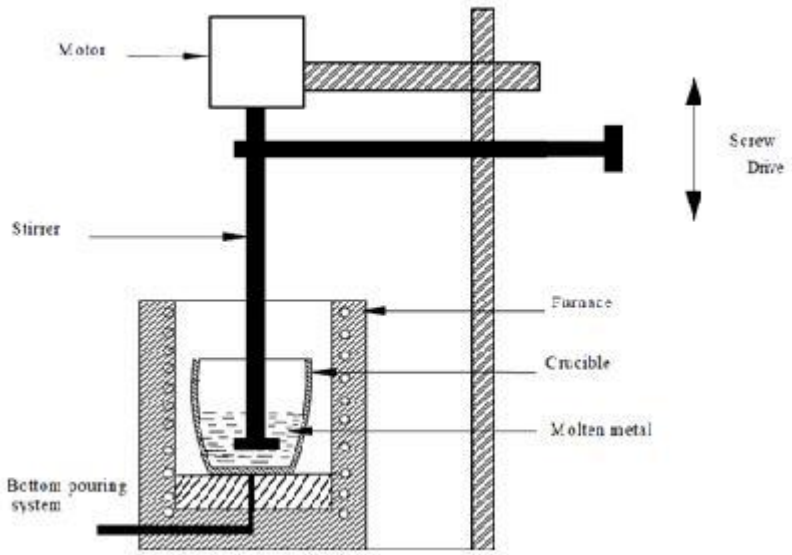

Figure 4.1 MMC preparations by Stir casting route [38]

Figure 4.2 Graphite stirrer

Figure 4.3 Muffle Furnace

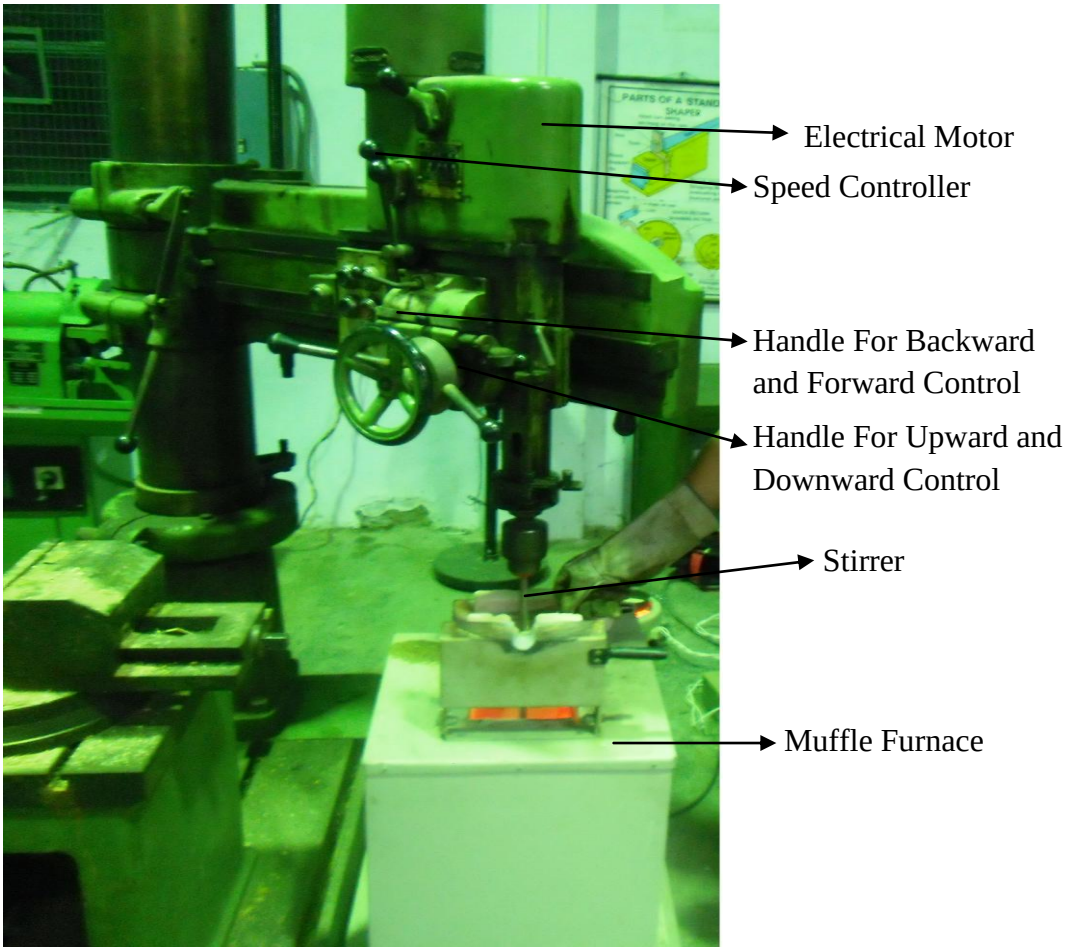

Figure 4.4 Arrangement of muffle furnace with verticle drilling machine

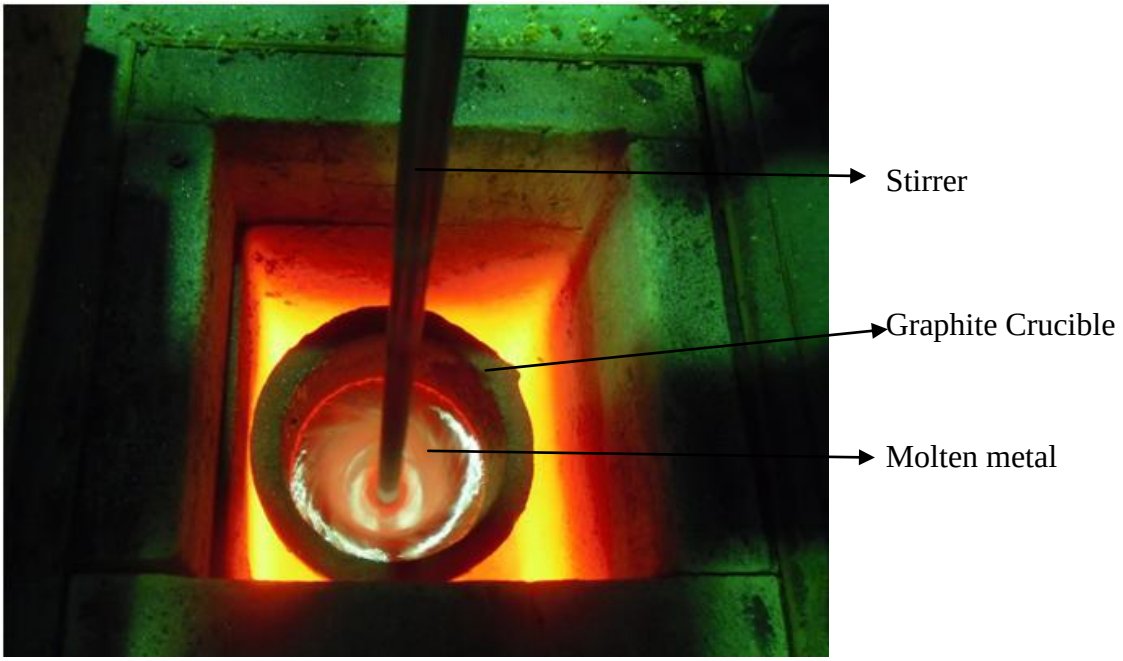

Figure 4.5 Preparation of Samples in Electrical Resistance furnace

The temperature of the furnace was gradually lowered until the melt reached a temperature in the liquid solid range while stirring was continued. Then the stirrer was positioned just below the surface of the slurry and the oxidized particles were added uniformly at a rate of 20 g/min over a time period of approximately 3–5 min. At the end of charging the slurry was allowed to mix in the semisolid state isothermally for another 15 min while the stirrer was positioned near the bottom of the crucible.

Figure 4.6 Crucible

Figure 4.7 Mould and cast product after casting

4.3.2 Important Parameters

Synthesis of composite is done by stir casting route. The parameters which are important in this work are stirrer design, preheating temperature for particulate and stirring speed. These parameters are discussed below.

A) Stirrer design

It is very important parameter for stir casting process. It is essentially requires for vortex formation for the uniformly dispersion of particles. There is different type of stirrer some 90º form the shaft and some are bent at 45º. There is a no uniform dispersion of particles in case of no vortex formation [38].

B) Particle preheating temperature

Preheating of particulate is necessary to avoid moisture from the particulate otherwise there is chance of agglomeration of particulate due moisture and gases. Along this Zircon Sand and SiC particles are heated at 800ºC to form a oxide layer on the Zircon Sand and SiC particles which make it chemically more stable and by the oxide layer formation wettability will increase so particles will effectively embedded in aluminium matrix and less number of porosities in casting.

C) Stirring speed

In stir casting process stirring speed is very important parameter for consideration. In this process stirring speed was 800 rpm which was effectively producing vortex without any spattering. Stirring speed is decided by fluidity of metal if metal having more fluidity then stirring speed will be low. It is also found that at less speed, dispersion of particulates is not proper because of ineffective vortex [38].

4.4 CORROSION TESTING

The electrodes used for corrosion studies were cut from the cast product having dimensions 30 mm x 15mm x 5 mm (L x b x t). They were polished using 100grit Silicon Carbide paper followed by 220, 400, 600 and 1000 grades of emery paper, degreased with acetone and rinsed with deionised water. The electrochemical measurements were performed using a potentiostat/frequency response analyzer (ACM instruments, UK) and a flat cell. A 3.5% NaCl solution was used as the electrolyte. Only 1 cm^2 of the sample was exposed to the electrolyte solution.

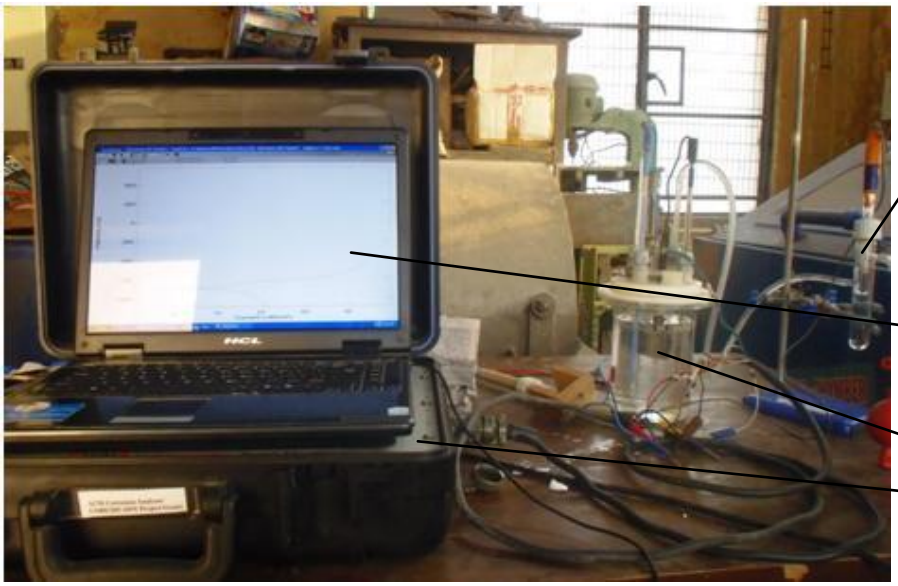

Figure 4.8 Experimental arrangements for electrochemical measurement

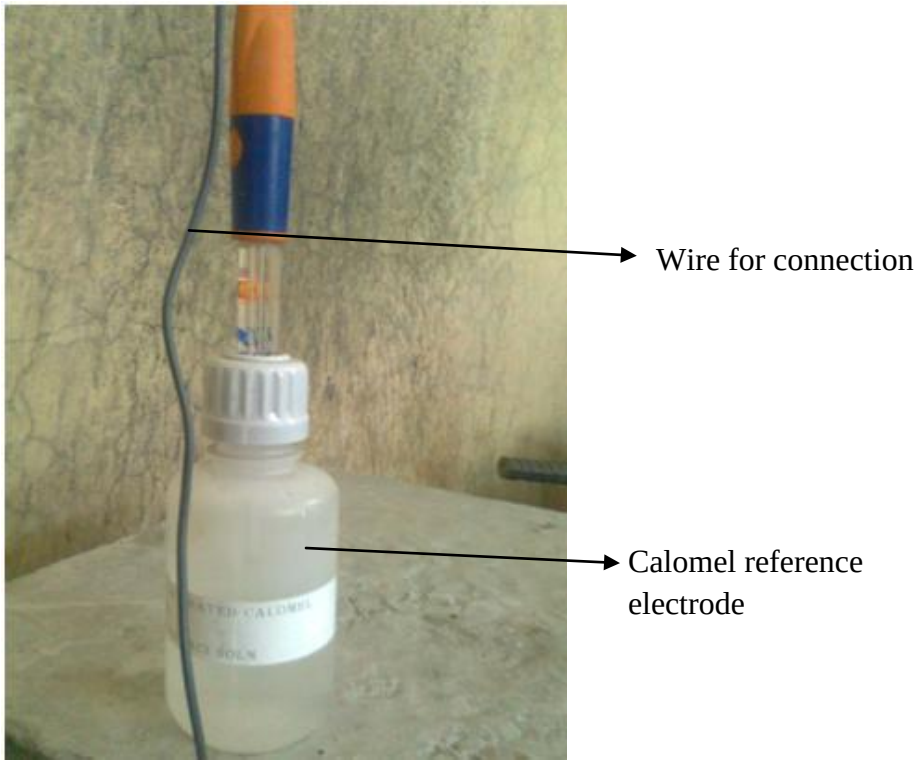

Figure 4.9 Saturated calomel electrode (SCE) served reference electrodes

A graphite rod and saturated calomel electrode (SCE) served as the counter and reference electrodes respectively. All experiments were performed at room temperature. Potentiodynamic polarization measurements were made at a potential scan rate of 60mV/min. The corrosion potential (Ecorr) and corrosion current density (icorr) were determined using the ACM field machine.

CHAPTER 5 RESULTS AND DISCUSSION

5.1 MICROSTRUCTURE OF ALUMINIUM ALLOY AND COMPOSITES BEFORE CORROSION

The casting procedure was examined under the optical microscope to determine the cast structure. For the sample preparation, first of all sample were cut down into small cuboids shapes then the sample grinded on different grit size paper sequentially by 100, 220, 320, 400, 600 and 1000. After grinding, the samples were polished by alumina paste and etched with Keller's solution. The samples were visualized on different magnifications. It is observed that there is a strong interfacial bonding between particles. Zircon Sand and Silicon Carbide particles are uniformly distributed throughout the matrix as shown in optical micrography.

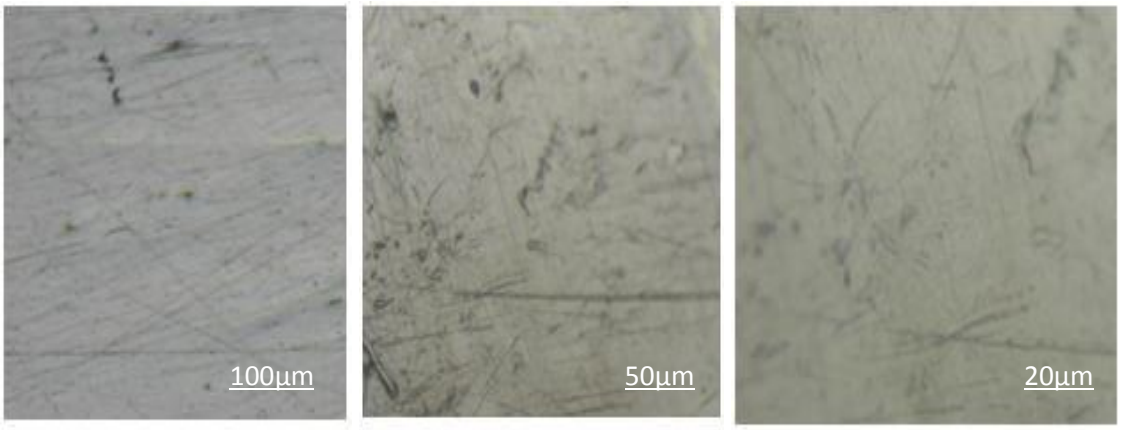

(a) (b) (c)

Figure 5.1 Optical micrographs of Base Alloy (a) 100X, (b) 200X, (c) 500X

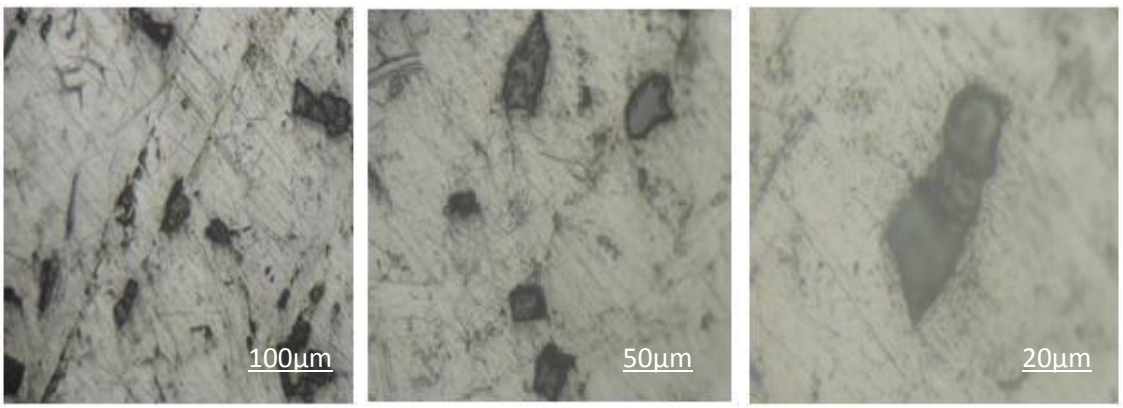

(a) (b) (c)

Figure 5.2 Optical micrographs of 2.5% SiC (a) 100X, (b) 200X, (c) 500X

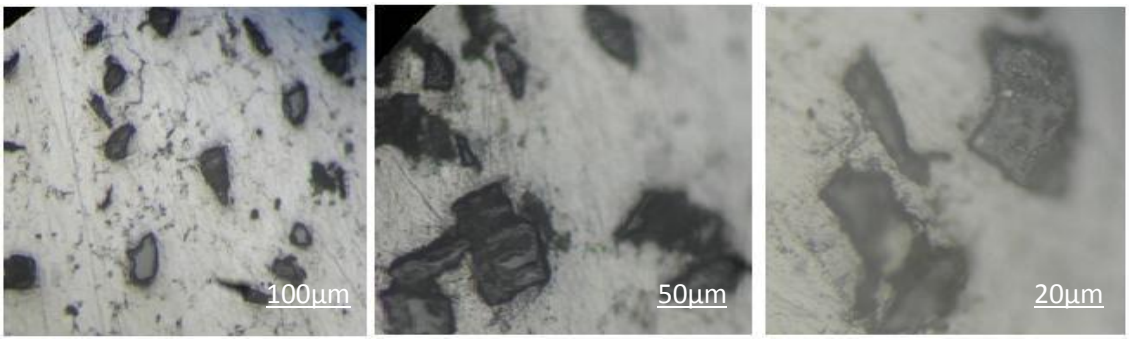

(a) (b) (c)

Figure 5.3 Optical micrographs of 5% SiC (a) 100X, (b) 200X, (c) 500X

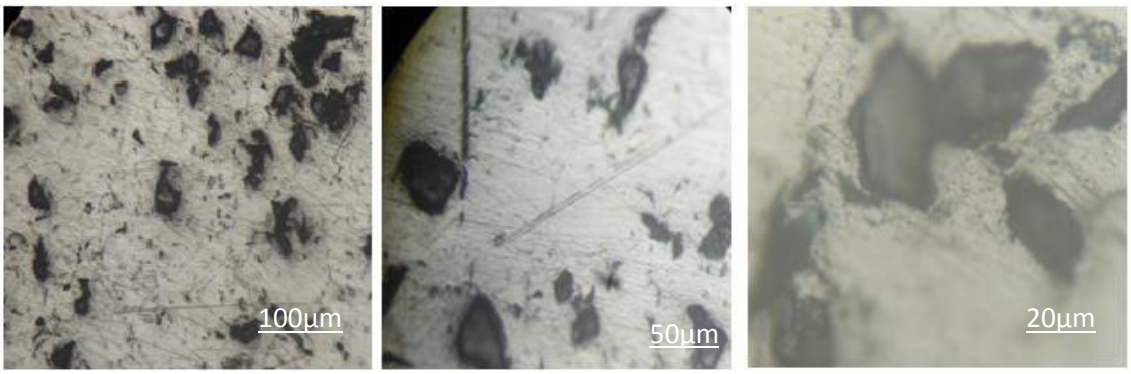

(a) (b) (c)

Figure 5.4 Optical micrographs of 7.5% SiC (a) 100X, (b) 200X, (c) 500X

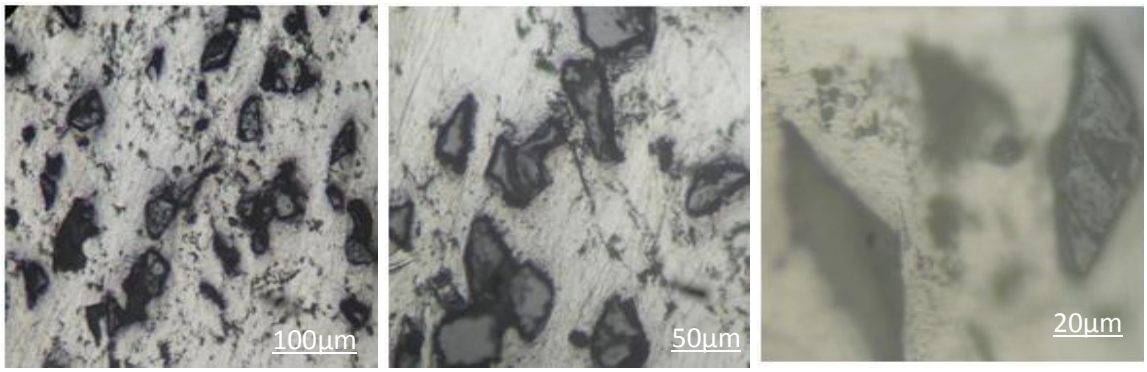

(a) (b) (c)

Figure 5.5 Optical micrographs of 10% SiC (a) 100X, (b) 200X, (c) 500X

It is clear from the figure 5.2-5.5 that the reinforcement in the aluminium alloy matrix is uniformly distributed. The average size of SiC particles is around 100µm-120µm.The shape of most SiC particles is angular and sub-angular. It is found that as the percentage of reinforcement increase the area fraction is also increases as shown in figure 5.2-5.5 in optical micrograph. It also observes that there is increase in hardness and corrosion

resistance this can be attributed to the increase in bonding of reinforcement with the aluminium matrix alloy.

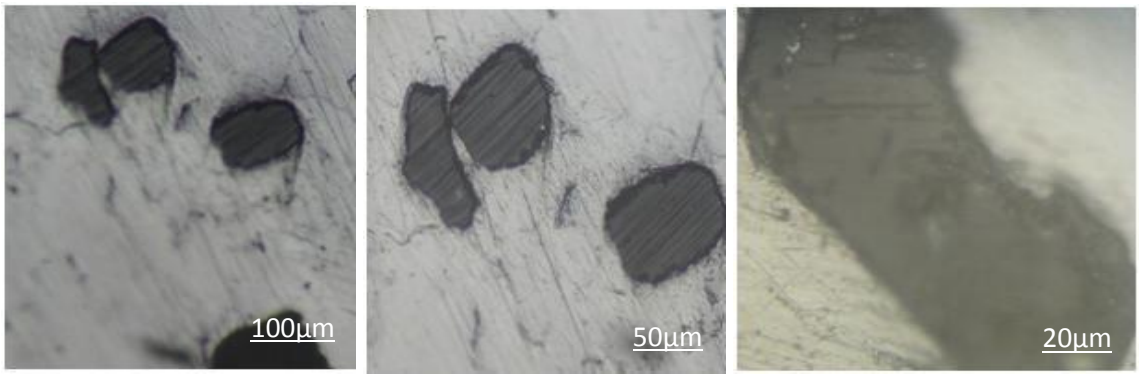

(a) (b) (c)

Figure 5.6 Optical micrographs of 2.5% Zircon Sand (a) 100X, (b) 200X, (c) 500X

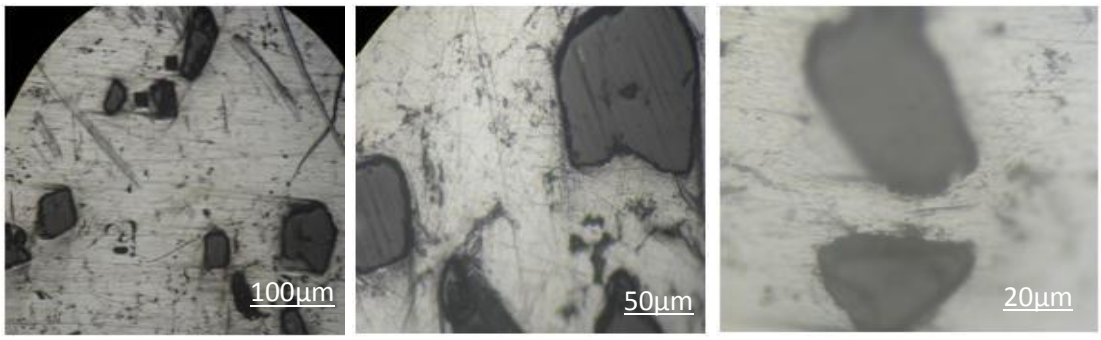

(a) (b) (c)

Figure 5.7 Optical micrographs of 5% Zircon Sand (a) 100X, (b) 200X, (c) 500X

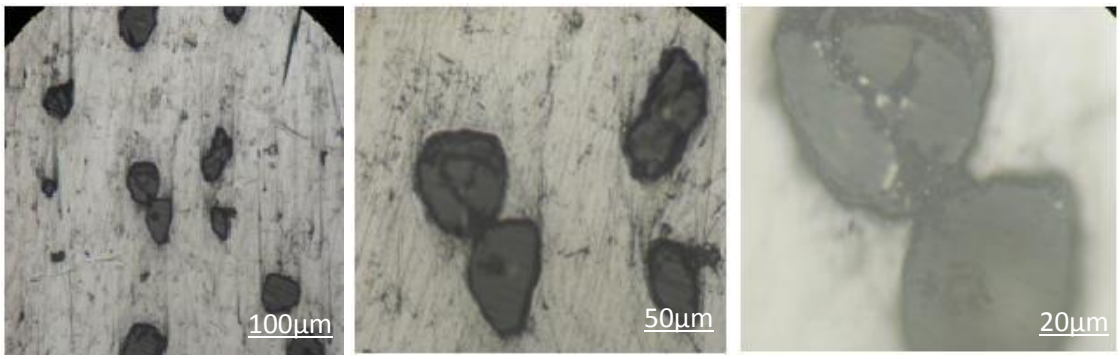

(a) (b) (c)

Figure 5.8 Optical micrographs of 7.5% Zircon Sand (a) 100X, (b) 200X, (c) 500X

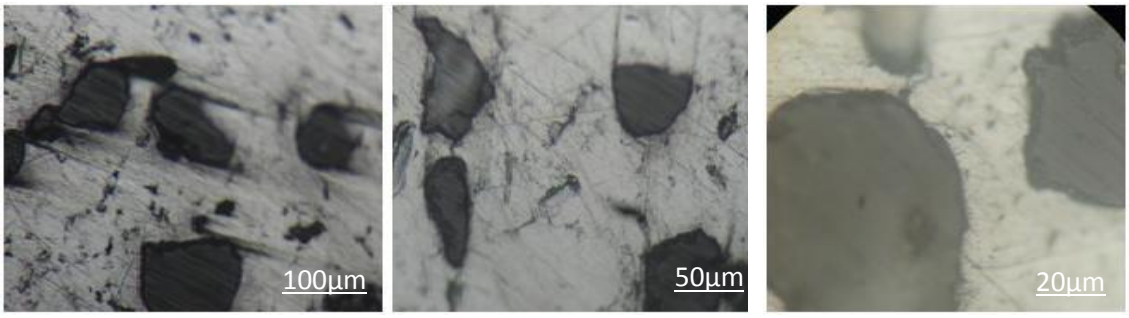

(a) (b) (c)

Figure 5.9 Optical micrographs of 10% Zircon Sand (a) 100X, (b) 200X, (c) 500X

It is clear from the figure 5.6-5.9 that the reinforcement in the aluminium alloy matrix is uniformly distributed. The average size of Zircon Sand particles is around 125µm-150µm.The shape of most Zircon Sand particles is mainly circular. It is found that as the percentage of reinforcement increase the area fraction is also increases as shown in figure 5.6-5.9 in optical micrograph. It also observes that there is increase in hardness and corrosion resistance this can be attributed to the increase in bonding of reinforcement with the aluminium matrix alloy.

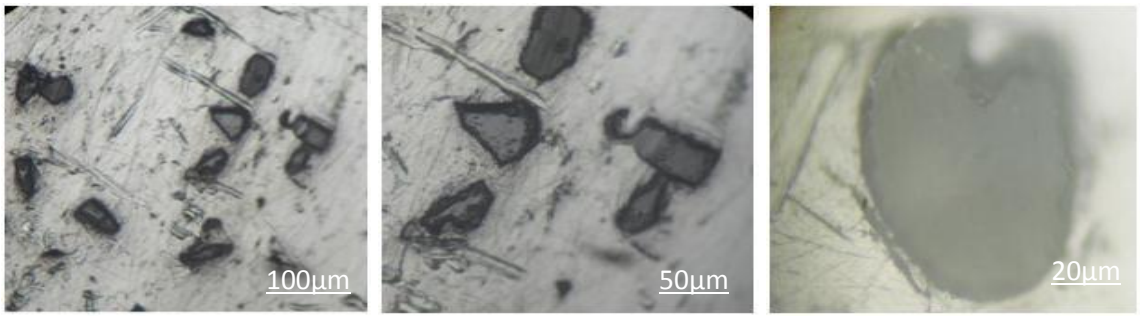

(a) (b) (c)

Figure 5.10 Optical micrographs of 5% Zircon Sand and SiC (a) 100X, (b) 200X, (c) 500X

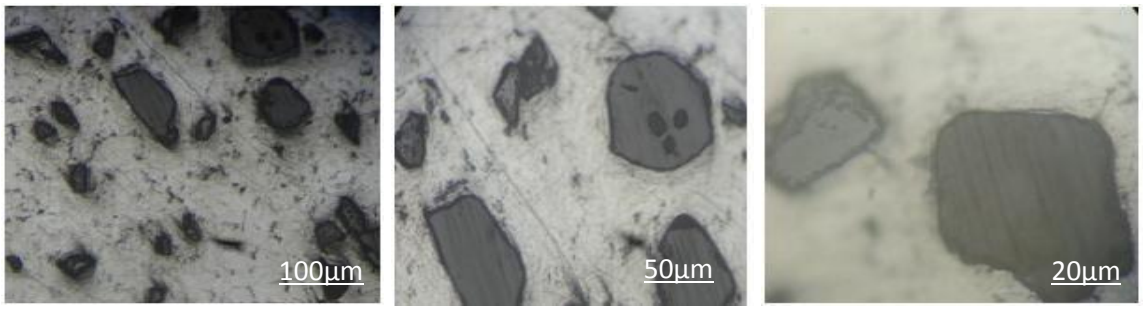

(a) (b) (c)

Figure 5.11 Optical micrographs of 10% Zircon Sand and SiC (a) 100X, (b) 200X, (c) 500X

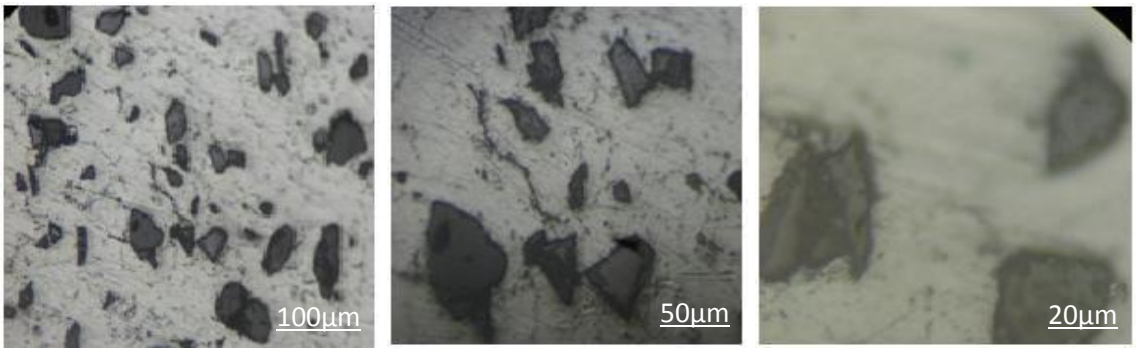

(a) (b) (c)

Figure 5.12 Optical micrographs of 15% Zircon Sand and SiC (a) 100X, (b) 200X, (c) 500X

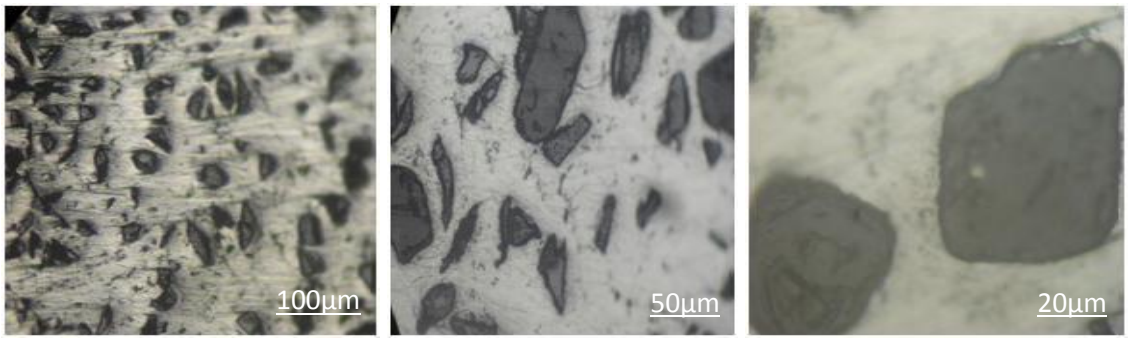

(a) (b) (c)

Figure 5.13 Optical micrographs of 20% Zircon Sand and SiC (a) 100X, (b) 200X, (c) 500X

It is clear from the figure 5.10-5.13 that the Silicon Carbide and Zircon Sand reinforcement in the aluminium alloy matrix is uniformly distributed. The shape of most Zircon Sand particles is mainly circular and the shape of SiC particle is angular and sub-angular. It is found that as the percentage of reinforcement increase the area fraction and hardness is also increases as shown in optical micrograph.

5.2 SCANNING ELECTRON MICROSCOPY BEFORE CORROSION

Figures 5.14-5.19 shows the scanning electron micrographs of the hybrid composite. It is observed that the particles are uniformly distributed throughout the matrix for the cast hybrid composite. Agglomeration of particles in some regions is clearly visible; this is due to the presence of porosity associated to it. Presence of entrapped air and moisture in the reinforcement particles results in the porosity after casting.

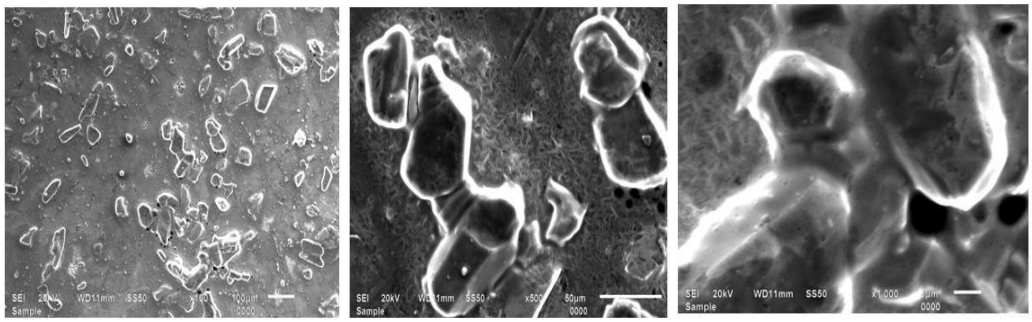

(a) (b) (c)

Figure 5.14 SEM of composite with 7.5% SiC at (a) 100X, (b) 500X, and (c) 1000X

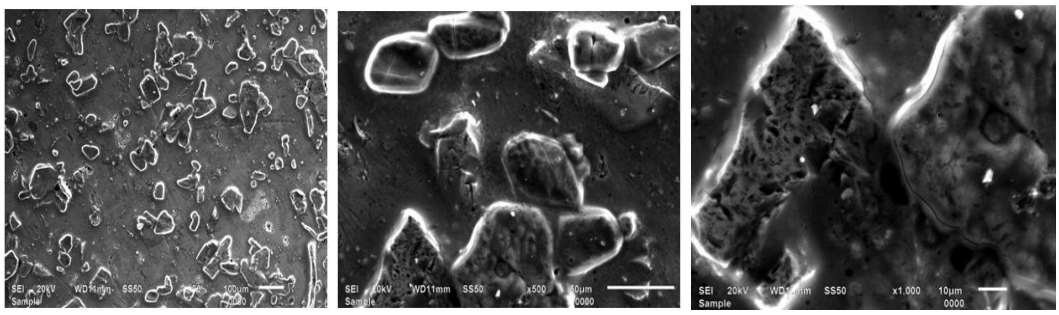

(a) (b) (c)

Figure 5.15 SEM of composite with 10% SiC at (a) 100X, (b) 500X, and (c) 1000X

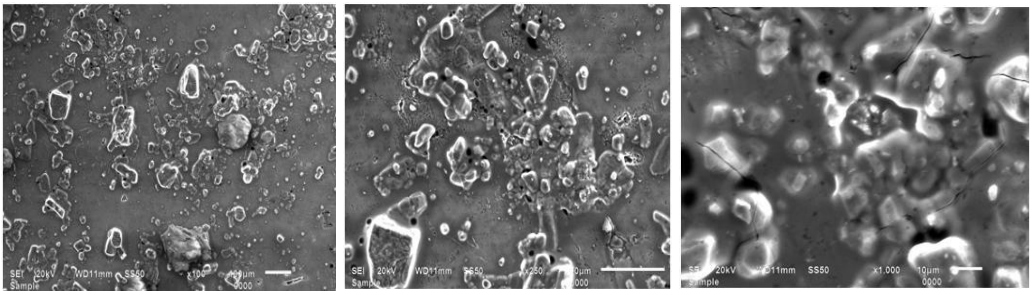

(a) (b) (c)

Figure 5.16 SEM of composite with 7.5% Zircon Sand at (a) 100X, (b) 250X, and (c) 1000X

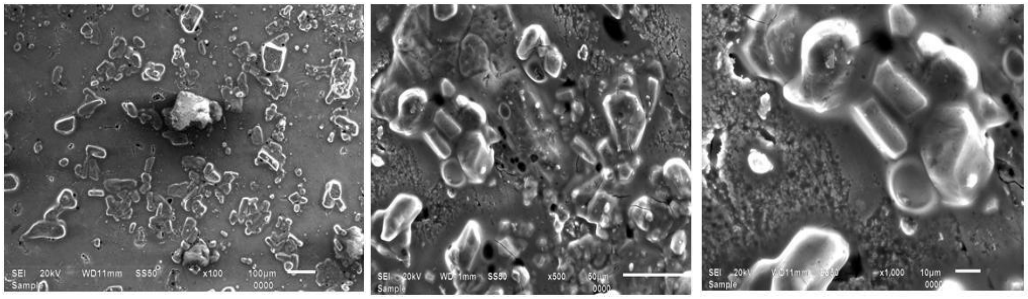

(a) (b) (c)

Figure 5.17 SEM of composite with 10% Zircon Sand at (a) 100X, (b) 500X and (c) 1000X

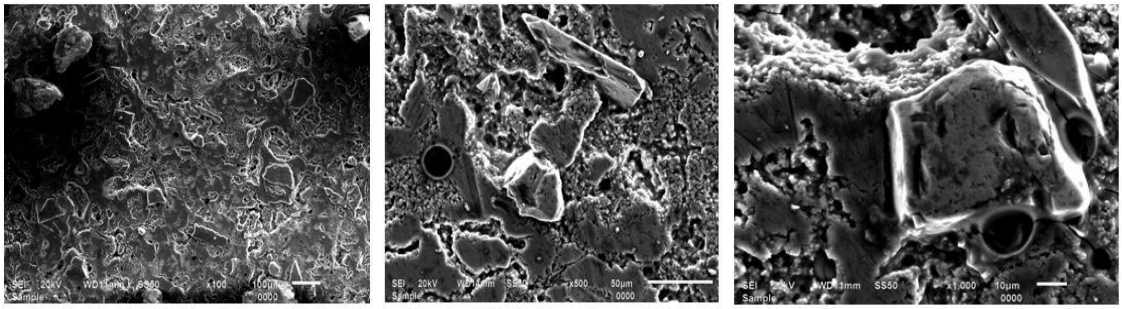

(a) (b) (c)

Figure 5.18 SEM of composite with 7.5% Zircon Sand and 7.5% SiC at (a) 100X, (b) 500X and (c) 1000X

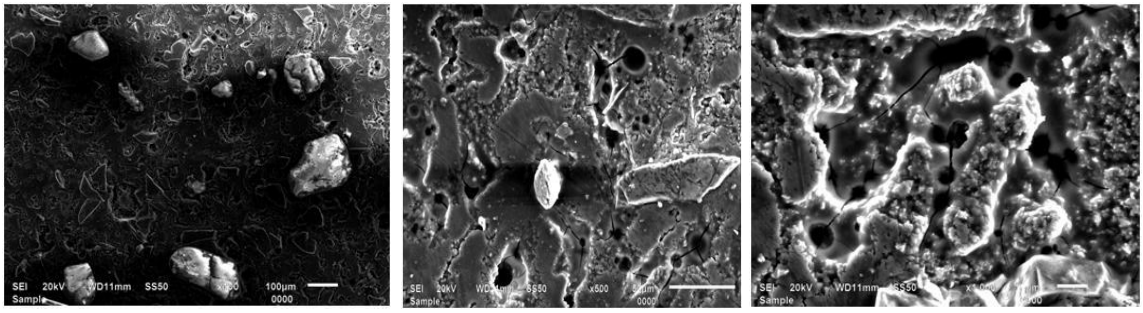

(a) (b) (c)

Figure 5.19 SEM of composite with 10% Zircon Sand and 10% SiC at (a) 100X, (b) 500X and (c) 1000X

The particle distribution is clearly visible in this micrograph. SiC and Zircon sand particles are visible in these micrographs. The shape of most Zircon Sand particles is mainly circular and the shape of SiC particle is angular and sub-angular.

5.3 MICROSTRUCTURE OF ALUMINIUM ALLOY AND COMPOSITES AFTER CORROSION

Microstructures of composites are visualized after subjecting to the corrosion test and microstructure are observed as shown below:

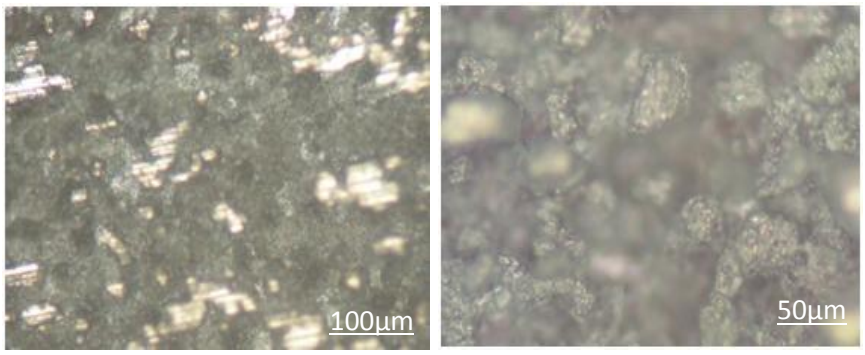

(a) (b)

Figure 5.20 Optical micrographs of Base Alloy (a) 100X, (b) 200X

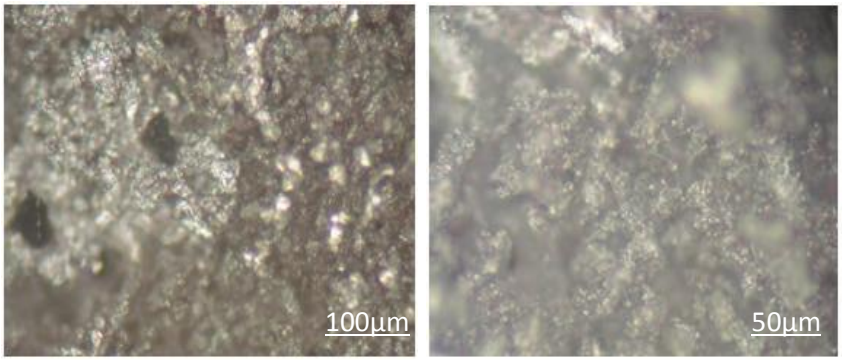

(a) (b)

Figure 5.21 Optical micrographs of 2.5% SiC (a) 100X, (b) 200X

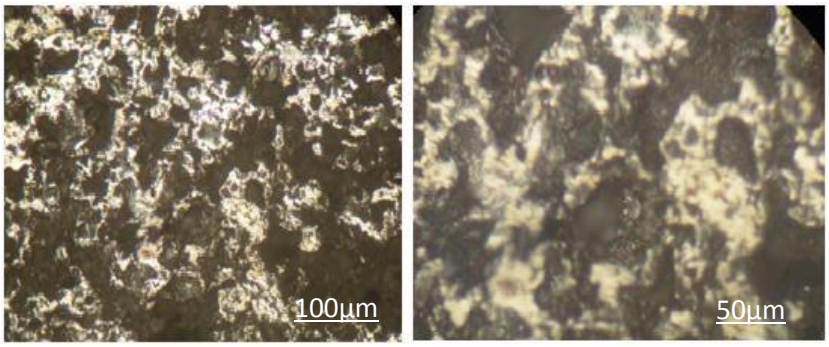

(a) (b)

Figure 5.22 Optical micrographs of 5% SiC (a) 100X, (b) 200X

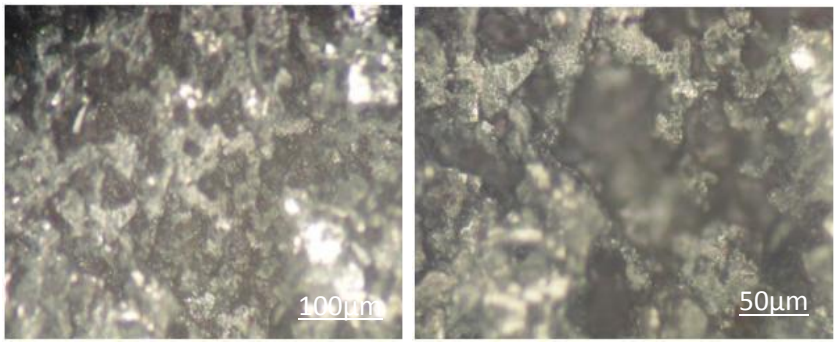

(a) (b)

Figure 5.23 Optical micrographs of 7.5% SiC (a) 100X, (b) 200X

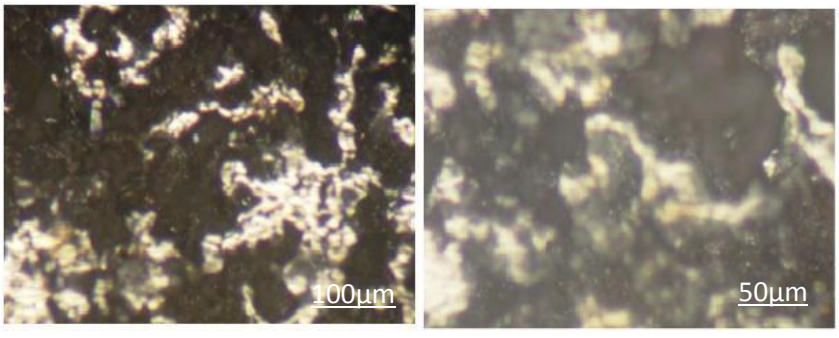

(a) (b)

Figure 5.24 Optical micrographs of 10% SiC (a) 100X, (b) 200X

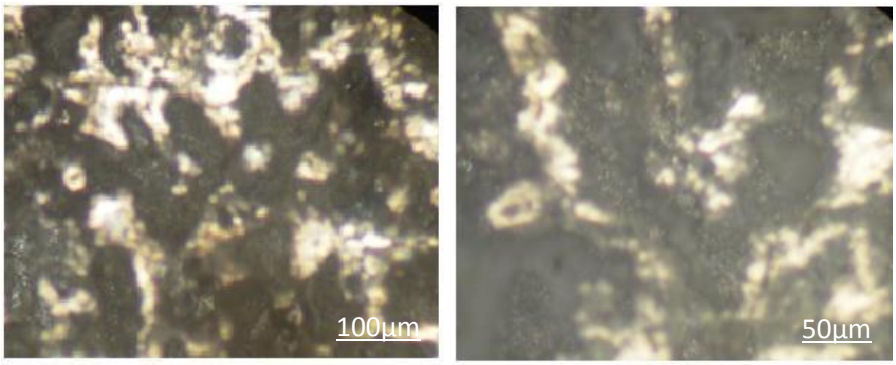

(a) (b)

Figure 5.25 Optical micrographs of 2.5% Zircon Sand (a) 100X, (b) 200X

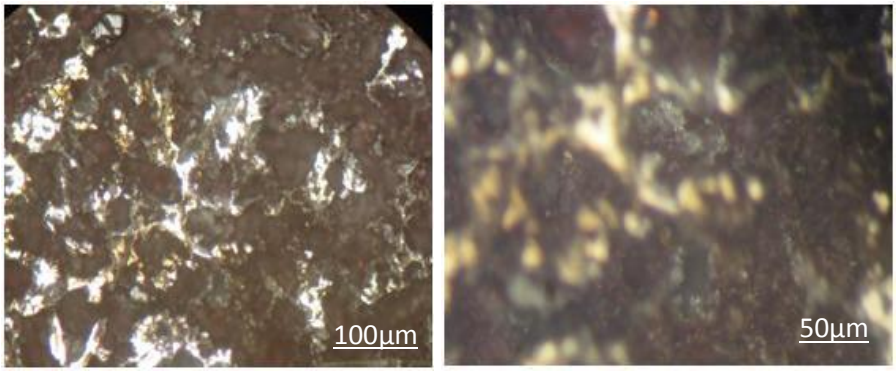

(a) (b)

Figure 5.26 Optical micrographs of 5% Zircon Sand (a) 100X, (b) 200X

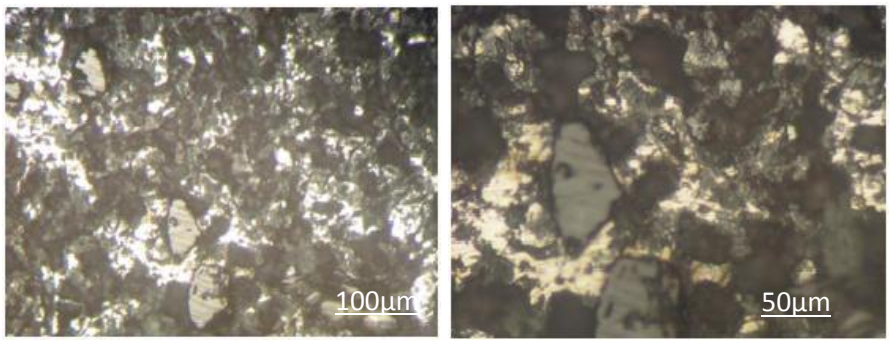

(a) (b)

Figure 5.27 Optical micrographs of 7.5% Zircon Sand (a) 100X, (b) 200X

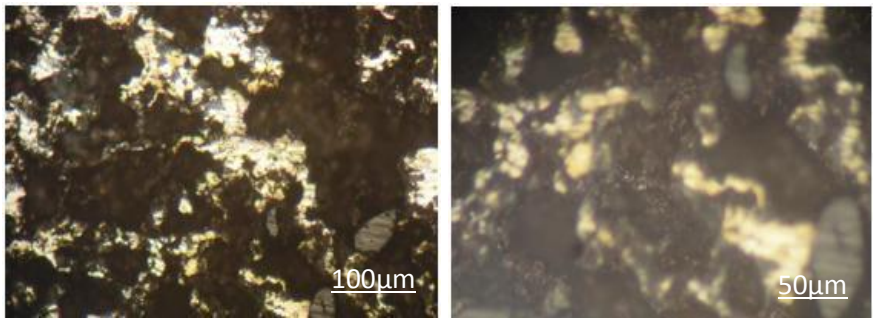

(a) (b)

Figure 5.28 Optical micrographs of 10% Zircon Sand (a) 100X, (b) 200X

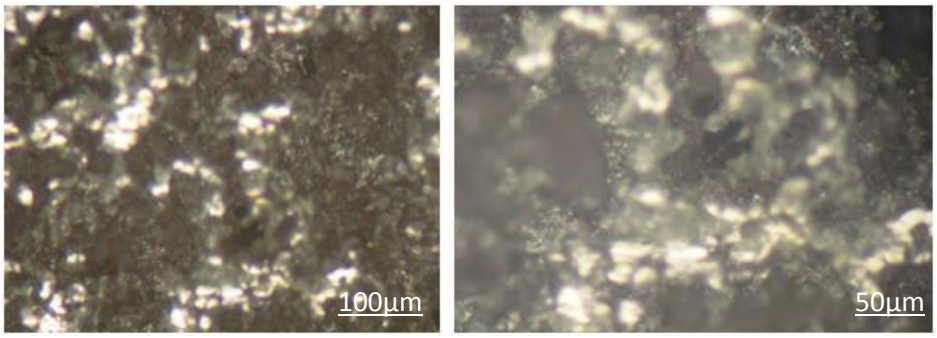

(a) (b)

Figure 5.29 Optical micrographs of 5% Zircon Sand and SiC (a) 100X, (b) 200X

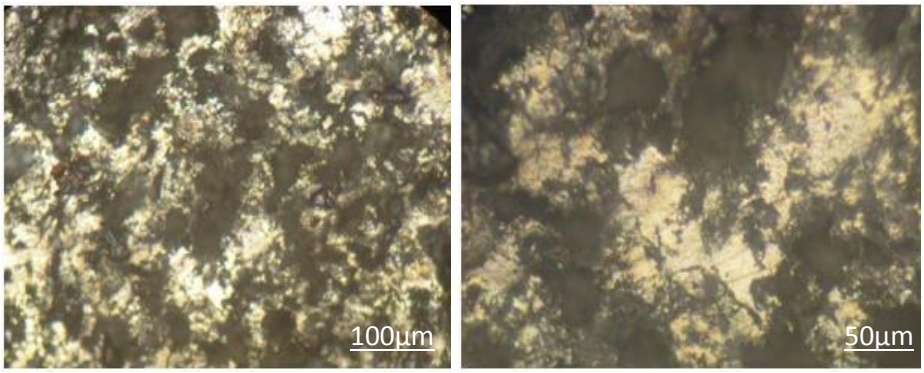

(a) (b)

Figure 5.30 Optical micrographs of 10% Zircon Sand and SiC (a) 100X, (b) 200X

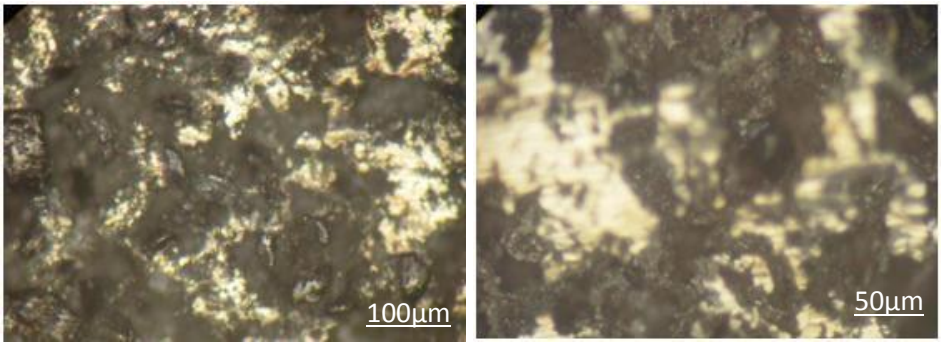

(a) (b)

Figure 5.31 Optical micrographs of 15% Zircon Sand and SiC (a) 100X, (b) 200X

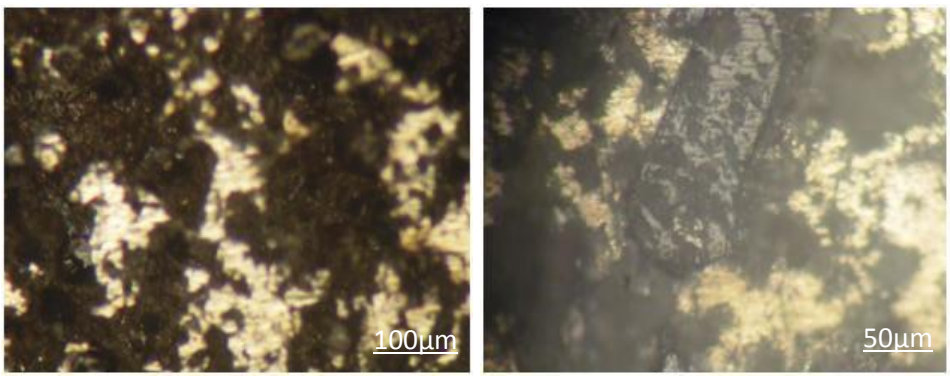

(a) (b)

Figure 5.32 Optical micrographs of 20% Zircon Sand and SiC (a) 100X, (b) 200X

5.4 SCANNING ELECTRON MICROSCOPY COMPOSITES AFTER CORROSION

Figures 5.33-5.38 shows the scanning electron micrographs of the hybrid composite after the corrosion testing. It is observed that the particles are uniformly distributed throughout the matrix for the cast hybrid composite. Pits in some regions are clearly visible. They were smaller and shallower than those on unreinforced alloy. Presence of entrapped air and moisture in the reinforcement particles results in the porosity after casting.

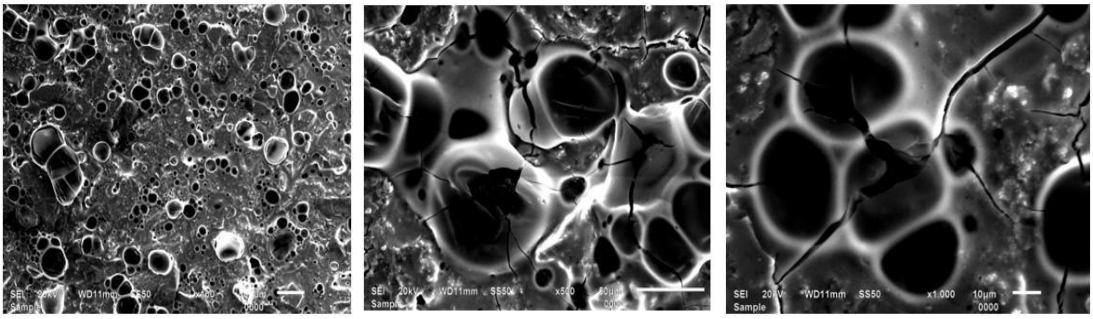

(a) (b) (c)

Figure 5.33 SEM of composite with 7.5% SiC at (a) 100X, (b) 500X, and (c) 1000X

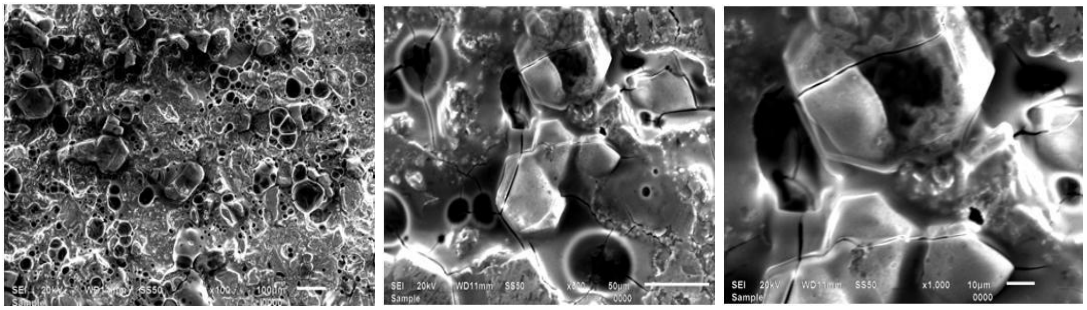

(a) (b) (c)

Figure 5.34 SEM of composite with 10 % SiC at (a) 100X, (b) 500X, and (c) 1000X

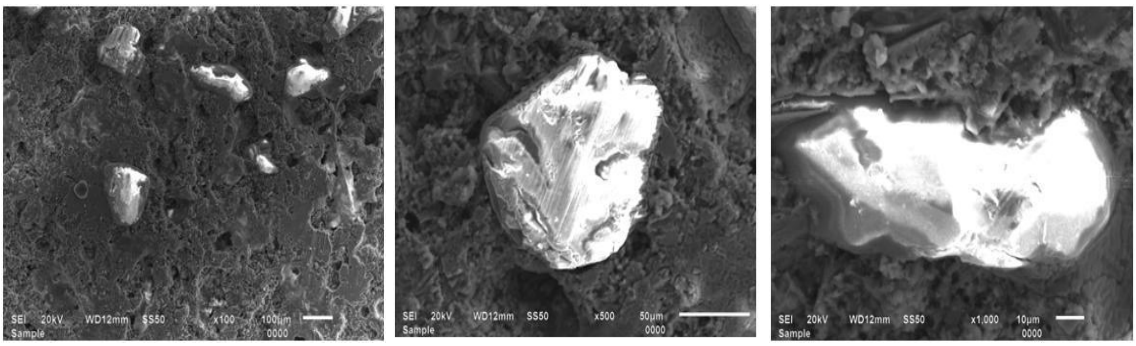

(a) (b) (c)

Figure 5.35 SEM of composite with 7.5 % Zircon sand at (a) 100X, (b) 500X, and (c) 1000X

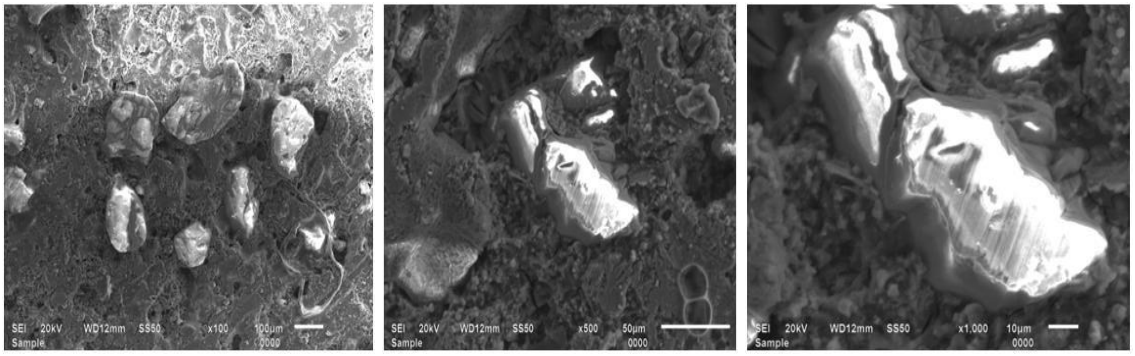

(a) (b) (c)

Figure 5.36 SEM of composite with 10 % Zircon sand at (a) 100X, (b) 500X, and (c) 1000X

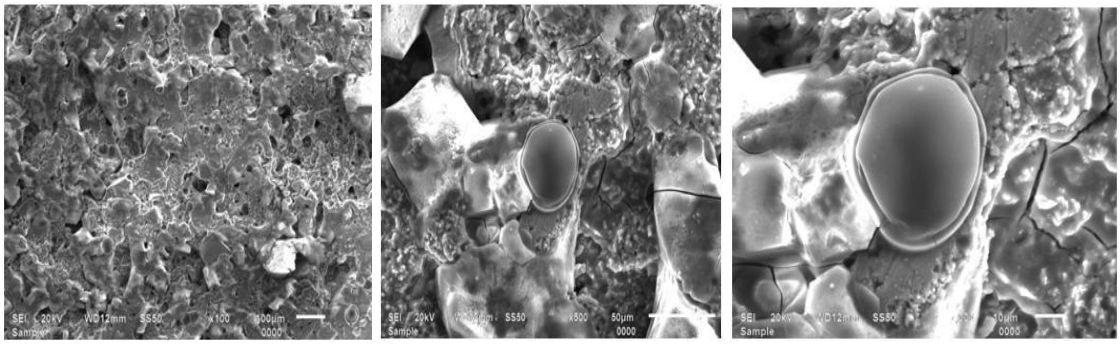

(a) (b) (c)

Figure 5.37 SEM of composite with 7.5 % Zircon sand and 7.5 % SiC at (a) 100X, (b) 500X, and (c) 1000X

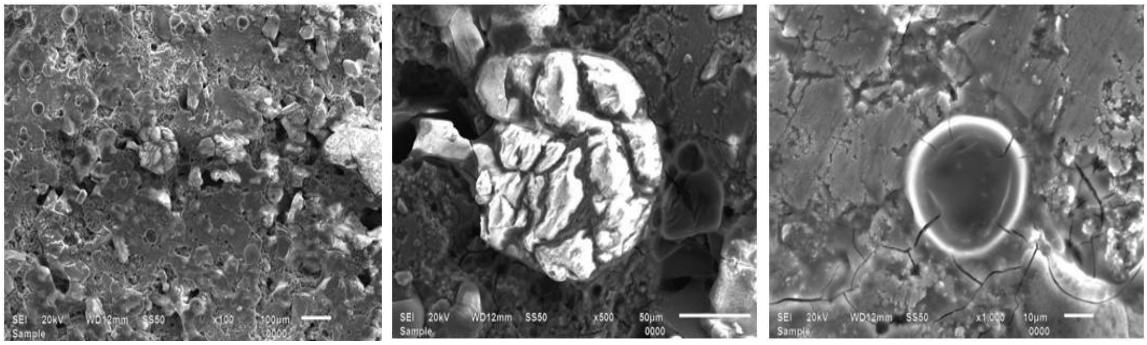

(a) (b) (c)

Figure 5.38 SEM of composite with 10 % Zircon sand and 10 % SiC at (a) 100X, (b) 500X, and (c) 1000X

5.5 CORROSION TESTING RESULT

The electrochemical measurements were performed using a potentiostat/frequency response analyzer (ACM instruments, UK). The test system is a 3-electrode system, the sample was the working electrode, and the reference electrode was a saturate calomel

electrode and a platinum plate serves as the counter electrode. The corrosion medium was 3.5wt% NaCl neutral solution, prepared by analytical sodium chloride and distilled water. Figure 5.39 and 5.40 show the samples before the corrosion and after the corrosion respectively. The samples were painted with nail paint to get the 1 cm^2 area so that corrosion would occur on the selected area.

Figure 5.39 Samples before corrosion testing

Figure 5.40 Samples after corrosion testing

5.5.1 Potentiodynamic Polarization

The polarization curve of base matrix and composites obtained in 3.5% sodium chloride solution is shown in Figures below respectively. The corrosion potential (*E*corr) and corrosion current density (Icorr) calculated using Tafel extrapolation method is given in Table 5.1.

Table 5.1 Corrosion behaviour of base matrix and composites in 3.5% sodium chloride solution evaluated by potentiodynamic polarization studies.

S.No	Percentage variation of different reinforcements	Corrosion potential, Ecorr (mV vs SCE)	Corrosion current density, Icorr (A/cm^2)	Corrosion rate (mm/year)
1	0% al	-822.85	3.2745	58.81
2	2.5% SiC	-864.67	2.8884	51.877
3	5% SiC	-999.78	2.7223	48.892
4	7.5% SiC	-1020.2	2.6549	47.683
5	10% SiC	-1058.9	2.4613	44.206
6	2.5% Zircon Sand	-986.69	2.8297	50.822
7	5% Zircon Sand	-998.9	2.7392	49.197
8	7.5% Zircon Sand	-1002.1	2.8392	50.992
9	10% Zircon Sand	-1003.9	2.6913	48.335
10	2.5% Zircon Sand + 2.5%SiC	-1002.9	2.9001	52.087
11	5% Zircon Sand +5% SiC	-1037.1	2.7042	48.569
12	7.5% Zircon Sand + 7.5% SiC	-1051.9	3.1064	55.791
13	10% Zircon Sand + 10% SiC	-1091.4	2.5719	46.191

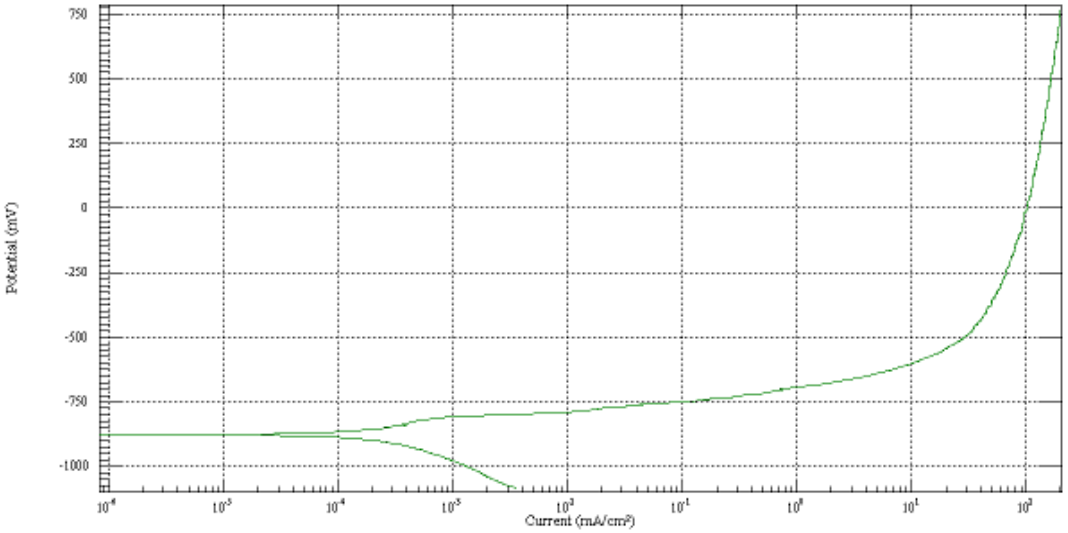

Figure 5.41 Polarization curve of base matrix

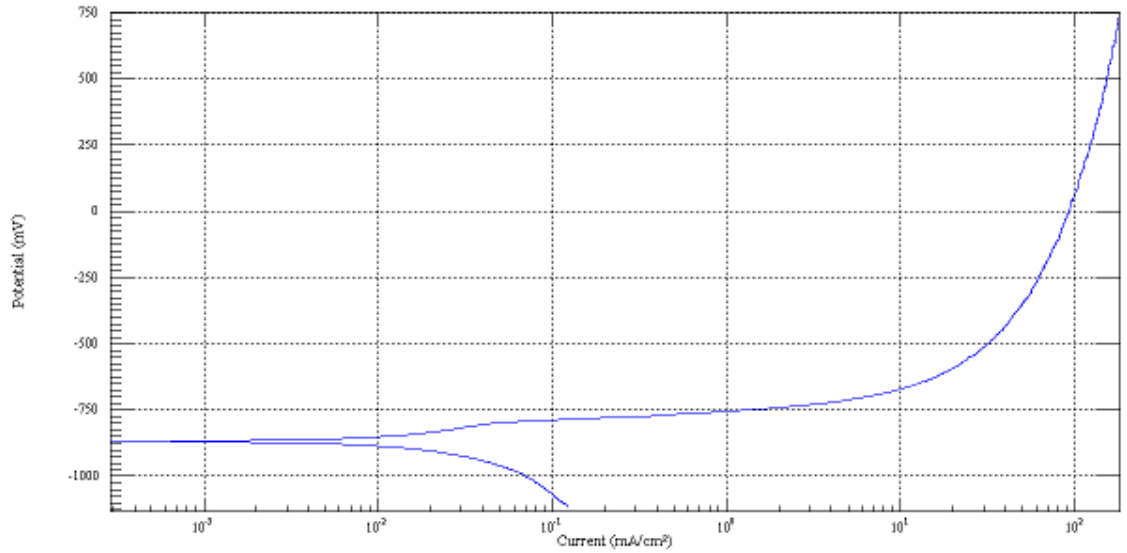
Potential (mV)
750
500
250
0
-250
-500
-750
-1000
Current (mA/cm²)

(a)

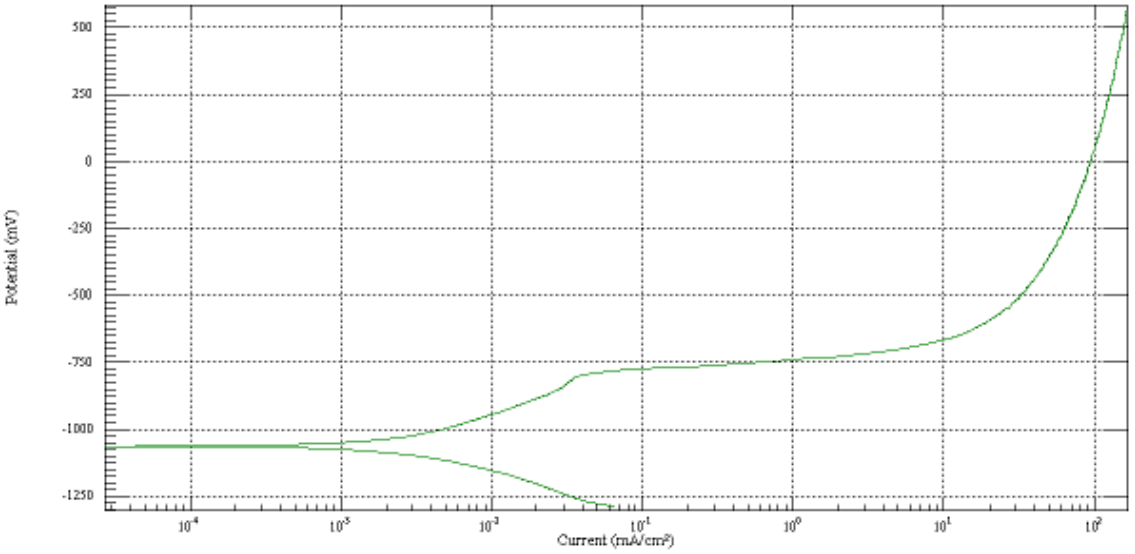
Potential (mV)
500
250
0
-250
-500
-750
-1000
-1250
Current (mA/cm²)

(b)

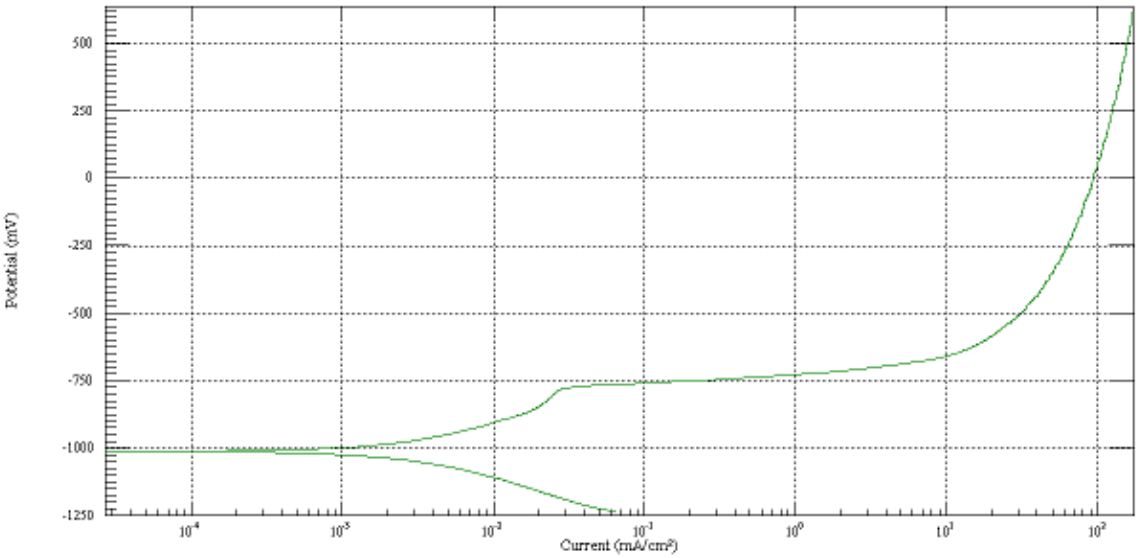
Potential (mV)
500
250
0
-250
-500
-750
-1000
-1250
Current (mA/cm²)

(c)

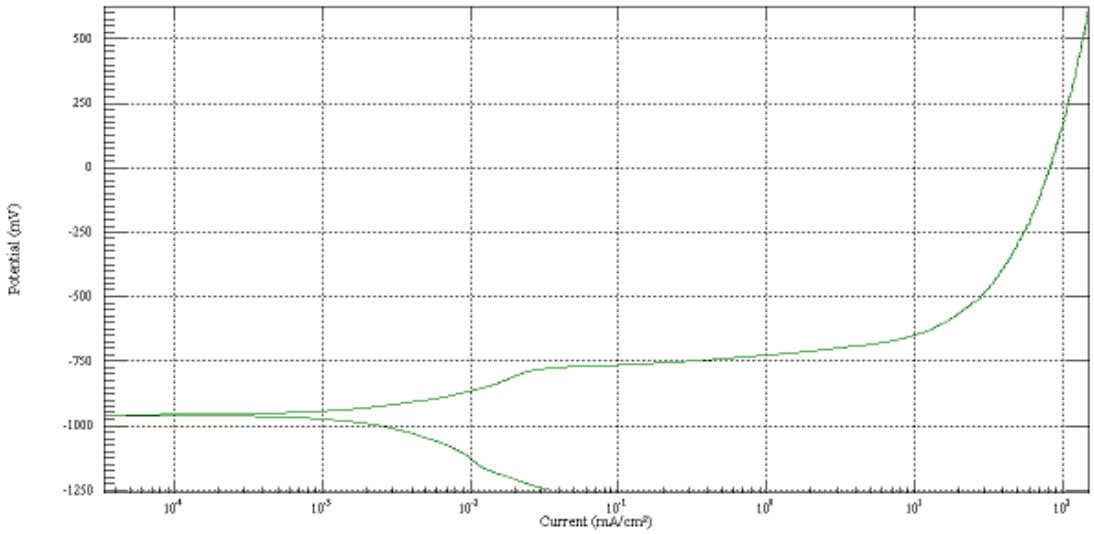

(d)

Figure 5.42 Polarization curves of (a) 2.5%SiC (b) 5%SiC (c) 7.5%SiC (d) 10% SiC in 3.5% sodium chloride solution

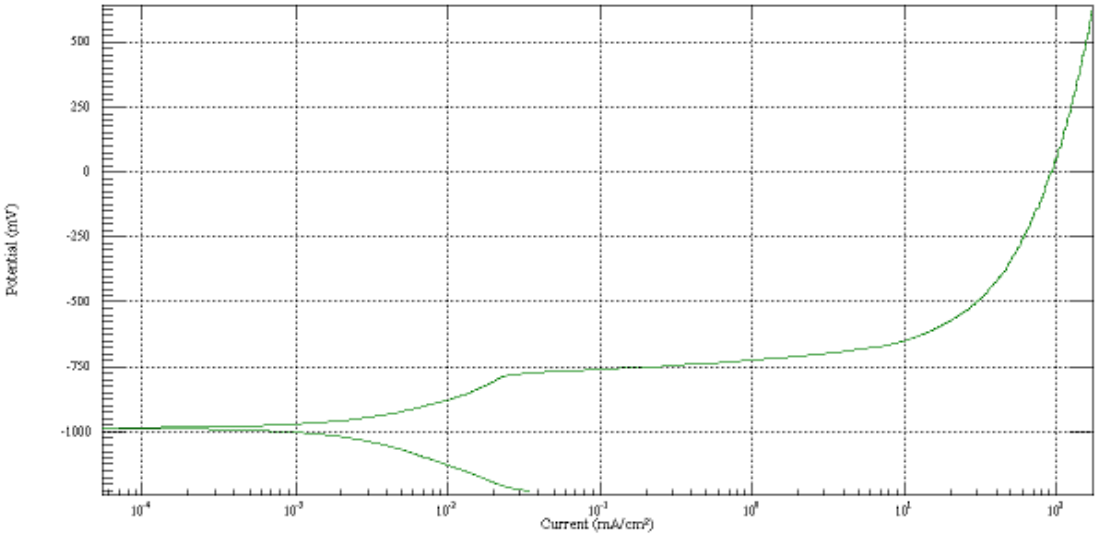

(a)

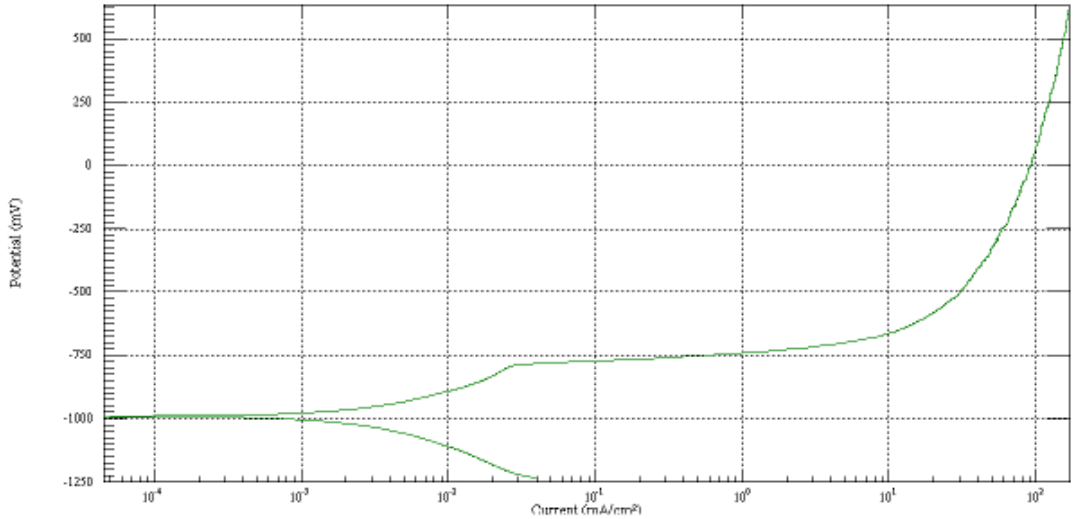

(b)

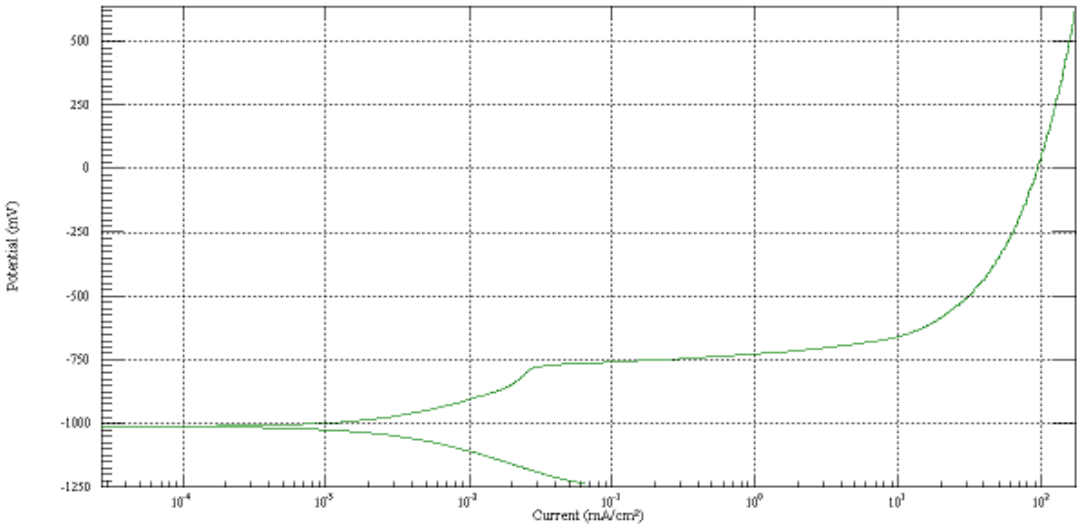

(c)

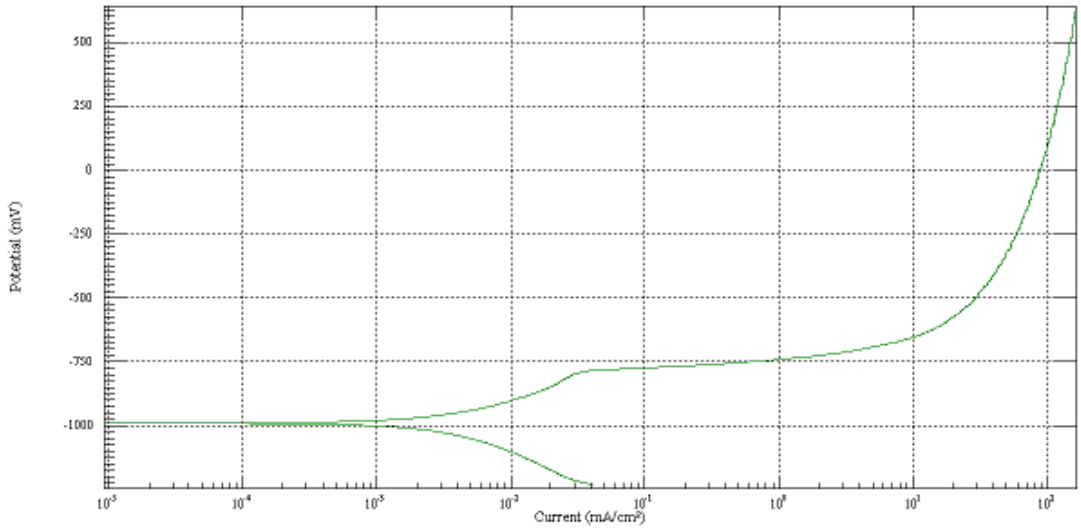

(d)

Figure 5.43 Polarization curves of (a) 2.5%Zircon Sand (b) 5% Zircon Sand (c) 7.5% Zircon Sand (d) 10% Zircon Sand in 3.5% sodium chloride solution

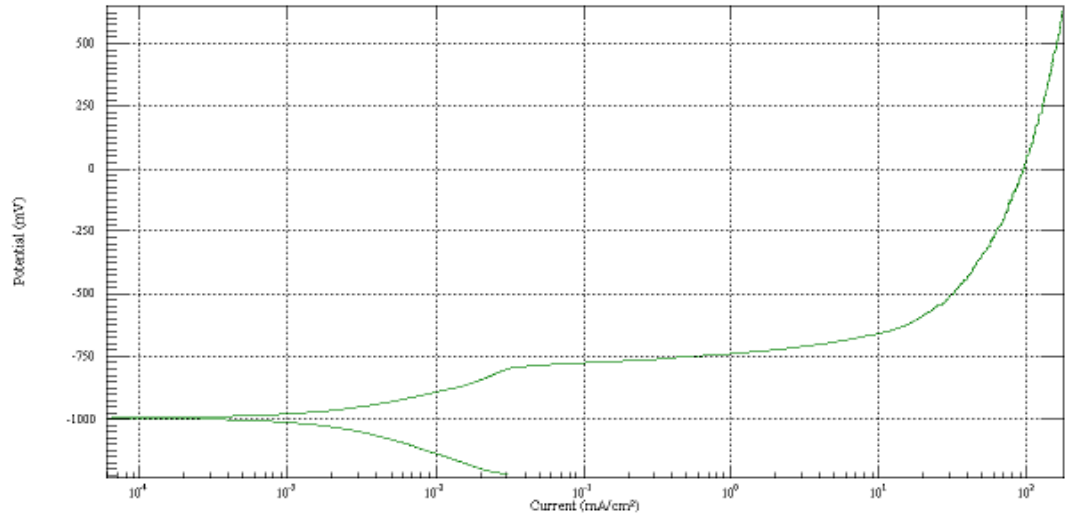

(a)

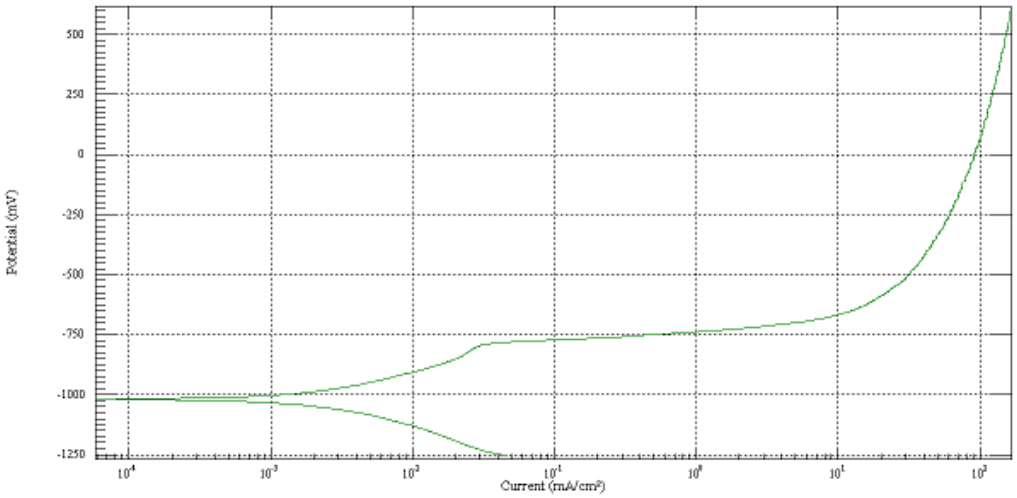

(b)

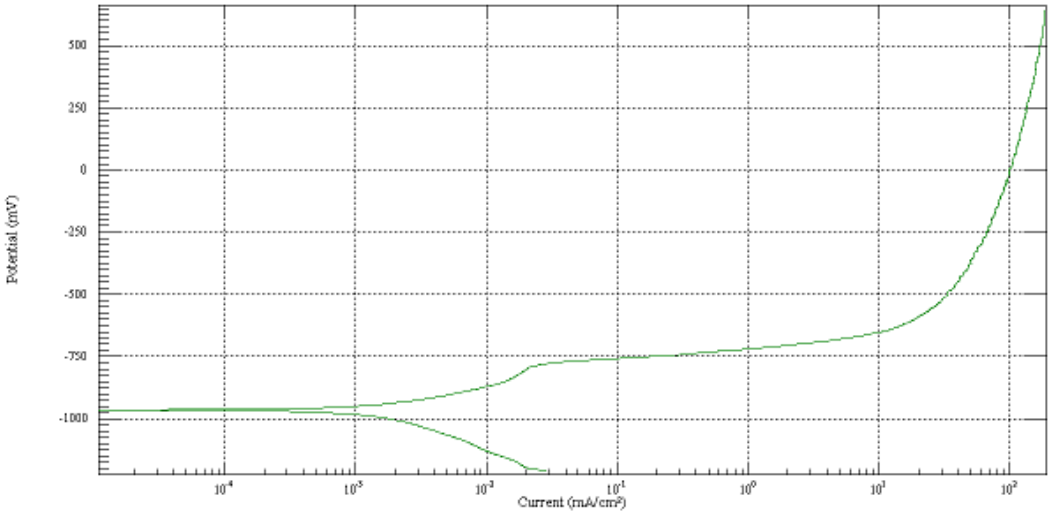

(c)

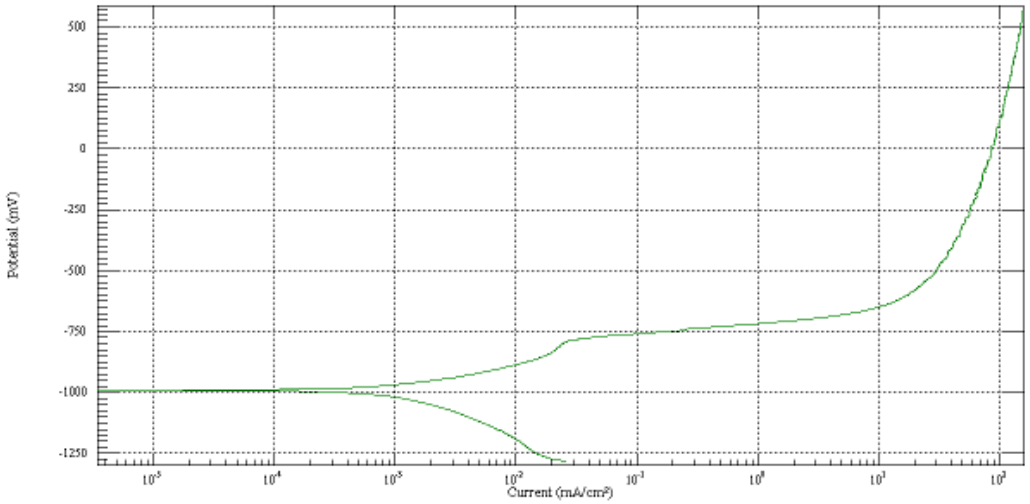

(d)

Figure 5.44 Polarization curves of (a) 2.5%Zircon Sand+2.5% SiC, (b) 5% Zircon Sand+5% SiC, (c) 7.5% Zircon Sand+7.5% SiC, (d) 10% Zircon Sand+10% SiC in 3.5% sodium chloride solution

In all the cases it is observed that the corrosion rate and the potential decreases in the beginning with increase in test duration and remains constant towards the end due to passivation. It is clear from the graph that the resistance of the composite to corrosion increases as the exposure time increases.

The phenomenon of gradually decreasing corrosion rate and potential indicates the possible passivation of the matrix alloy. Visual inspection of the specimens after the tests revealed the presence of a black film covering the surface and that might have retarded the corrosion. In case of base alloy the strength of the media used induces crack formation on the surface, which eventually leads to the formation of pits, thereby causing the loss of material.

5.5.2 Potential measurement

It is clear from the graph that with increase in the weight percentage of different reinforcement particles the potential of the different composites with different weight percentage of reinforcement decreases. The initial decrease in the potential is due the corrosion process which takes place on the surface of the composites. It is clear from the graph that the percentage variation of the Zircon Sand, SiC and Zircon Sand & SiC both as reinforcement lead to the decrease in the potential.

A) Percentage variation of Zircon Sand

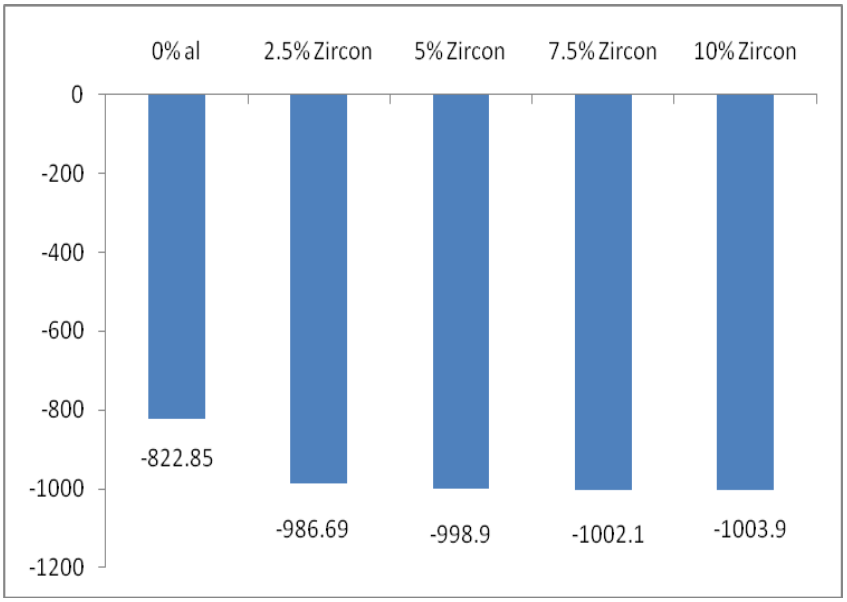

Figure 5.45 Potential measurement for different weight percentage of Zircon Sand

B) Percentage variation of SiC

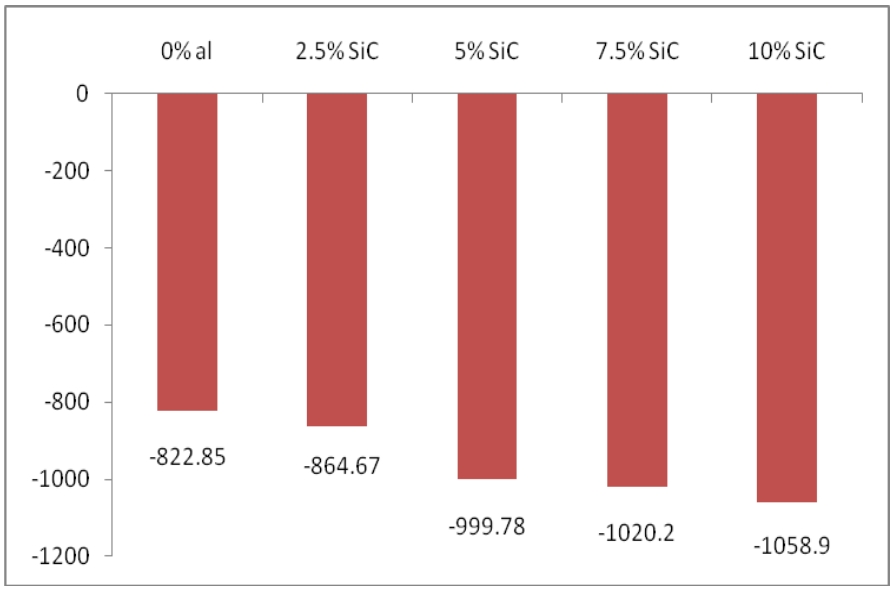

Figure 5.46 Potential measurement for different weight percentage of SiC

C) Percentage variation of SiC+Zircon Sand

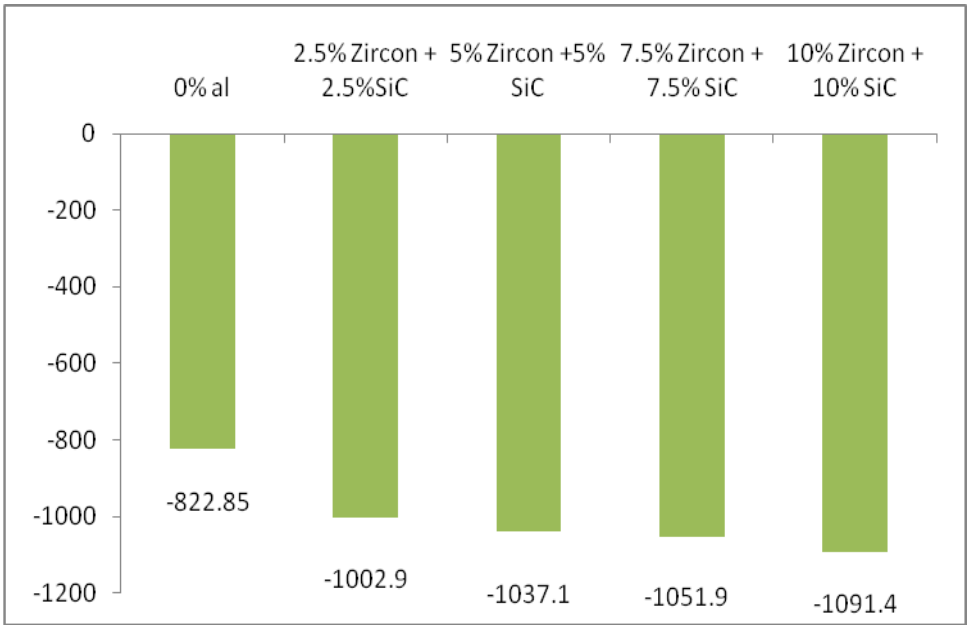

Figure 5.47 Potential measurement for different weight percentage of Zircon Sand & SiC

5.5.3 Corrosion Current Density (Icorr)

It is clear from the graph that the percentage variation of the Zircon Sand, SiC and Zircon Sand & SiC both as reinforcement lead to the decrease in corrosion current density. From the graphs it can also be clearly seen that the ceramic reinforcement particles act as insulator and remain inert in the corrosion medium during the test. Thus

the corrosion current density decreases with increase in the percentage of different reinforcement contents.

A) Percentage variation of Zircon Sand

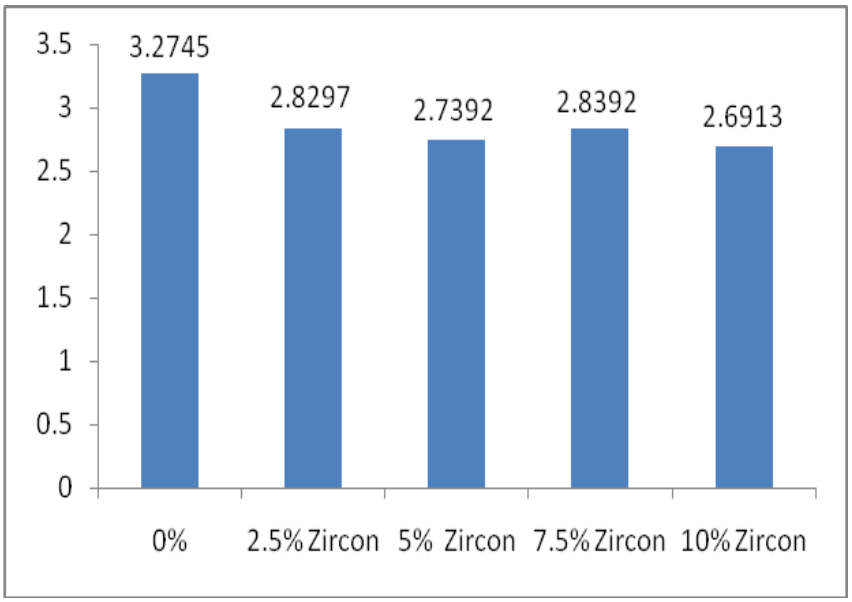

Figure 5.48 Corrosion current density for different weight percentage of Zircon Sand

B) Percentage variation of SiC

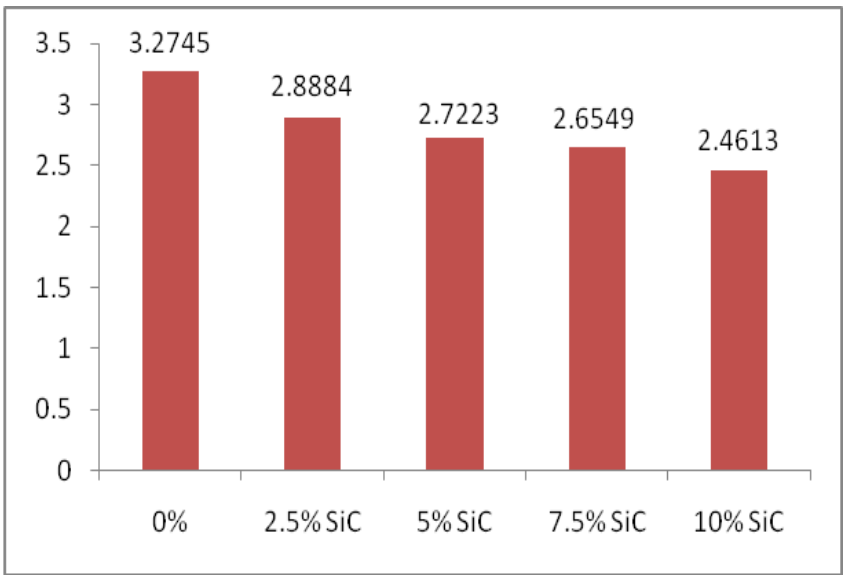

Figure 5.49 Corrosion current density for different weight percentage of SiC

C) Percentage variation of SiC+Zircon Sand

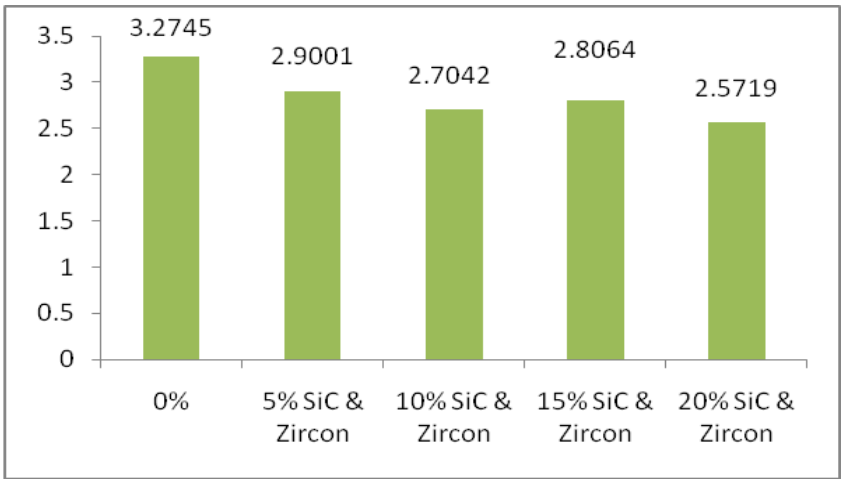

Figure 5.50 Corrosion current density for different weight percentage of Zircon Sand & SiC

5.5.4 Half cell potential measurement

The half-cell potential is measure of electrode potential, represents the potential difference between the composite and the adjacent electrolyte. Thus in a given environment it may serve as an indicator of corrosion initiation since the threshold of depassivation depends mainly on the potential compared. The half-cell potential value is measured with reference to a standard reference electrode. The various reference electrodes used for the potential measurement are standard hydrogen electrode (SHE), copper-copper sulphate electrode (Cu/CuSO4), saturated calomel electrode (SCE), silver-silver chloride electrode (Ag/AgCl).

A) Percentage variation of SiC

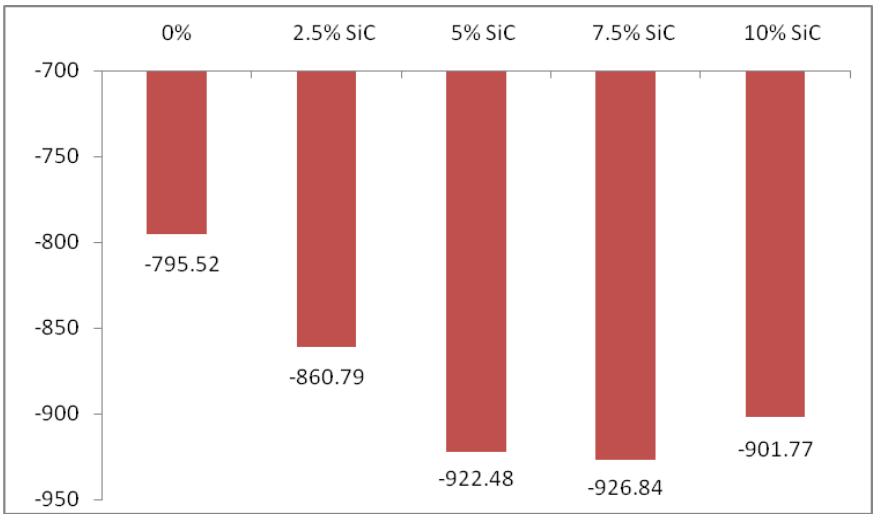

Figure 5.51 Half cell potential of different weight percentage of SiC

B) Percentage variation of Zircon Sand

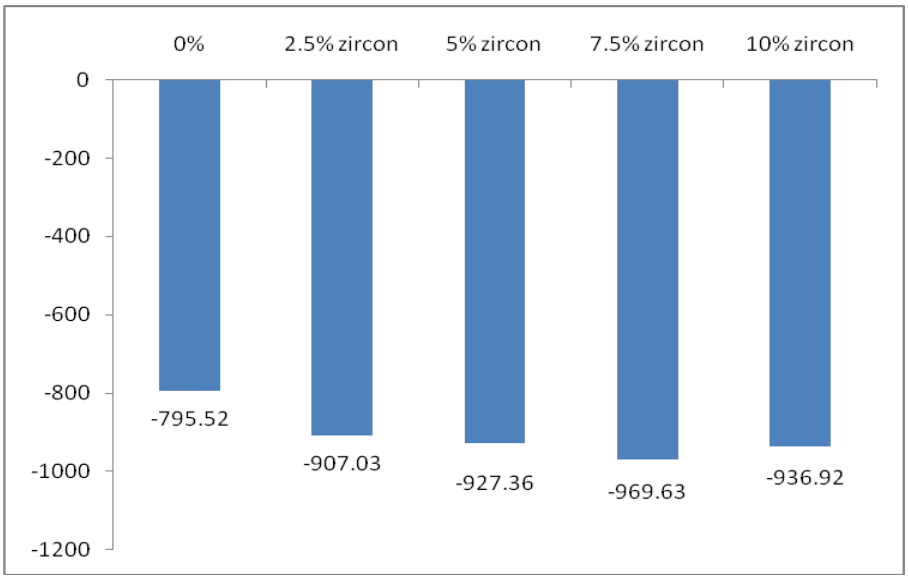

Figure 5.52 Half cell potential of different weight percentage of Zircon Sand

C) Percentage variation of SiC+Zircon Sand

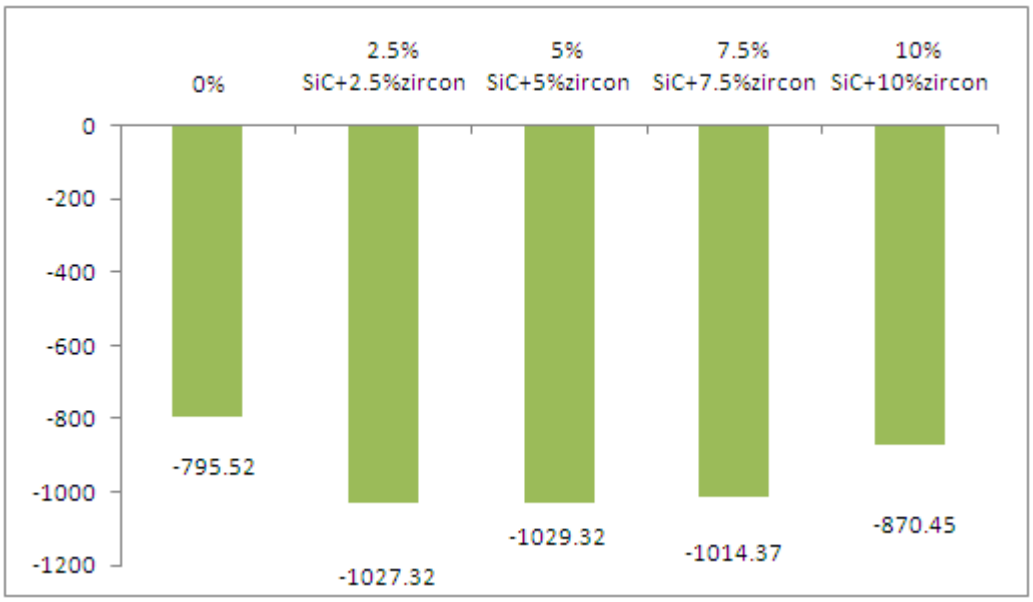

Figure 5.53 Half cell potential of different weight percentage of SiC + Zircon Sand

It is clear from the graph that with increase in the weight percentage of different reinforcement particles the half cell potential of the different composites with different weight percentage of reinforcement decreases. But after some passes of time half cell potential start increases.The initial decrease in the potential is due the corrosion process which takes place on the surface of the composites.But after some time a oxide layer is

formed on the surface of composite which further prevent the corrosion of the composite thus the half cell potential start increases.

5.5.5 Corrosion rate

It is clear from the graph that the corrosion rate decreases with increase in the percentage of different reinforcement contents. Less exposure of the MMCs area to corrosive environments in corrosion testing led to lesser pitting as well as corrosion than that of the matrix alloy. Since the lesser surface area is provided by the MMCs as compared to the matrix alloy lesser is the corrosion rate.

Zircon Sand and SiC being the ceramic material remains inert and is hardly affected by corrosion medium during the test and is not expected to affect the corrosion mechanism of the composites. The results indicate that there is an improvement in corrosion resistance as the percentage of Zircon Sand and SiC particulates increased in the composite which shows that Zircon Sand and SiC particulates directly or indirectly influence the corrosion property of the composites. Zircon Sand and SiC particulates act as a physical barrier to the initiation and development of corrosion pits and also modifies the micro structure of the matrix material and hence reduces the corrosion rate as well as the potential.

A) Percentage variation of SiC

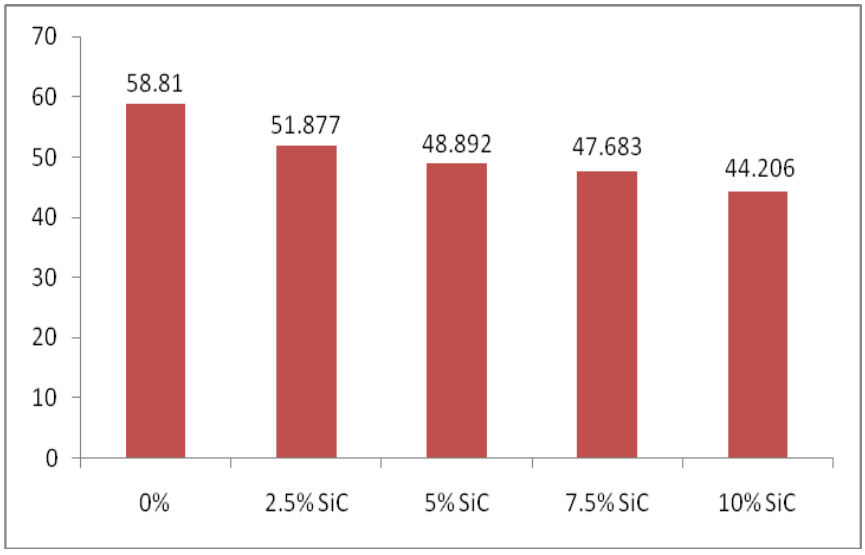

Figure 5.54 Corrosion rate for different weight percentage of SiC

B) Percentage variation of Zircon Sand

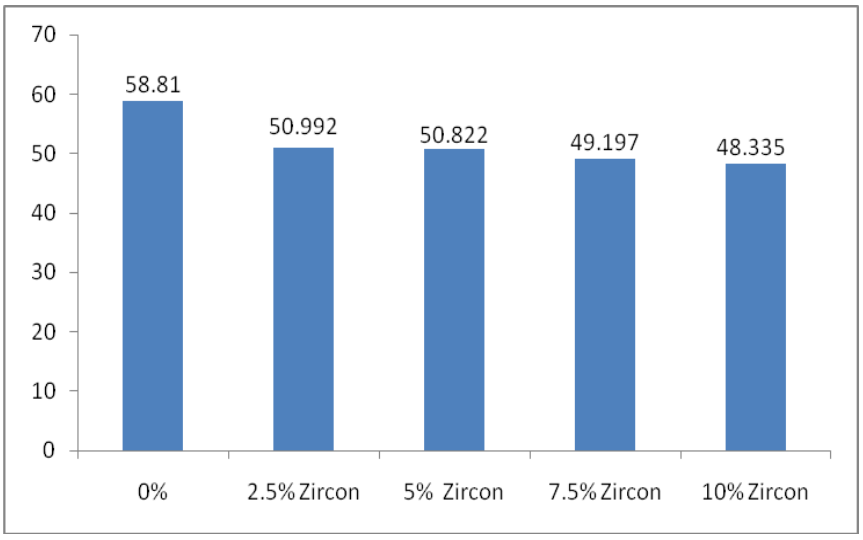

Figure 5.55 Corrosion rate for different weight percentage of Zircon Sand

C) Percentage variation of SiC+Zircon Sand

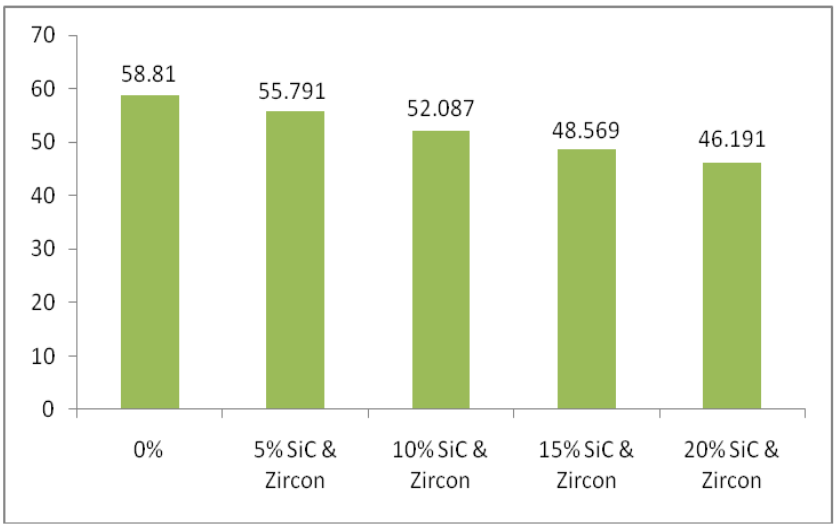

Figure 5.56 Corrosion rate for different weight percentage of Zircon Sand & SiC

The phenomenon of gradually decrease in the corrosion rate, corrosion current density and potential indicates the possible passivation of the matrix alloy. Visual inspection of the specimens after the tests revealed the presence of a black film covering the surface and that might have retarded the corrosion. In case of base alloy the strength of the media used induces crack formation on the surface, which eventually leads to the formation of pits, thereby causing the loss of material. The presence of cracks and pits on the base alloy surface was observed clearly on visual inspection of the specimens after the test. Since there is no reinforcement added in any form, the base alloy fails to provide any sort of resistance to the corrosion medium.

From the graphs it can be clearly seen that the ceramic reinforcement particles act as insulator and remain inert in the corrosion medium during the test. Hence the corrosion rate, corrosion current density and potential decreases with increase in Zircon Sand and SiC content in MMCs. The pits on the matrix alloy were more when compared with those of MMCs. This may be due to the exposure of less matrix alloy surface in MMCs than matrix alloy, by the addition of reinforcement.

5.6 MICROHARDNESS TEST

The term micro hardness test usually refers to static indentations made with loads not exceeding 1 kgf. The testing is done on a microscopic scale with higher precision instruments. The surface being tested generally requires a metallographic finish and it was done with the help of 100, 220, 400, 600, 800 and 1000 grit size emery paper. Load used on micro hardness machine used was 200 gms at 100x optical zoom.

A) Percentage variation of Zircon Sand

Table-5.2 Results of Vicker's Microhardness Test for the percentage variation of Zircon Sand.

Samples	Trial 1	Trial 2	Trial 3	Average
Base alloy 6063	93.32776	94.02126	89.97054	92.43985
2.5% SiC	99.16645	94.43701	96.8881	96.83052
5% SiC	95.39883	101.9312	99.66764	98.99922
7.5% SiC	102.407	99.23139	96.84344	99.49394
10% SiC	104.4641	102.5808	97.18865	101.4112

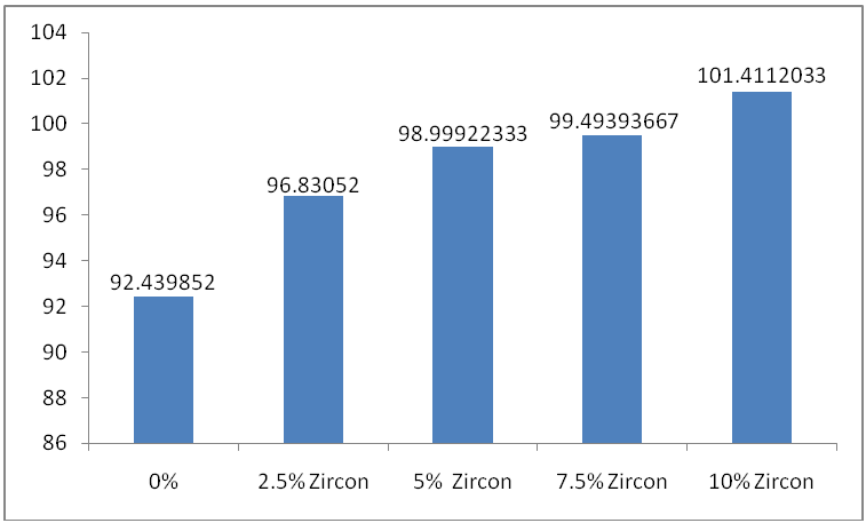

Figure 5.57 Hardness with percentage variation of Zircon Sand

B) Percentage variation of SiC

The results obtained on Micohardness test for the percentage variation of SiC are as follows:

Table-5.3 Results of Vicker's Microhardness Test for the percentage variation of SiC.

Samples	Trial 1	Trial 2	Trial 3	Average
Base alloy 6063	93.32776	94.02126	89.97054	92.43985
2.5% SiC	89.02652	90.31209	113.7657	97.70143
5% SiC	117.1045	92.14009	97.31129	102.1853
7.5% SiC	101.681	95.79014	113.9041	103.7918
10% SiC	101.5469	117.5735	96.23019	105.1169

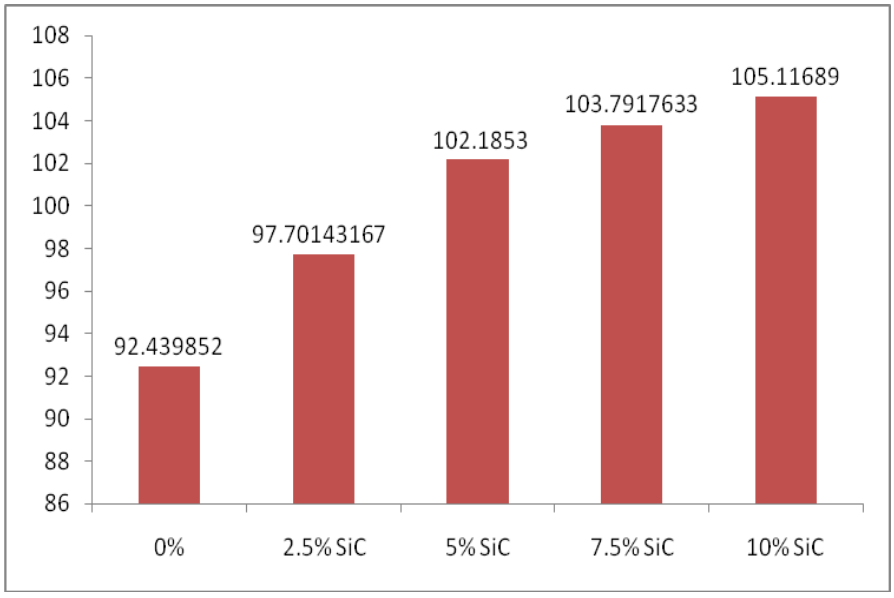

Figure 5.58 Hardness with percentage variation of SiC

C) Percentage variation of SiC+Zircon Sand

Table-5.4 Results of Vicker's Microhardness Test for the percentage variation of SiC+Zircon Sand.

Samples	Trial 1	Trial 2	Trial 3	Average
Base alloy 6063	93.32776	94.02126	89.97054	92.43985
2.5% SiC	101.8966	98.823	107.1213	102.6136
5% SiC	104.5843	120.8878	94.67971	106.7173
7.5% SiC	112.57	95.43242	130.7894	112.9306
10% SiC	151.0782	130.98	121.8103	134.6228

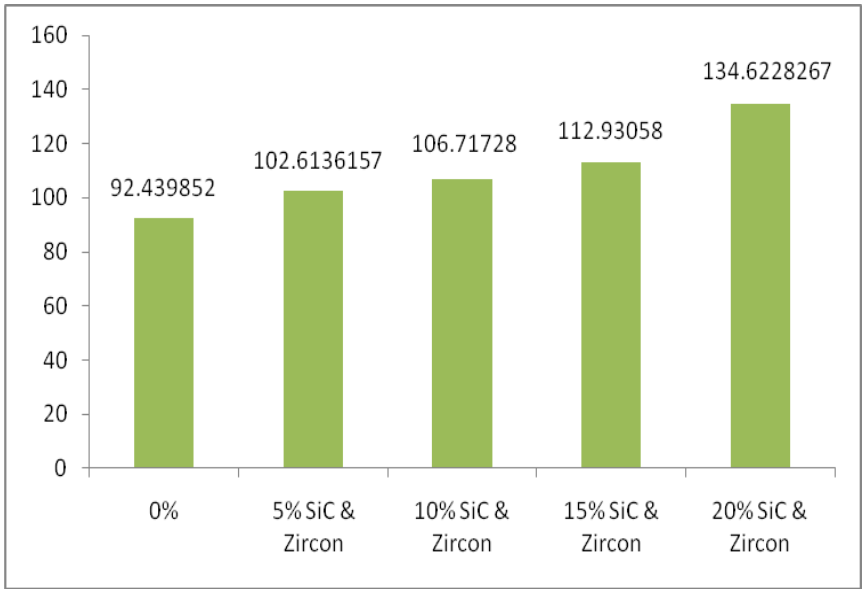

Figure 5.59 Hardness with percentage variation of SiC & Zircon Sand

D) Comparison of hardness of the composites with Zircon Sand,SIC and Sic+Zircon Sand

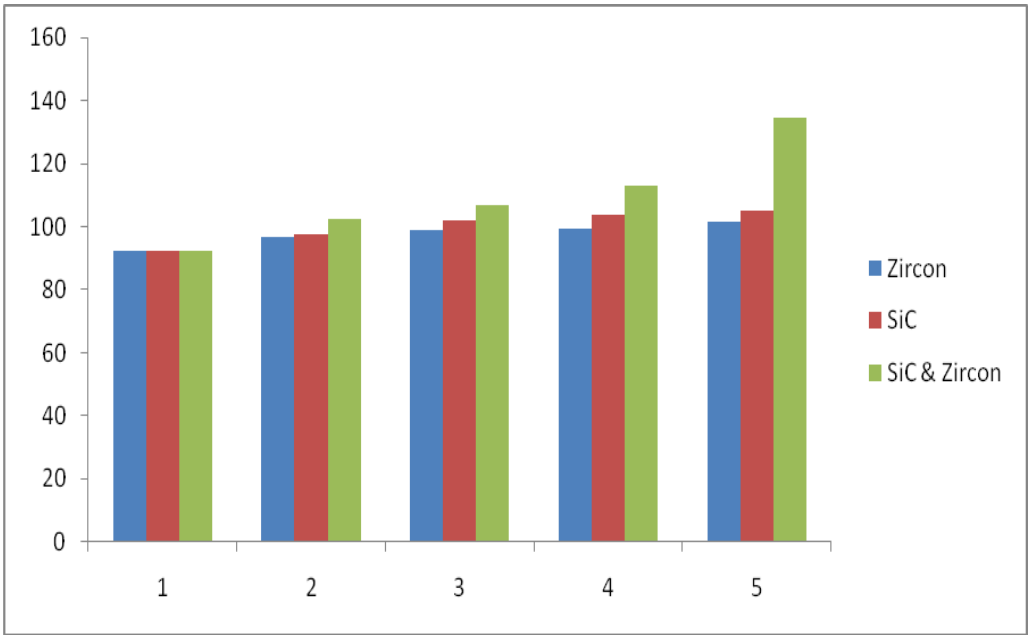

Figure 5.60 Comparison of hardness of the composites with Zircon Sand, SiC and SiC & Zircon Sand.

The above graphs and tables show that incorporation of SiC, Zircon Sand and SiC & Zircon Sand particles in Aluminium matrix causes reasonable increase in hardness. The strengthening of the composite can be due to dispersion strengthening as well as due to particle reinforcement. Thus SiC and Zircon Sand as filler in aluminium matrix casting increase hardness which is needed in various industries like automotive etc.

5.7 RESULT OF X-RD

In XRD, the physical content of the constituents present in the samples are indicated in the form of a graph. X-ray powder diffraction (XRD) pattern of Aluminium alloy and Aluminium matrix composite is shown in Figures below. X-ray diffraction of the aluminium alloy was carried out using X'PERT PRO of PAN ANALYTICAL. Figures below shows the XRD of various Samples and Tables shows the percentage of material present in respective Samples.

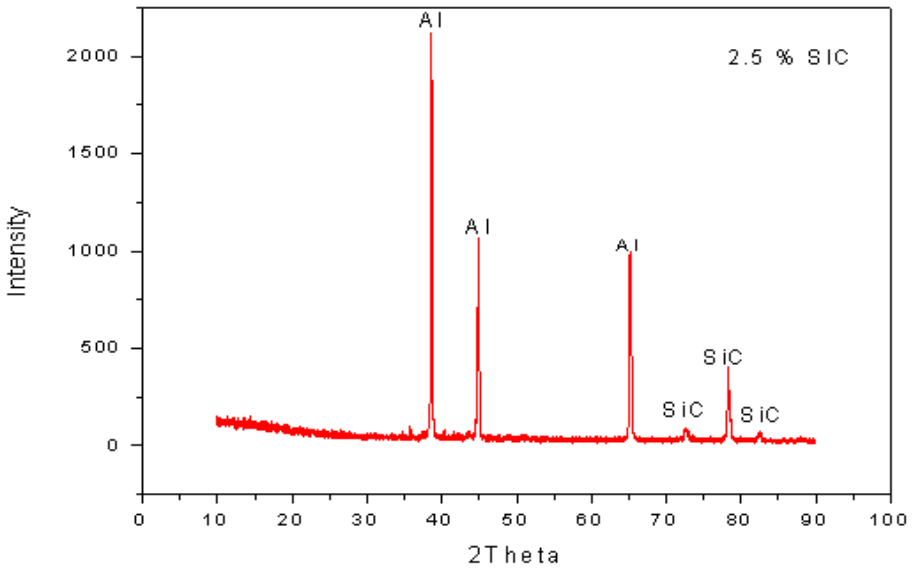

Figure 5.61 X-RD of AA6063 with 2.5% SiC

Table 5.5 X-RD results of alloy reinforced with 2.5% SiC

S.NO.	Rel. Int. [%]	Displacement [°2Th.]	Compound Name	Chemical Formula
1	100.00	38.6507	Aluminium	Al
2	47.31	44.8655	Aluminium	Al
3	45.67	65.1522	Aluminium	Al
4	17.50	78.2633	Silicon carbide	SiC
5	2.94	72.6282	Silicon carbide	SiC
6	1.83	82.5173	Silicon carbide	SiC

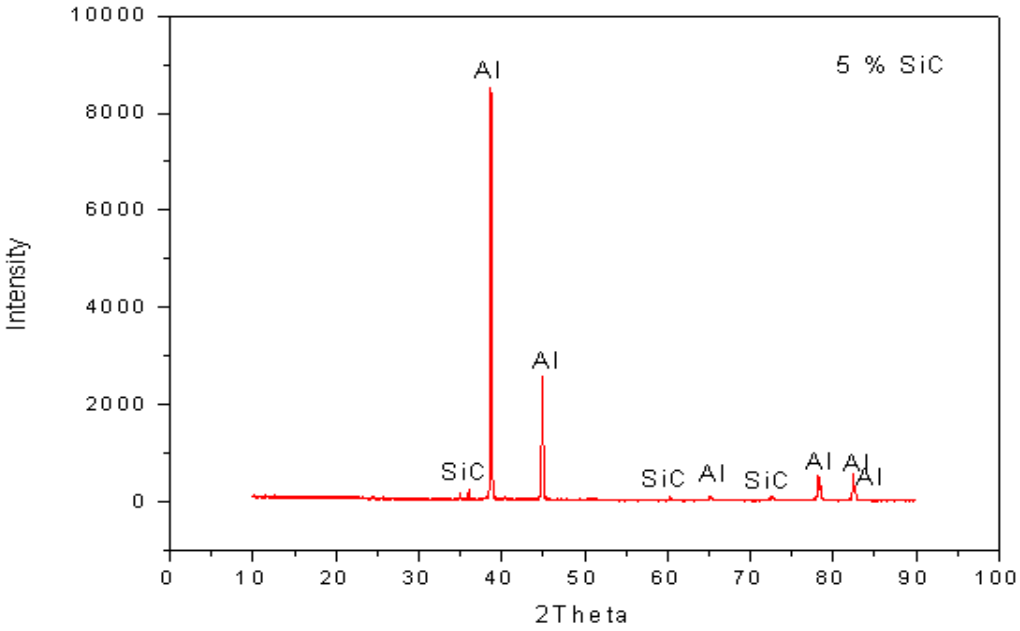

Figure 5.62 X-RD of AA6063 with 5% SiC

Table 5.6 X-RD results of alloy reinforced with 5% SiC

S.NO.	Rel. Int. [%]	Displacement [°2Th.]	Compound Name	Chemical Formula
1	100.00	38.6735	Aluminium	Al
2	48.76	48.7847	Aluminium	Al
3	5.89	82.4105	Aluminium	Al
4	5.66	78.1951	Aluminium	Al
5	3.20	82.6610	Aluminium	Al
6	0.88	65.1693	Aluminium	Al
7	0.86	72.6110	Silicon carbide	SiC
8	0.77	34.9600	Silicon carbide	SiC
9	0.09	60.2879	Silicon carbide	SiC

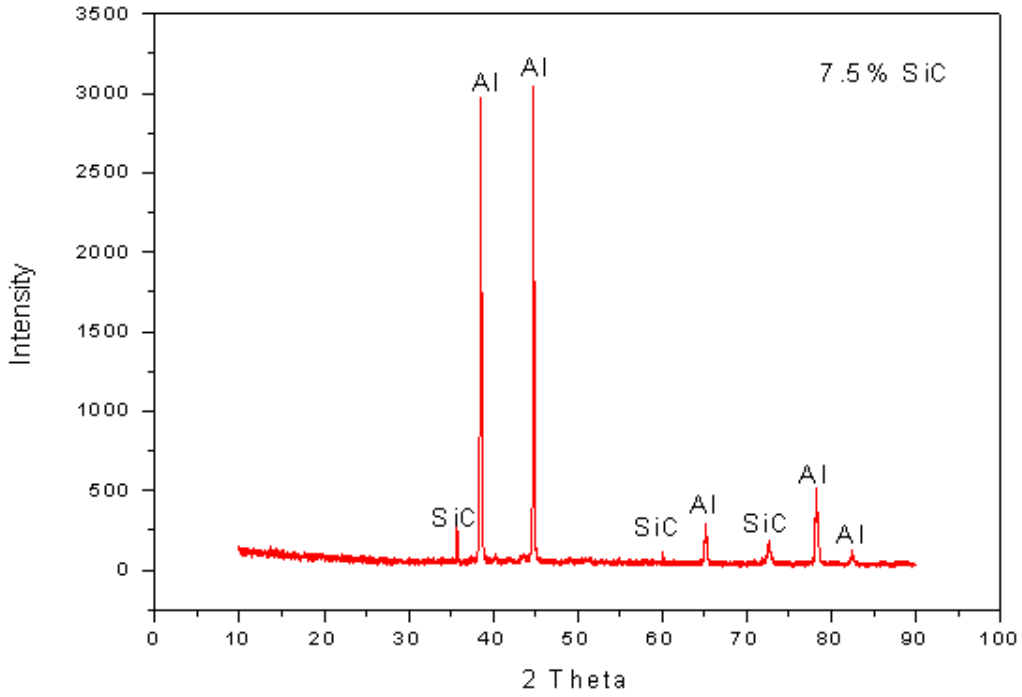

Figure 5.63 X-RD of AA6063 with 7.5% SiC

Table 5.7 X-RD results of alloy reinforced with 7.5% SiC

S.NO.	Rel. Int. [%]	Displacement [°2Th.]	Compound Name	Chemical Formula
1	100.00	44.7487	Aluminium	Al
2	98.95	38.5371	Aluminium	Al
3	15.71	78.1640	Aluminium	Al
4	7.66	65.1103	Aluminium	Al
5	3.86	72.6126	Silicon carbide	SiC
6	3.02	35.7854	Silicon carbide	SiC
7	2.01	82.4515	Aluminium	Al
8	0.70	60.1187	Silicon carbide	SiC

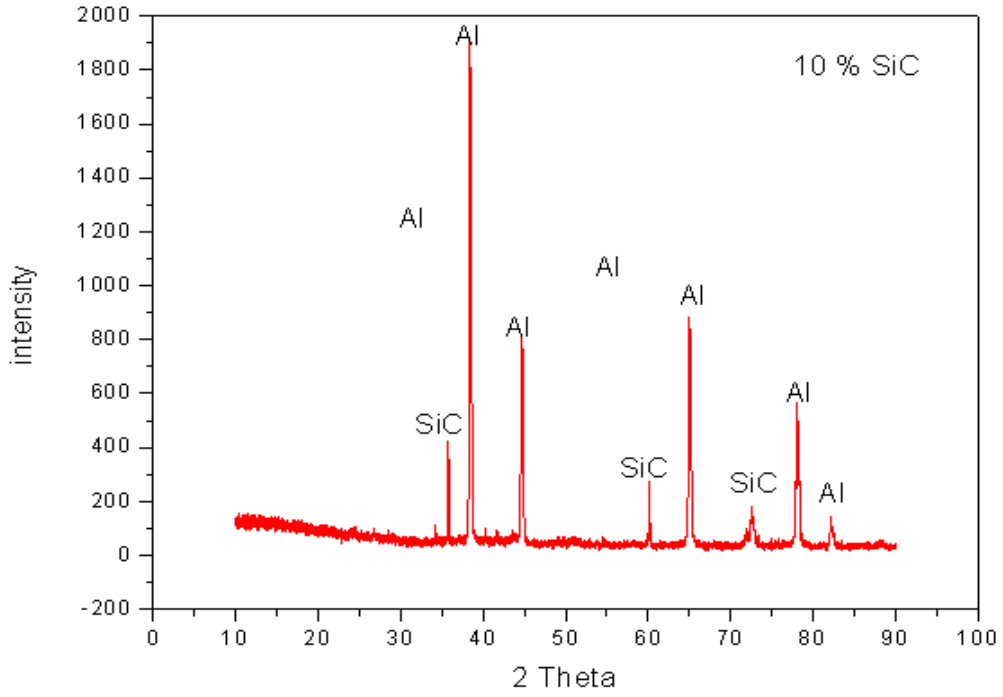

Figure 5.64 X-RD of AA6063 with 10% SiC

Table 5.8 X-RD results of alloy reinforced with 10% SiC

S.NO.	Rel. Int. [%]	Displacement [°2Th.]	Compound Name	Chemical Formula
1	100.00	38.4332	Aluminium	Al
2	45.88	65.0369	Aluminium	Al
3	40.15	44.7309	Aluminium	Al
4	27.31	78.5879	Aluminium	Al
5	16.41	35.8209	Silicon carbide	SiC
6	5.80	72.5879	Silicon carbide	SiC
7	4.98	82.1953	Aluminium	Al
8	4.09	60.1666	Silicon carbide	SiC

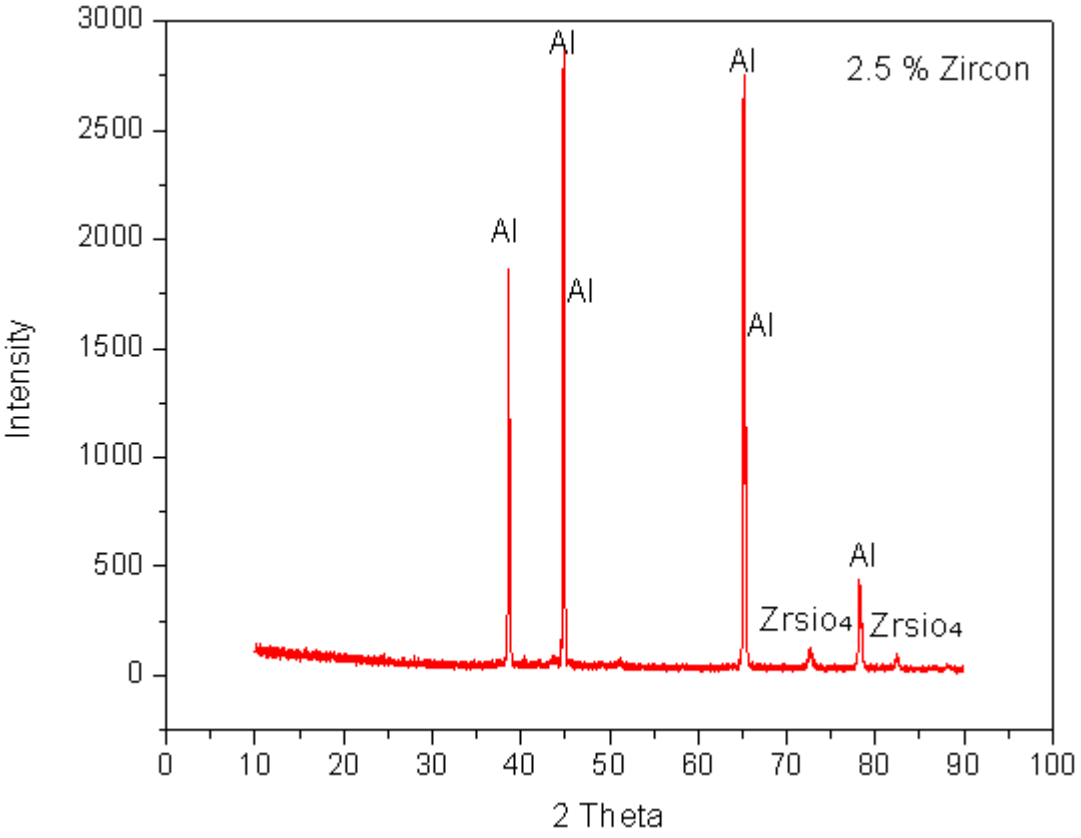

Figure 5.65 X-RD of AA6063 with 2.5% Zircon Sand

Table 5.9 X-RD results of alloy reinforced with 2.5% Zircon Sand

S.NO.	Rel. Int. [%]	Displacement [°2Th.]	Compound Name	Chemical Formula
1	100.00	44.8141	Aluminium	Al
2	98.17	65.1138	Aluminium	Al
3	64.76	38.5808	Aluminium	Al
4	53.60	65.2932	Aluminium	Al
5	51.77	44.9382	Aluminium	Al
6	13.93	78.1778	Aluminium	Al
7	2.81	72.6211	Zirconium Silicate	$Zrsio_4$
8	1.12	43.6746	Zirconium Silicate	$Zrsio_4$

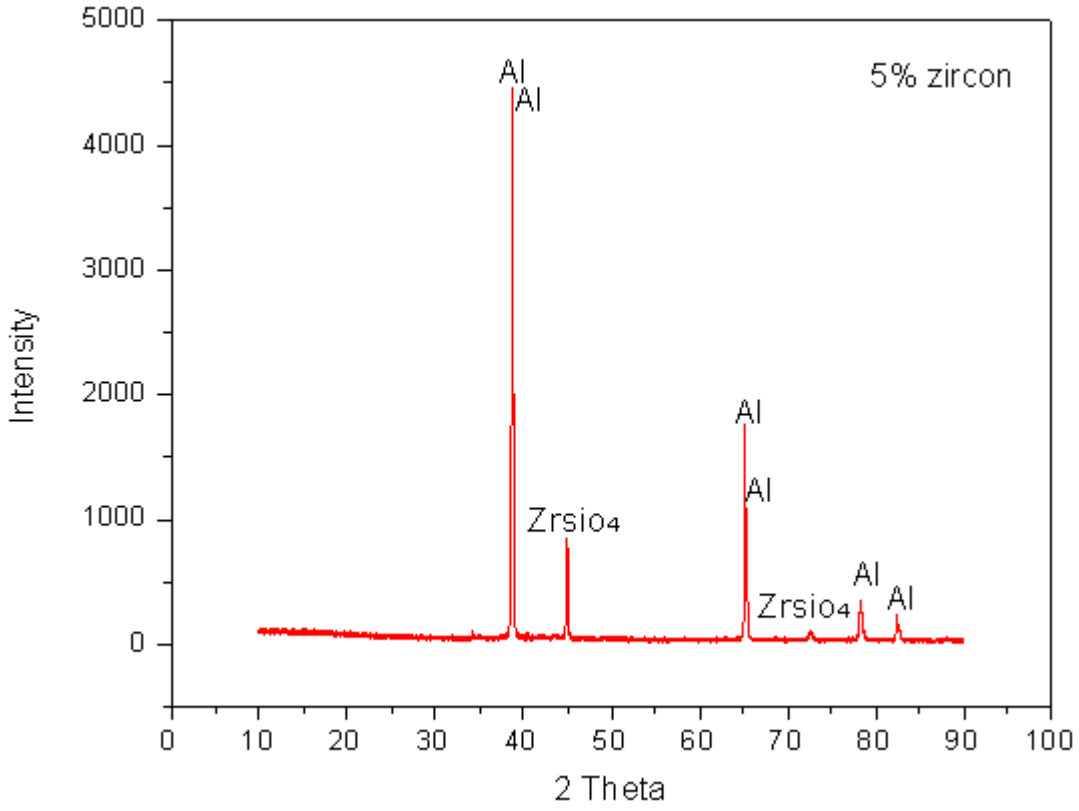

Figure 5.66 X-RD of AA6063 with 5% Zircon Sand

Table 5.10 X-RD results of alloy reinforced with 5% Zircon Sand

S.NO.	Rel. Int. [%]	Displacement [°2Th.]	Compound Name	Chemical Formula
1	100.00	38.7609	Aluminium	Al
2	88.61	38.6635	Aluminium	Al
3	38.88	65.1806	Aluminium	Al
4	22.09	65.3534	Aluminium	Al
5	18.08	78.2868	Aluminium	Al
6	3.09	82.5077	Aluminium	Al
7	0.59	72.4962	Zirconium Silicate	$Zrsio_4$
8	0.44	43.5901	Zirconium Silicate	$Zrsio_4$

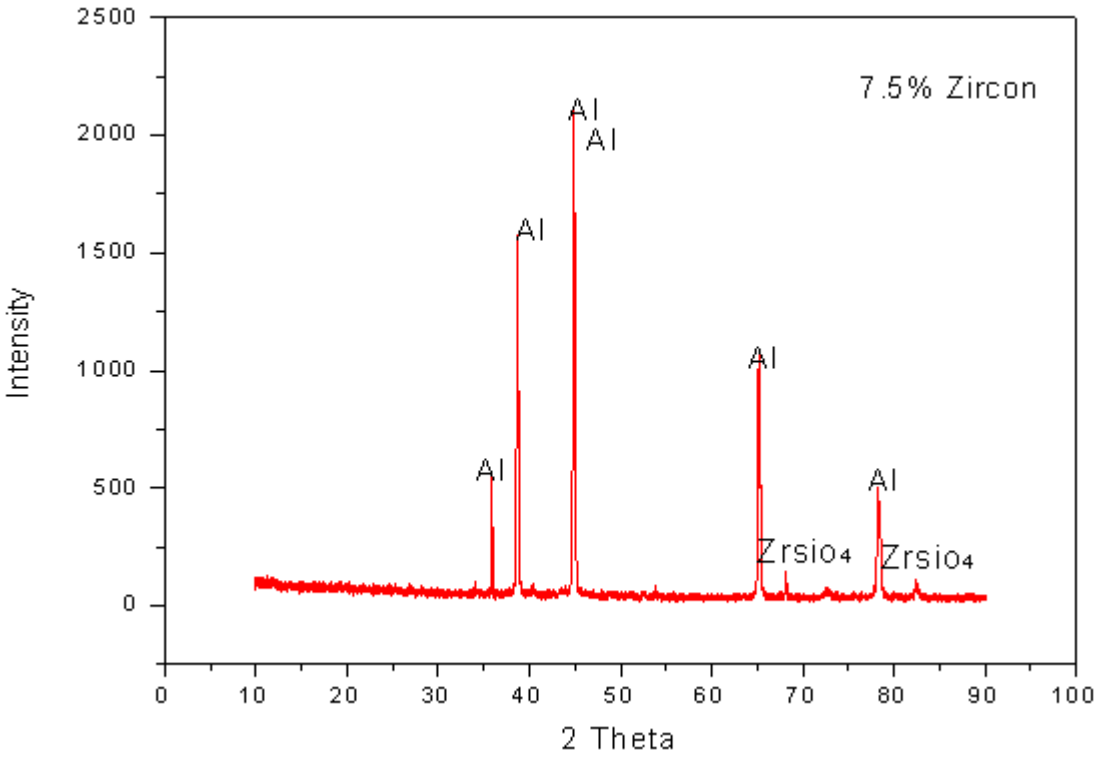

Figure 5.67 X-RD of AA6063 with 7.5% Zircon Sand

Table 5.11 X-RD results of alloy reinforced with 7.5% Zircon Sand

S.NO.	Rel. Int. [%]	Displacement [°2Th.]	Compound Name	Chemical Formula
1	100.00	44.8509	Aluminium	Al
2	74.41	38.6803	Aluminium	Al
3	49.98	65.1597	Aluminium	Al
4	22.36	35.8750	Aluminium	Al
5	21.73	78.2646	Aluminium	Al
6	5.26	65.0881	Aluminium	Al
7	3.39	82.4263	Zirconium Silicate	$Zrsio_4$
8	1.72	68.0881	Zirconium Silicate	$Zrsio_4$

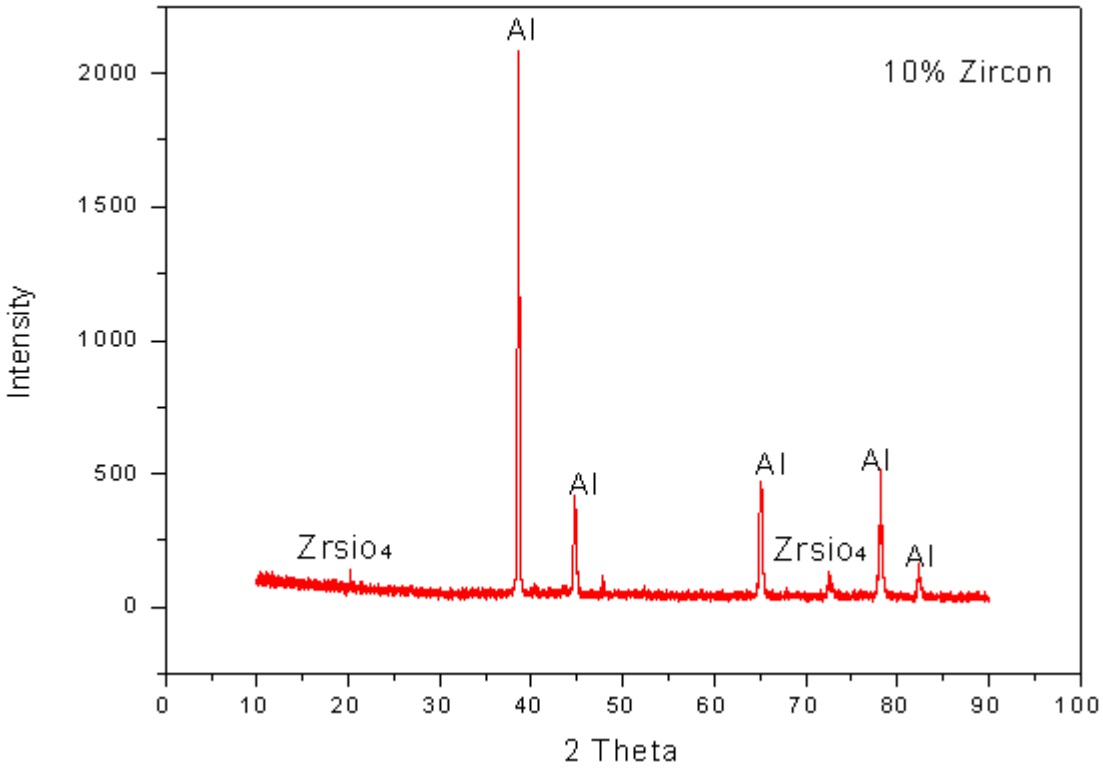

Figure 5.68 X-RD of AA6063 with 10% Zircon Sand

Table 5.12 X-RD results of alloy reinforced with 10% Zircon Sand

S.NO.	JCPDS code	Rel. Int. [%]	Displacement [°2Th.]	Compound Name	Chemical Formula
1	851327	100.00	38.5849	Aluminium	Al
2	851327	23.37	78.1674	Aluminium	Al
3	851327	20.75	64.9863	Aluminium	Al
4	851327	17.56	44.6836	Aluminium	Al
5	030932	4.97	82.3228	Aluminium	Al
6	751564	2.37	20.2134	Zirconium Silicate	$Zrsio_4$
7	831383	0.84	72.9504	Zirconium Silicate	$Zrsio_4$

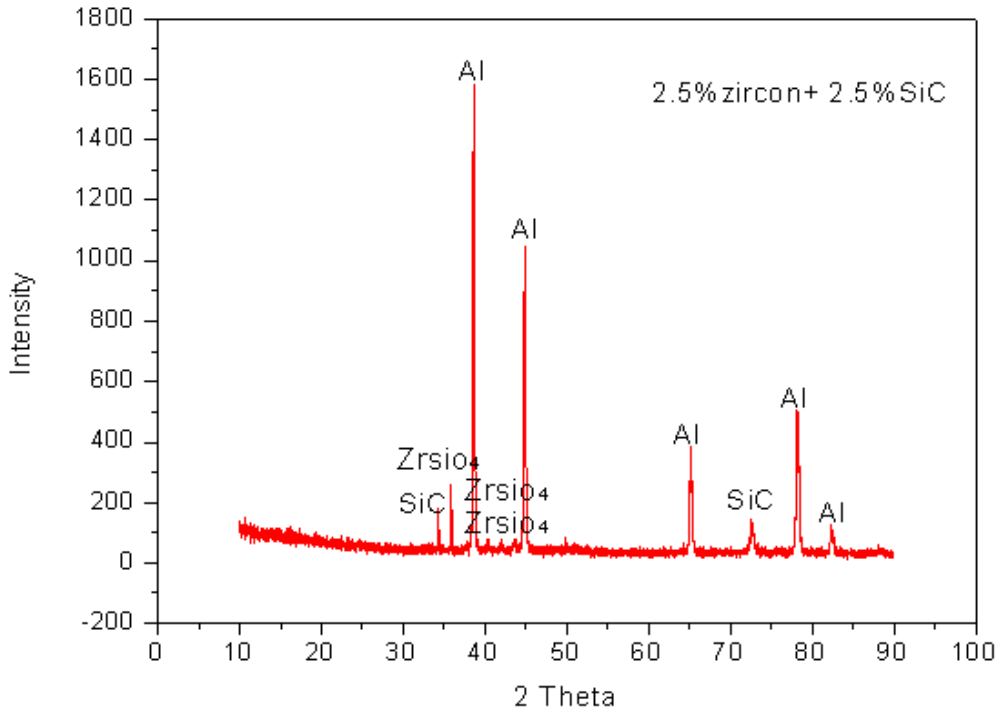

Figure 5.69 X-RD of AA6063 with 2.5% Zircon Sand and2.5% SiC

Table 5.13 X-RD results of alloy reinforced with 2.5% Zircon Sand and 2.5% SiC

S.NO.	JCPDS code	Rel. Int. [%]	Displacement [°2Th.]	Compound Name	Chemical Formula
1	011180	100.00	38.6197	Aluminium	Al
2	011180	64.60	44.8516	Aluminium	Al
3	030932	29.77	78.1768	Aluminium	Al
4	030932	22.40	65.1326	Aluminium	Al
5	030932	5.85	72.5878	Silicon carbide	SiC
6	732082	5.52	82.3572	Aluminium	Al
7	831383	4.87	35.8829	Zirconium Silicate	$Zrsio_4$
8	021464	4.32	34.3638	Silicon carbide	SiC
9	030457	1.71	40.3874	Zirconium Silicate	$Zrsio_4$
10	030630	1.32	43.5995	Zirconium Silicate	$Zrsio_4$

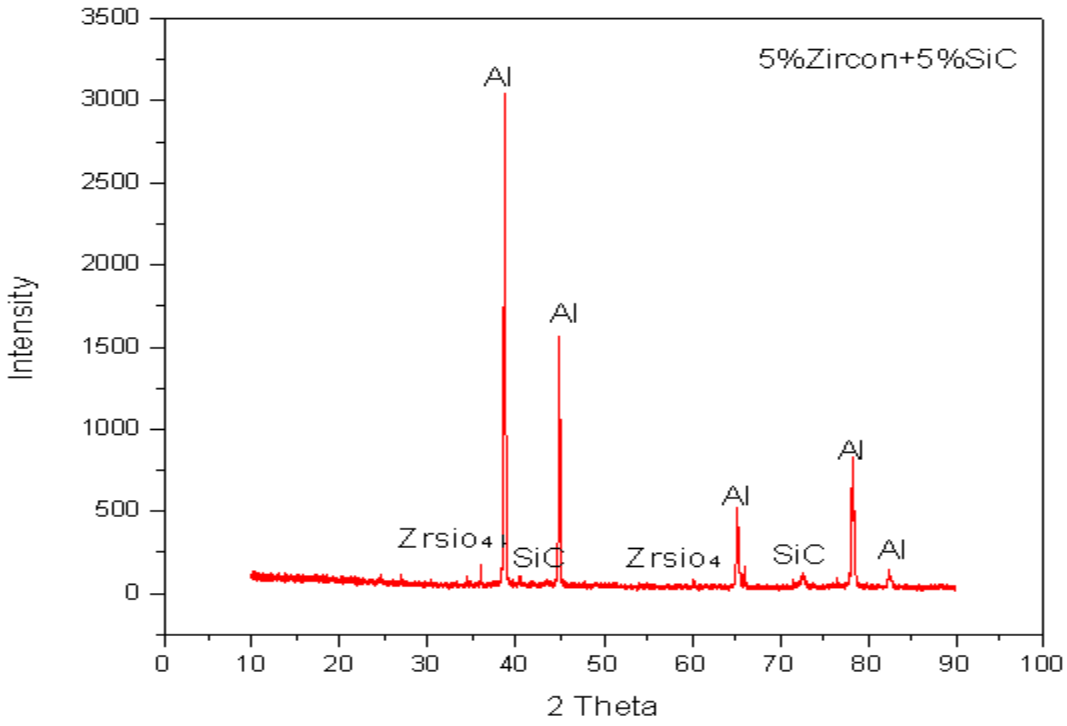

Figure 5.70 X-RD of AA6063 with 5% Zircon Sand and5% SiC

Table 5.14 X-RD results of alloy reinforced 5% Zircon Sand and5% SiC

S.NO.	JCPDS code	Rel. Int. [%]	Displacement [°2Th.]	Compound Name	Chemical Formula
1	030932	100.00	38.7023	Aluminium	Al
2	040787	49.88	44.8979	Aluminium	Al
3	851327	26.31	78.2286	Aluminium	Al
4	851327	15.30	65.1733	Aluminium	Al
5	831383	2.83	36.0214	Zirconium Silicate	$Zrsio_4$
6	040787	2.80	82.4169	Aluminium	Al
7	732082	2.28	72.6230	Silicon carbide	SiC
8	831379	0.54	60.2748	Zirconium Silicate	$Zrsio_4$
9	021462	0.37	48.9893	Silicon carbide	SiC

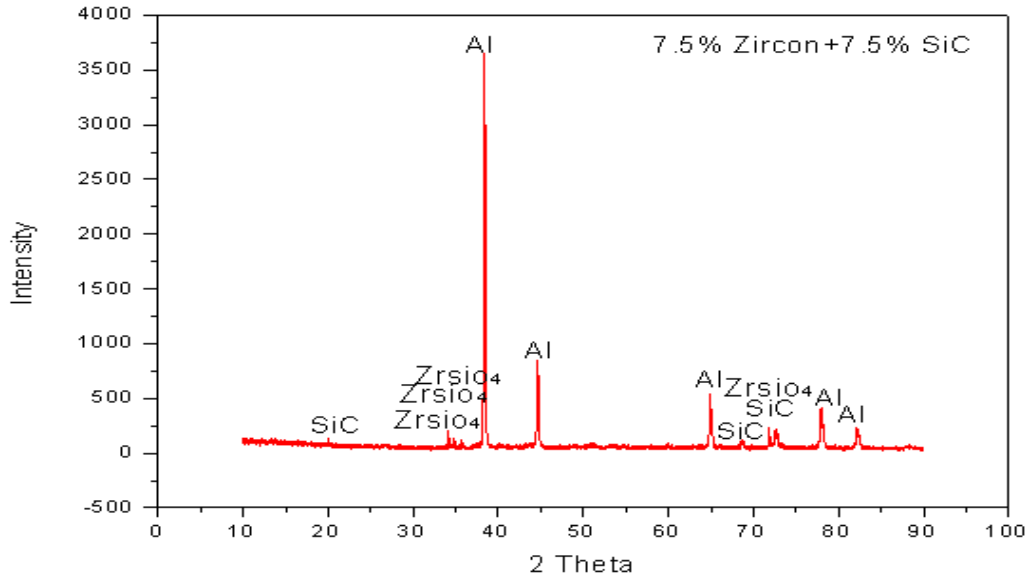

Figure 5.71 X-RD of AA6063 with 7.5% Zircon Sand and7.5% SiC

Table 5.15 X-RD results of alloy reinforced with 7.5% Zircon Sand and7.5% SiC

S.NO.	JCPDS code	Rel. Int. [%]	Displacement [°2Th.]	Compound Name	Chemical Formula
1	011176	100.00	38.4030	Aluminium	Al
2	030932	21.93	44.6181	Aluminium	Al
3	851327	13.30	64.9102	Aluminium	Al
4	851327	9.47	77.9692	Aluminium	Al
5	030932	4.84	82.1561	Aluminium	Al
6	732082	4.00	72.5865	Silicon carbide	SiC
7	831383	2.13	34.1265	Zirconium Silicate	$Zrsio_4$
8	831383	1.54	71.8774	Zirconium Silicate	$Zrsio_4$
9	831375	1.20	34.7149	Zirconium Silicate	$Zrsio_4$
10	831377	0.56	70.0084	Silicon carbide	SiC
11	421360	0.38	21.7688	Silicon carbide	SiC

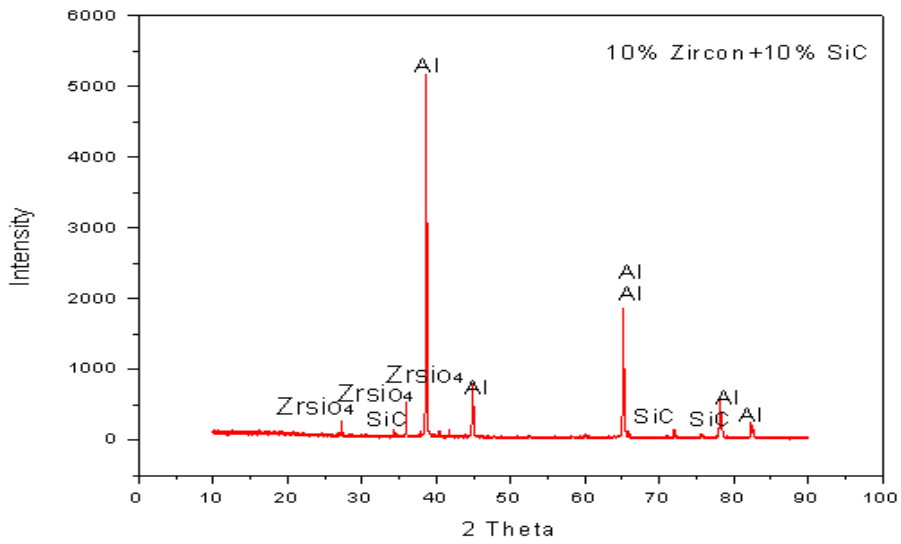

Figure 5.72 X-RD of AA6063 with 10% Zircon Sand and 10%SiC

Table 5.16 X-RD results of alloy reinforced with 10% Zircon Sand and10% SiC

S.NO.	JCPDS code	Rel. Int. [%]	Displacement [°2Th.]	Compound Name	Chemical Formula
1	030932	100.00	38.6572	Aluminium	Al
2	030932	53.91	48.7603	Aluminium	Al
3	851327	36.48	65.1450	Aluminium	Al
4	851327	19.11	65.3197	Aluminium	Al
5	851327	10.09	78.1932	Aluminium	Al
6	831383	9.64	35.9179	Zirconium Silicate	$Zrsio_4$
7	751541	5.66	78.4136	Silicon carbide	SiC
8	030932	4.14	82.3444	Aluminium	Al
9	030457	1.04	40.4336	Zirconium Silicate	$Zrsio_4$
10	021464	0.84	34.4155	Silicon carbide	SiC
11	732082	0.83	72.0894	Silicon carbide	SiC

In X-ray diffraction as shown in Figure 5.69- 5.72, different peaks have been obtained in the 2θ span ranging from 10 to 90. Applying extinction rules, these peaks and associated d-values have been found to correspond to the aluminium matrix composite are given in Table from 5.5-5.16.Different peaks in the pattern can be indexed to a mixture of different compounds such as Al, SiC and Zircon sand. Minor peaks attributed to impurity.

CHAPTER 6 CONCLUSION

The following conclusions can be drawn from the present investigation:

1. AA 6063 alloy matrix composites reinforced with Zircon Sand particles and Silicon Carbide particles can be successfully synthesized by the stir casting method.

2. For synthesizing of hybrid composite by stir casting process, stirrer design and position, stirring speed and time, melting and pouring temperature, particle-preheating temperature, particle incorporation rate, mould type and size, and reinforcement particle size and amount are the important process parameters.

3. Microstructural observations shows that the Zircon Sand particles and Silicon Carbide particles are uniformly distributed in the AA6063 alloy matrix and good interfacial bonding between reinforcing particles and matrix.

4. With the addition of Zircon Sand and SiC particles the hardness of the composite increased. The Specimen with highest percentage of Zircon Sand and SiC particles has highest hardness value.

5. XRD results showed the presence Zircon Sand and SiC particles in alloy matrix.

6. Corrosion behaviours of Al 6063/Zircon Sand/ SiC MMCs is tested by potential measurement, corrosion current density measurement and potentiodynamic polarization method. Increase in the percentage of Zircon Sand and SiC particles will reduce the potential, corrosion current density and corrosion rate.

7. The Zircon Sand and SiC content in Al 6061 alloys plays a significant role in the corrosion resistance of the material. Increase in the percentage of Zircon Sand and SiC will be advantageous to reduce the density and increase the strength of the alloy. However, there is a significant reduction in the potential and corrosion rate.

6.1 Scope of Future Work

1) Other Metal Matrix Composites can be manufactured and tested by using stir casting method.

2) The concentration of corrosive medium and temperature of the corrosive medium can be changed and the effect on corrosion rate and corrosion behaviour can be studied.

3) Different corrosive medium can be used and their effect on metal matrix composites can be investigated.

CHAPTER 7 REFERENCES

1. Sudipt Kumar, J. Ananda Theerthan, "Production and Characterisation of Aluminium-Fly Composites using Stir Casting Method", Department of Metallurgical & Materials Engineering National Institute of Technology Rourkela, 2008.

2. Zuhair M. Gasem and Amro M. Al-Qutub, "Corrosion Behaviour of Powder Metallurgy Aluminium Alloy 6061/AL_2O_3 Metal Matrix Composites", 6th Saudi engineering conference, 2002.vol 5 P. 271-280.

3. Karl Ulrich Kainer, "Basics of Metal Matrix Composites", custom-made material for automotive and aerospace engineering, *McGraw-Hill,* 2004.

4. Vishal Sharma, "Synthesis and Interfacial Charaterization of Al-4.5wt%Cu/Zircon /SiliconCarbide Hybrid Composite", *ME Thesis,* Thapar University Patiala 2007.

5. Shailove kumar, "Effect of thermal ageing on Al -SiC MMC", *ME Thesis*, Thapar University Patiala, 2010.

6. Daniel B. Miracle and Steven L. Donaldson, "Introduction to Composites", *ASM Hand Book of Composite Materials*, volume-21.

7. Sanjeev Das V. Udhayabanu S. Das K. Das, "Synthesis and characterization of Zircon Sand/Al-4.5 wt% Cu Composite produced by Stir Casting Route", *J Mater Sci* (2006) 41:4668–4677.

8. Subhakanta sarangi, Deepak kumar, "Fabrication and characterisation of Aluminium-fly Ash composite using Stir Casting method", *ME Thesis,* NIT Rourkela, 2009.

9. T. P. D. Rajan, R.M. Pillai, B.C. Pai, K.G. Satyanarayana, P.K. Rohatgi, "Fabrication and characterisation of Al–7Si–0.35Mg/fly ash metal matrix composites processed by different stir casting routes", *Composites Science and Technology* 67 (2007) 3369–3377.

10. Nigamanada ray, Dilip kumar kerketta, "Some Studies on Aluminium Matrix in Situ Composites Produced by Stir Casting Method", *ME Thesis* NIT Rourkela, 2010.

11. J. E. Breakell, M. Siegwart, K. Foster, "Management of Accelerated Low Water Corrosion in Steel Maritime Structures", *ISBN* 0-86017-634-7.

12. http://corrosion-doctors.org/Forms-Uniform/lamppost-weathering-hues.htm.

13. J. W. Oldfield, "Electrochemical theory of galvanic corrosion", *ASTM*, STP 978, 1988, p. 5-22.

14. M. G. Fontana, N. D. Greene, "Corrosion engineering", *McGraw-Hill*, New York, 1998.

15. R. Takabeya, "Aluminium corrosion products formed in atmospheric environments", *Corrosion Engineering*, vol. 36, 1987, p. 279-286.

16. S. J. Ketcham, I. S. Shaffer, "Exfoliation corrosion of Aluminium alloys", *ASTM, STP*, vol. 516, 1972, p. 3-16.

17. M. O. Speidel, "Stress-corrosion cracking of cast aluminium alloys", *NATO, Advanced study Institute on stress-corrosion cracking, Denmark*, 1975, p. 97-115.

18. I. L. Rozenfeld, "Crevice corrosion of metals and alloys", *NACE*, 3, 1974, p. 373-398.

19. J. M. Bryan, "Mechanism of the corrosion of aluminium", *Chemistry & Industry*, 1948, p. 135-136.

20. Y. L. Cheng, Z. H. Chen, H. L. Wu and H. M. Wang, "The corrosion behaviour of the Aluminium alloy 7075/SiCp metal matrix composite prepared by spray deposition", *Materials and Corrosion 2007*, 58, No. 4.

21. Geetha Mable Pinto, Jagannath Nayak, A Nityananda Shetty, **"**Corrosion Behaviour of 6061 Al - 15vol. Pct. SiC Composite and its Base Alloy in a Mixture of 1:1 Hydrochloric and Sulphuric Acid Medium", *J. Electrochem. Sci*., 4 (2009) 1452 – 1468.

22. A. Abdul Jameel1, H. P. Nagaswarupa, P. V. Krupakara and T. R. Shashi Shekhar, "Evaluation of Corrosion Rate of Al 6061 / Zircon Sand Metal Matrix Composites in Sea Water", *International Journal of Oceans and Oceanography* ISSN 0973-2667 Volume 3, Number 1 (2009), pp. 37-42.

23. B. Bobic, S. Mitrovic, M. Babic, I. Bobic, "Corrosion of Metal-Matrix Composites with Aluminium Alloy Substrate", *McGraw-Hill*, New York, 2010.

24. C. Monticelli, F. Zucchi, G. Brunoro, G.Trabanelli, "Corrosion and corrosion inhibition of alumina particulate/aluminium alloys metal matrix composites in neutral chloride solutions", *Journal of Applied Electrochemistry* 27 (1997) 325-334.

25. C. Chen and F. Mansfeld, "Corrosion protection of an Al 6092/SiC Metal Matrix Composite', *Corrosion Science* Vol. 39, No. 6, pp. 1075-1082, 1997.

26. Florian B. Manfeld, Westlake village, Calif. Hong shih, Qingdao, You Wang, jingshou, "Method for creating a Corrosion-Resistant Aluminium Surface", *United states patent*, patent number: 5,194,138 and date:Mar.16,1993.

27. G. B. Veeresh Kumar, C. S. P. Rao, N. Selvaraj, M. S. Bhagyashekar, "Studies on Al6061-SiC and Al7075-Al2O3 Metal Matrix Composites, *Journal of Minerals & Materials Characterization & Engineering*", Vol. 9, No.1, pp.43-55, 2010.

28. Hosni Ezuber , A. El-Houd , F. El-Shawesh, "A study on the corrosion behavior of Aluminium alloys in seawater", *Materials and Design* 29 (2008) 801–805.

29. H.J. Greene and F. Mansfeld, **"**Corrosion Protection of Aluminium Metal-Matrix Composites", *Corrosion science*, Volume 53, Number 12, nov 1997.

30. J. Bienia, M. Walczak, B. Surowska, J. Sobczaka, "Microstructure and Corrosion behaviour of Aluminium Fly ash Composites", *Journal of Optoelectronics and Advanced Materials* Vol. 5, No. 2, June 2003, p. 493 – 502.

31. J. Zhu, L.H. Hihara, "Corrosion of continuous alumina-fibre reinforced Al–2 wt.% Cu–T6 metal–matrix composite in 3.15 wt.% NaCl solution*", Corrosion Science* 52 (2010) 406–415.

32. L. A. Dobrza nski, Structure, "properties and corrosion resistance of PM composite materials based on EN AW-2124 Aluminium alloy reinforced with the Al_2O_3 ceramic particles", *Journal of Materials Processing Technology* 162–163 (2005) 27–32.

33. Manoj Singla, D. Deepak Dwivedi, Lakhvir Singh, Vikas Chawla, **"**Development of Aluminium Based Silicon Carbide Particulate Metal Matrix Composite", *Journal of Minerals & Materials Characterization & Engineering*, Vol. 8, No.6, pp 455-467, 2009.

34. M. K. Surappa, "Aluminium matrix composites: Challenges and opportunities", Sadhana Vol. 28, Parts 1 & 2, February/April 2003, pp. 319–334.

35. Olivier Beffort, Siyuan Long, Cyril Cayron, Jakob Kuebler, "Composites Science and Technology", 67 (2007) 737–745.

36. P. B. DA Silva-Mala, F. Velasco, N. Aanton, C.E. DA Costa and W.C. Zapata, **"**Corrosion Resistance of 2014 Aluminium Matrix Composites Reinforced with Atomised Ni3Al", *Advanced Performance Materials* 6, 117–127 (1999).

37. S. Balasivanandha Prabu , L. Karunamoorthy, S. Kathiresan , B. Mohan, "Influence of stirring speed and stirring time on distribution of particles in cast metal matrix composite", *Journal of Materials Processing Technology* 171 (2006) 268–273.

38. Sanjeev Das V. Udhayabanu S. Das K. Das, "Synthesis and characterization of Zircon Sand/Al-4.5 wt% Cu Composite produced by Stir Casting Route", *Journal of Material Science* (2006) 41:4668–4677.

39. S.L. Colenman, V. D. Scott, "Materials Science", University of Bath, UK, *Journal of Materials Science* 29 (1994) 2826-2834.